

MECHANISM OF DEPOSIT FORMATION ON FUEL-WETTED HOT METAL SURFACES

**INTERIM REPORT
BFLRF No. 290**

By

**L.L. Stavinoha
S.R. Westbrook
L.A. McInnis**

**Belvoir Fuels and Lubricants Research Facility (SwRI)
Southwest Research Institute
San Antonio, Texas**



Under Contract to
**U.S. Army TARDEC
Mobility Technology Center-Belvoir
Fort Belvoir, Virginia**

Contract No. DAAK70-92-C-0059

Approved for public release; distribution unlimited

19950117 120

January 1995 [DTIC QUALITY INSPECTED 3]

Disclaimers

The findings in this report are not to be construed as an official Department of the Army position unless so designated by other authorized documents.

Trade names cited in this report do not constitute an official endorsement or approval of the use of such commercial hardware or software.

DTIC Availability Notice

Qualified requestors may obtain copies of this report from the Defense Technical Information Center, Cameron Station, Alexandria, Virginia 22314.

Disposition Instructions

Destroy this report when no longer needed. Do not return it to the originator.

REPORT DOCUMENTATION PAGE

Form Approved
OMB No. 0704-0188

Public reporting burden for this collection of information is estimated to average 1 hour per response, including the time for reviewing instruction, searching existing data sources, gathering and maintaining the data needed, and completing and reviewing the collection of information. Send comments regarding this burden estimate or any other aspect of this collection of information, including suggestions for reducing this burden, to Washington Headquarters Services, Directorate for Information Operations and Reports, 1215 Jefferson Davis Highway, Suite 1204, Arlington, VA 22202-4302, and to the Office of Management and Budget, Paperwork Reduction Project (0704-0188), Washington, DC 20503.

1. AGENCY USE ONLY (Leave blank)		2. REPORT DATE Jan 95	3. REPORT TYPE AND DATES COVERED Interim; May 89 to Dec 92	
4. TITLE AND SUBTITLE Mechanism of Deposit Formation on Fuel-Wetted Hot Metal Surfaces			5. FUNDING NUMBERS DAAK70-87-C-0043; WD 30 DAAK70-92-C-0059	
6. AUTHOR(S) Stavinocha, Leo L., Westbrook, Steven R., and McInnis, Lona A.				
7. PERFORMING ORGANIZATION NAME(S) AND ADDRESS(ES) U.S. Army Belvoir Fuels and Lubricants Research Facility (SwRI) Southwest Research Institute P.O. Drawer 28510 San Antonio, Texas 78228-0510			8. PERFORMING ORGANIZATION REPORT NUMBER BFLRF No. 290	
9. SPONSORING/MONITORING AGENCY NAME(S) AND ADDRESS(ES) Department of the Army Mobility Technology Center-Belvoir 10115 Gridley Road, Suite 128 Ft. Belvoir, Virginia 22060-5843			10. SPONSORING/MONITORING AGENCY REPORT NUMBER	
11. SUPPLEMENTARY NOTES				
12a. DISTRIBUTION/AVAILABILITY STATEMENT Approved for public release; distribution unlimited			12b. DISTRIBUTION CODE	
13. ABSTRACT (Maximum 200 words) Experiments were performed in a Single-Tube Heat Exchanger (STHE) apparatus and a Hot Liquid Process Simulator (HLPS) configured and operated to meet Jet Fuel Thermal Oxidation Tester (JFTOT) ASTM D 3241 requirements. The HLPS-JFTOT heater tubes used were 1018 mild steel, 316 stainless steel (SS), 304 SS, and 304 SS tubes coated with aluminum, magnesium, gold, and copper. A low-sulfur Jet A fuel with a breakpoint temperature of 254°C was used to create deposits on the heater tubes at temperatures of 300°C, 340°C, and 380°C. Deposit thickness was measured by dielectric breakdown voltage and Auger ion milling. Pronounced differences between the deposit thickness measuring techniques suggested that both the Auger milling rate and the dielectric strength of the deposit may be affected by deposit morphology/composition (such as metal ions that may have become included in the bulk of the deposit). Carbon burnoff data were obtained as a means of judging the validity of DMD-derived deposit evaluations. ESCA data suggest that the thinnest deposit was on the magnesium-coated test tube. The Scanning Electron Microscope (SEM) photographs showed marked variations in the deposit morphology and the results suggested that surface composition has a significant effect on the mechanism of deposition. The most dramatic effect observed was that the bulk of deposits moved to tube locations of lower temperature as the maximum temperature of the tube was increased from 300° to 380°C, also verified in an STHE. The results indicate that the deposition rate and quantity at elevated temperatures is not completely temperature dependent, but is limited by the concentration of dissolved oxygen and/or reactive components in the fuel over a temperature range. Experiments were done for several fuels using the STHE apparatus to evaluate deposit formation rates with fuel at measured temperatures. The STHE test tubes were 0.64 cm O.D., 304 SS test tubes, heated at 340°, 380°, 420°, 460°, 500°, and 540°C for 4 hours with a fuel flow of 10 mL/min. The position of the fuel deposit in the tube versus the fuel temperature at various bath set temperatures very closely approximates what was observed for HLPS heater tubes. These data support the observation based on HLPS data that the depositing position on the tube is temperature dependent. Furthermore, the magnitude of the deposit is essentially the same at all three temperatures. Oxygen measurements in both HLPS and STHE tests indicate that oxygen is depleted at temperatures below 260°C. At higher temperatures (set temperature of 420°C) for the STHE, methane generation is observed due to pyrolysis of the fuel. At pyrolysis temperatures, surface deposit formation is fuel composition dependent.				
14. SUBJECT TERMS Diesel Fuel Fuel Injection Adiabatic Engine Fuel Instability Thermal Oxidative Stability JFTOT Single Tube Heat Exchanger DMD			15. NUMBER OF PAGES 91 16. PRICE CODE	
17. SECURITY CLASSIFICATION OF REPORT Unclassified	18. SECURITY CLASSIFICATION OF THIS PAGE Unclassified	19. SECURITY CLASSIFICATION OF ABSTRACT Unclassified		20. LIMITATION OF ABSTRACT

EXECUTIVE SUMMARY

Problems: In the development of high-efficiency/advanced engine technology such as low-heat rejection engines and injection systems, the thermal stability of the fuel is an important concern. Limited data from Jet Fuel Thermal Oxidation Test (JFTOT) rigs show that heat-treated aluminum tubes with magnesium-enriched surfaces tend to retard deposit formation and accumulation. Basic problem areas for investigation of fuel thermal stability should include (1) a measure of the deposition rates on different surface compositions, and (2) the effect of fuel composition on possible changes in surface chemistry. Furthermore, an evaluation of nascent deposit formation versus subsequent thick deposits on hot surfaces is needed to ascertain to what degree surface composition controls deposition.

Objective: The objective of this program was to investigate the role of surface composition in the mechanism of deposit formation on fuel-wetted hot surfaces. The effect of surface composition on the tendency of fuels containing a relatively broad range of components to form deposits was evaluated. Goals include the following: 1) measurement of the relative rates of deposit formation on several surface materials, 2) determination of the effect of the surface material on the composition and structure at the surface/deposit interface and in the bulk of the deposit, and 3) determination of the effects of prestressing and surface temperature on the formation of nascent deposits.

Importance of Project: The role of fuel stability must be considered in the development of high-efficiency/advanced engine technology. Neglecting fuel stability, especially in new engines with higher operating temperatures, could lead to serious problems with reliability and reduced engine (component) life. Based on the results of previous studies, it is possible to predict the deposit-forming tendencies of various fuel types at the operating temperatures of actual engines. However, very little work has been done on the effects of surface composition on deposit formation at higher operating temperatures. Understanding the surface interaction could not only be helpful in selecting the most benign metallurgy, but it may also lead to methods of inhibiting the formation of deposits and designing of fuel-pretreatment units for high heat rejection engine fuel delivery without fouling of fuel system components.

Technical Approach: Major emphasis was placed on obtaining deposit quantitation versus temperature on various metal surfaces using both the Hot Liquid Process Simulator (HLPS) and the Single Tube Heat Exchanger (STHE). Surface metallurgy was also varied in the STHE using the approach developed for gravimetric Jet Fuel Thermal Oxidation Tester (JFTOT) by the Naval Research Laboratories.

Accomplishments: This project was initiated in 1989 as an In-house Laboratory Independent Research (ILIR) project. Three groups of four stainless steel (SS) (304) test tubes were coated with aluminum, gold, carbon, magnesium, and copper. The instrumentation configuration was defined for the HLPS using ASTM D 3241 JFTOT standard conditions, except for eliminating the Triton-treated fuel prefilter. Preheating fuel at 150°F (66°C) and 200°F (93°C) at heater tube temperatures of 300°C and 340°C did not demonstrate any hot zone broadening advantages over fuel at room temperature. Experiments were performed in an HLPS configured and operated such that it performed under conditions similar to JFTOT ASTM D 3241 requirements. The

JFTOT heater tubes used were 1018 mild steel, 304 SS, and 304 SS tubes coated with aluminum, magnesium, gold, and copper. A low-sulfur Jet A fuel with a breakpoint temperature of 254°C was used to create deposits on the heater tubes at temperatures of 300°C, 340°C, and 380°C. Deposit thickness was measured by dielectric breakdown voltage and Auger ion milling. Auger ion milling of the deposits showed the order of deposition to be copper > mild steel > gold > aluminum > magnesium. The dielectric strength method indicated deposit thickness ranking of mild steel > 304 SS > gold > magnesium = aluminum = copper. The pronounced differences between the deposit thickness measuring techniques suggested that both the Auger milling rate and the dielectric strength of the deposit may be affected by deposit morphology/composition (such as metal ions that may have become included in the bulk of the deposit). Subsequent carbon burnoff results ranked the deposit level at 340°C as copper > 304 SS > magnesium > gold > aluminum. ESCA data had suggested that the thinnest deposit was on the magnesium-coated test tube. The Scanning Electron Microscope (SEM) photographs showed marked variations in the deposit morphology, and the results suggested that surface composition has a significant effect on the mechanism of deposition. Aside from variations in the thickness of deposits due to metallurgy, the most dramatic effect observed was that the bulk of deposits moved to tube locations of lower temperature as the maximum temperature of the tube was increased from 300 to 380°C, also verified in a single-tube heat exchanger. The results indicate that the deposition rate is highly temperature-dependent and may be limited by the concentration of dissolved oxygen and/or reactive components in the fuel. The overall results show that the surface temperature and composition play an important role in deposition. Additional fuels were evaluated by HLPS and in an STHE. A gas chromatograph was successfully installed in-line in the HLPS to facilitate the measurement of oxygen and methane in the fuel after heating. Data generated using the HLPS and the STHE provide a correlation between results of the two bench test units and allowed determination of mechanism regimes. The oxygen/methane data were used to help identify the transition points for oxidative degradation and pyrolysis of the test fuels. Plots of the energies of activation for each of the fuels were also prepared based on deposit formation rates versus STHE bath temperatures. These data, combined with oxygen/methane data, have clearly defined fuel deposit formation mechanism temperature regimes. Analytical data for oxygen depletion, methane generation, and carbon burnoff from deposits have provided a correlation between HLPS and STHE results and test conditions. Limited metallurgical effects as well as fuel additive effects were evaluated for mechanism influence using the STHE.

Military Impact: The role of fuel stability must be considered in the development of high-efficiency/advanced engine technology. Fuel instability, especially in new engines with higher operating temperatures, could lead to serious problems with reliability and reduced engine life. Based on the results of previous studies, it is possible to predict the deposit-forming tendencies of various fuel types at the operating temperatures of actual engines. However, very little work has been done on the effects of surface composition on deposit formation at elevated temperatures. Understanding the mechanism of fuel deposit formation will be helpful in selecting the most benign metallurgy, as well as lead to methods of inhibiting the formation of deposits and designing of fuel-pretreatment units for high heat rejection engine fuel delivery without fouling of fuel system components.

FOREWORD/ACKNOWLEDGEMENTS

This work was performed at the U.S. Army Belvoir Fuels and Lubricants Research Facility (BFLRF) located at Southwest Research Institute (SwRI), San Antonio, TX, during the period May 1989 to December 1992 under Contract Nos. DAAK70-87-C-0043 and DAAK70-92-C-0059 with the U.S. Army TARDEC, Mobility Technology Center-Belvoir (MTCB). Mr. T.C. Bowen (AMSTA-RBFF) of MTCB served as the contracting officer's representative, and Mr. M.E. LePera (AMSTA-RBF) served as the project technical monitor.

The authors would like to acknowledge the technical assistance provided by SwRI personnel in conducting this work. Mr. K.E. Hinton performed the STHE experiments, and Dr. D.W. Naegeli assisted in the initial evaluation of HLPS data during the early phases of this program.

The authors would also like to acknowledge the editorial assistance provided by Mr. J.W. Pryor, Ms. M.M. Clark, and Ms. L.A. Pierce in the preparation of the report.

Accession For	
NTIS	CRA&I <input checked="checked" type="checkbox"/>
DTIC	TAB <input type="checkbox"/>
Unannounced <input type="checkbox"/>	
Justification	
By	
Distribution /	
Availability Codes	
Dist	Avail and/or Special
A-1	

TABLE OF CONTENTS

<u>Section</u>	<u>Page</u>
I. INTRODUCTION AND BACKGROUND	1
II. OBJECTIVE	5
III. EXPERIMENTAL APPROACH	5
A. Hot Liquid Process Simulator	5
B. Deposit Measuring Device	6
C. Single Tube Heat Exchanger	6
D. Carbon Burnoff Procedure	9
E. Test Fuels	10
IV. RESULTS	11
V. DISCUSSION OF RESULTS	11
VI. CONCLUSIONS	21
VII. RECOMMENDATIONS	22
VIII. LIST OF ABBREVIATIONS	23
IX. LIST OF REFERENCES	24
APPENDICES	
A. Summary of Hot Liquid Process Simulator (HLPS) Data	27
B. Summary of Single Tube Heat Exchanger (STHE) Data	51
C. Quantitation of Fuel Deposition on Hot Metal Surfaces	69

LIST OF ILLUSTRATIONS

<u>Figure</u>	<u>Page</u>
1 Schematic of Single Tube Heat Exchanger	7
2 Fuel Temperature Versus Location in STHE	7
3 Carbon Data for Four Fuels on Various HLPS Metal Test Tubes	8
4 Fuel Nitrogen Purge Effect on Deposit Level on HLPS Metal Tubes	12
5 HLPS: Temperature Effects on Oxygen and Methane	13
6 STHE: Temperature Effects on Oxygen and Methane	14
7 Carbon Data for Three Fuels at Various STHE Bath Temperatures	15
8 Fuel Microparticulate Levels After STHE Stressing at Various Temperatures Using 304 SS and 316 SS Test Tubes	16
9 1% S Fuel Microparticulate Levels at Room Temperature After STHE Stressing at Various Temperatures and Flowing Through In-Line Metal Filters	18
10 Nitrogen Purge Effect on 1% S Fuel Deposit Level in STHE 316 SS Metal Tubes at 364°C	19
11 Reference No. 2 Diesel Fuel Deposit Level on STHE 316 SS and 304 SS Serial Metal Tubes at 364°C	19
12 Arrhenius Energies of Activation for Three Fuels on 304 SS and 316 SS STHE Metal Tubes Using Carbon Levels for the Whole Tube and Two Sections of the Tube	20

LIST OF TABLES

<u>Table</u>	<u>Page</u>
1 Comparison of Stainless Steel Composition Requirement With STHE Test Tube Analyses	9
2 Chemical and Physical Properties of Test Fuels	10

I. INTRODUCTION AND BACKGROUND

The effect of fuel system metallurgy on fuel stability is an important concern in the development of high efficiency/advanced engine technology such as adiabatic, low-heat rejection engines. Several studies have shown that trace metals adversely affect the thermal stability of hydrocarbon fuels.(1, 2) Metal concentrations as low as 15 ppb of copper, 25 ppb of iron, 100 ppb of zinc, and about 200 ppb of lead have been found to cause significant change in the thermal stability of jet fuels. These studies suggest that the slightest metallic contamination could cause a significant change in the thermal oxidative stability of hydrocarbon fuels. In fact, the theory has been advanced that all hydrocarbon auto-oxidations are trace metal catalyzed.(3) Recent work (4) in which only limited data are available, suggests that aluminum tubes with magnesium-enriched surfaces tend to have lower deposit buildups than the standard aluminum tubes. If such minor changes in surface metallurgy cause significant differences in the rate of deposit formation, major changes in surface composition could dramatically affect processes such as deposit adherence and oxidation catalysis.(5) Experiments with metal deactivator in dodecane using JFTOT equipment suggest that the effect on deposit reduction may be a consequence of interactions in the liquid phase rather than a reduced adherence to the hot metal surface.(6)

One measure of the thermal stability of aviation fuels is the quantity of deposits formed on heated metal surfaces.(7) In accelerated stability tests conducted in accordance with the JFTOT procedure (ASTM D 3241) (8), the rating methods currently employed involve either visual comparisons or measurements of reflected light by the tube deposit rater (TDR), both of which are sensitive to deposit color and surface texture. Morris and Hazlett (7) examined deposits formed on stainless steel JFTOT heater tubes in several ways including TDR, gravimetric carbon combustion, and two new nondestructive techniques for determining deposit volumes based on dielectric strength and optical interference. Measurements of total carbon content by combustion were used as a reference. They found that the dielectric and interference methods correlated well with the combustion analyses and each other, while the total TDR often gave misleading results.

* Underscored numbers in parentheses refer to the list of references at the end of this report.

The rate of deposit formation in and by fuels is generally both time- and temperature-dependent. The hotter the fuel, the lower the time needed to form deleterious products. However, the hotter the wall (surface) used to heat the fuel, the greater are the wall (surface) deposits, as long as adequate reactants remain available or are not depleted. Examples of deleterious products are listed below.

- Microparticulates – particulates filterable by porous membranes.
- Sediment – agglomerated particulates settled to the bottom.
- Surface deposits – insoluble fuel products formed on heated walls by one of several mechanisms.

Mechanisms of deposit formation include the following:

- Auto-oxidation – self-catalyzed oxidation not directly involving the container surface. This is typical in long-term storage environments and accelerated tests up to approximately 150°C.
- Thermal Oxidation – fuel flowing over hot surfaces as in JFTOT, HLPS, or STHE with set temperatures of 200°C and hotter. Relates to deposits in higher temperature surfaces of heat exchanger/fuel nozzle-injector.
- Pyrolysis – decomposition of fuel and thermal-oxidative deposits on very hot surfaces. Relates to deposits on nozzle/injector tips and combustion chamber deposits.

Typical forms of deterioration related to fuel types are as follows:

- Gasoline
 - Auto-oxidation in the storage of fuel.

- Rapid auto-oxidation and thermal oxidation, i.e., engine induction system depositing (ISD) in vehicle fuel system.
- Diesel
 - Storage auto-oxidation, condensation, esterification, and acid-base reactions forming fuel-insoluble microparticulates and sediment (agglomerated microparticulates).
 - Thermal oxidation forming surface deposits in injectors.
 - Pyrolysis forming deposits on injector tips and combustion chamber fuel-wetted surfaces.
- Jet/Gas Turbine
 - Auto-oxidation forming soluble gum, peroxides, and color bodies.
 - Thermal-oxidation formation of deposits on fuel-wetted hot surfaces of heat exchangers, control arms, divider valves, nozzles (during operation and shut-down soak-back).

In a previous paper "Quantitation of Fuel Deposition on Hot Metal Surfaces," presented at the 4th International Conference on Stability and Handling of Liquid Fuels (9), data for a Jet A fuel was presented which led to the following conclusions:

- Under JFTOT D 3241 test conditions, thickness profiles of deposits formed on a variety of surfaces including mild steel, 304 SS, Al, Mg, Cu and Au, were compared using the DMD (dielectric breakdown voltage) and Auger milling.
- Except for gold and aluminum, the deposit thicknesses measured by DMD were substantially lower than those measured by Auger milling, and the disparity in the two

methods seemed to grow with increased temperature and deposit thickness. The disparities in the thicknesses measured by DMD and Auger milling were most pronounced in the copper-coated heater tubes.

- Using carbon burnoff data for quantitation allowed for the observation that the deposit magnitude was essentially the same, except it seemed dramatically lower for aluminum. The highest value was 416 μg for Mg at 380°C while the lowest value at 380°C was 153 μg C for aluminum.
- Aside from variations in the thickness of deposits due to metallurgy, the most dramatic effect observed was that the bulk of deposits moved to tube locations of lower temperature as the maximum temperature of the tube was increased from 300 to 380°C. This effect was somewhat greater on the copper-coated tubes. Deposition rate is highly temperature-dependent and may be quantitatively limited by the concentration of dissolved oxygen and/or reactive components in the fuel.
- Surface analysis by ESCA showed that the deposits consisted of a highly oxygenated aliphatic hydrocarbon film containing alcohol, ether, ester, and carboxylic acid groups.
- The SEM photographs showed marked variations in the deposit morphology among the surface materials tested. The results suggested that surface composition has a significant effect on the mechanism of deposition. In general, it appears that insolubles coalesce in the fuel to form microspheres less than 1000 Å in diameter. The microspheres then either deposit directly onto the surface, forming a relatively smooth platelet-type structure, or they agglomerate into macrospheres (1 to 3 μm in diameter) before adhering to the surface. The former is observed on aluminum and gold, while the latter is particularly evident in deposits formed on magnesium. For copper, mild steel, and 304 SS, the deposits appear to form from several particle sizes ranging from micro- to macrospheres.

- STHE experiments using 304 SS tubing has confirmed the temperature dependence of fuel deposits and limited depositing capacity (with oxygen starvation) for the Jet A fuel based on HLPS data.

In this report, the earlier report is expanded by evaluating three additional fuels covering a wide range of composition from a very stable Jet A-1 to a Referee one-percent No. 2 diesel fuel and emphasizes the utility of results of quantitation of fuel deposits on hot metal surfaces. This data is provided in Appendices A and B. Data for the Jet A fuel is summarized in Appendix C.(9)

II. OBJECTIVE

The objective of this program was to investigate the role of surface composition in the mechanism of deposit formation on fuel-wetted hot surfaces. The effect of surface composition on the tendency of fuels containing a relatively broad range of components to form deposits was evaluated. Specific goals included measurement of the relative rates of deposit formation on several surface materials, determination of the effect of the surface material on the composition and structure at the surface/deposit interface and in the bulk of the deposit, and determination of the effects of prestressing and surface temperature on the formation of nascent deposits.

III. EXPERIMENTAL APPROACH

A. Hot Liquid Process Simulator

Experiments were performed in an Alcor model HLPS300 Hot Liquid Process Simulator (HLPS), which is a modular version of the JFTOT apparatus used for the ASTM D 3241 method. The HLPS was operated to give conditions equivalent to D 3241 requirements except that Triton-treated fuel prefilters were not used. Preparation of JFTOT tubes for carbon burnoff involved removing both of the tube end grips using a fine tooth jeweler's saw. Special care is taken not to handle the test section of the tube. After SEM evaluation, the test section is then

placed in a pre-labeled test tube and cleaned with toluene followed by n-hexane. After decanting the solvents, the test tube is placed in a vacuum oven and dried at 75°C for approximately one hour. The specimens are now ready for carbon burnoff analysis.

B. Deposit Measuring Device

The deposit measuring device (DMD) determines the thickness of a deposit on a conductive surface by applying a voltage across the deposit while measuring the dielectric breakdown of the layer at various points.⁽¹⁰⁾ The DMD used in this work was first reported in the Proceedings of the 2nd International Conference on Long-Term Storage Stabilities of Liquid Fuels.⁽¹¹⁾ The DMD voltage measurements were shown to relate thickness of deposits with 350 volts equal to 1 micrometer.⁽¹¹⁾ Methods for calculating deposit volume on JFTOT heater tubes were also discussed in Reference 11. This procedure was used to develop DMD data correlations to carbon burnoff values reported in Reference 7. Based on deposit density calculations, assuming that a density value of 1.0 to 1.5 g/cm³ is reasonable, deposit volumes greater than 0.0800 mm³ (and ranging up to 0.6365 mm³) by DMD seemed most reliable in this work. These DMD deposit volumes correspond to carbon burnoff values of 95 µg to 877 µg of carbon, respectively.

C. Single Tube Heat Exchanger

Figure 1 is a schematic description of the single tube heat exchanger (STHE). Figure 2 summarizes the thermocouple-measured fuel temperatures at various positions in the test tubes at the indicated bath temperatures. The bath set temperatures ranged from 340°C to 540°C, with actual temperatures ranging from 326°C to 519°C, respectively, as shown in Fig. 3. The points at which the bath media contact the test tube are 15.2 cm and at 86.3 cm leaving the bath. Overall length of the tube was 101.6 cm. Prior to a run, the test fuel is filtered and aerated according to the procedures outlined in ASTM D 3241 (the JFTOT test). It is then pumped through the system for 15 minutes to flush the lines of all residue from the previous run or cleanup. The pumping is done with a standard HPLC pump set to deliver 10 mL/min. The pressure in the system fluctuates (due to the pulsing action of the pump) between 800 and 950

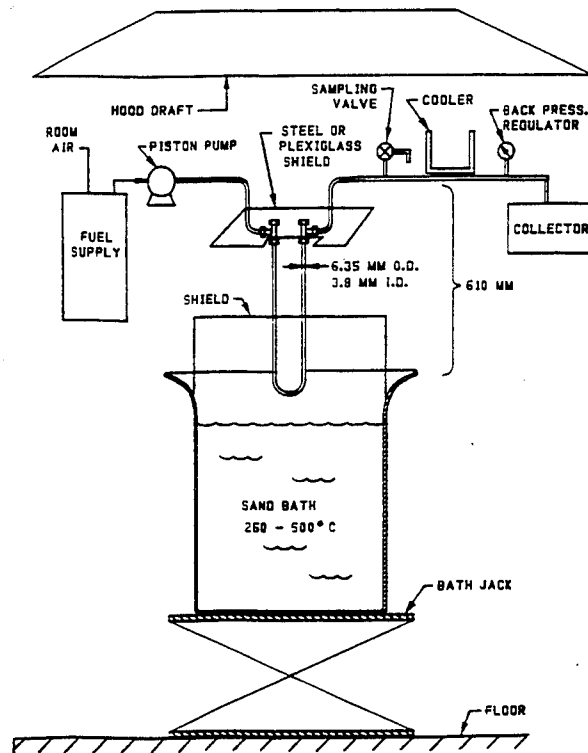


Figure 1. Schematic of Single Tube Heat Exchanger

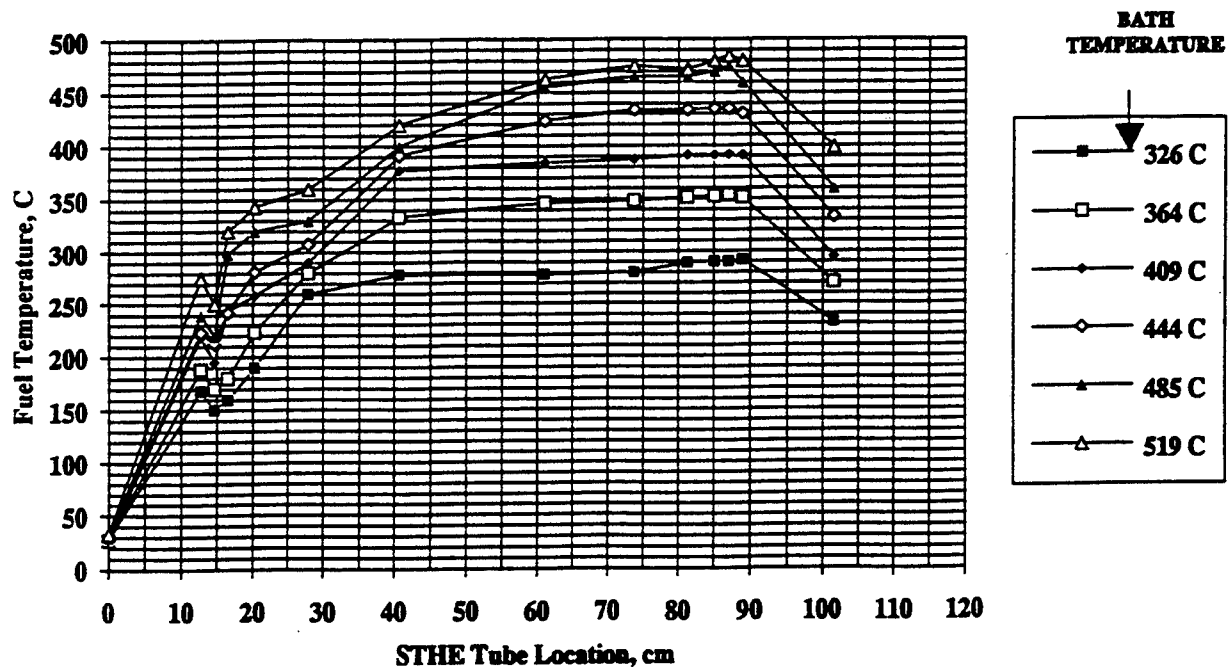


Figure 2. Fuel temperature versus location in STHE

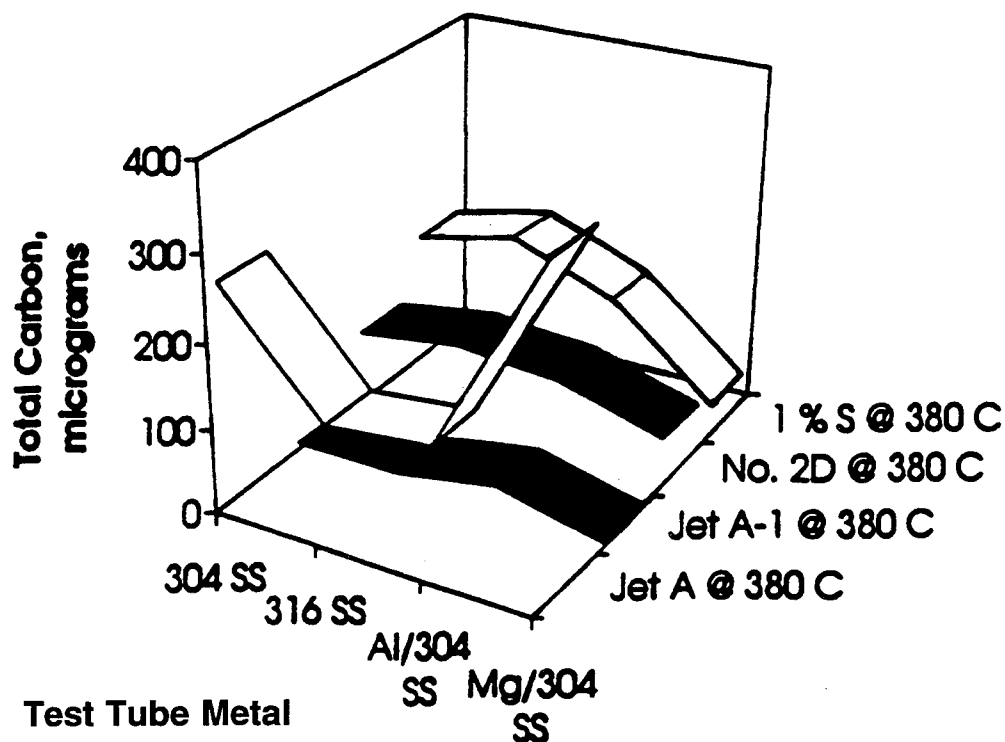


Figure 3. Carbon data for four fuels on various HLPS metal test tubes

psig with the help of a back pressure regulator. A safety pressure relief valve is set at 1000 psig. The flush is performed with no heat applied to the heat exchanger tube. Once the flush is complete, the heating bath (a Techne Fluidized Bath Model SBL-2D) is raised into position around the heat exchanger tube. This point is the beginning of the four-hour run. At this time, a zero-hour oxygen/methane analysis is made using gas chromatography. Additional oxygen/methane analyses are conducted throughout the run, once every 10 minutes for the first hour and every 30 minutes thereafter. An end-of-test analysis at ambient temperature is also made for comparison purposes. At the end of a STHE run, the heating bath is lowered away from the U-tube. Fuel is allowed to flow through the tube for approximately 10 more minutes to cool the tube. The pressure is released and the U-tube is removed from the STHE. Next, the U-tube is rinsed with heptane and air-dried. The tube is then clamped in a bench vise and straightened. The longitudinal center of the tube is marked. Measuring from the center point, marks are made at 3-inch (7.6-cm.) intervals along the entire length of the tube. Beginning at the inlet end of the tube, each marked-off section is inscribed with a letter, starting with "A" and ending with "N." The tube is cut at each of the 3-inch scribe marks using a tubing cutter. Since the tubing cutter will tend to close the openings at each end of the 3-inch sections, use a 1/4-inch

drill bit to open the holes to original diameter. The sections (B through M) are now ready for carbon burnoff analysis. TABLE 1 provides the composition of both 316 and 304 SS compared to 304 SS and 316 SS test tubes used in the STHE.

TABLE 1. Comparison of Stainless Steel Composition Requirement With STHE Test Tube Analyses

316 Stainless Steel STHE Samples

<u>Property</u>	<u>316 SS, wt%</u>	<u>STHE B-18, wt%</u>	<u>STHE B-19, wt%</u>
Sulfur	0.025, max	0.006	0.006
Phosphorous	0.025, max	0.019	0.020
Manganese	2.0, max	1.65	1.65
Silica	1.0, max	0.37	0.36
Chrome	16 to 18	17.41	17.37
Nickel	10 to 14	12.66	12.39
Molybdenum	2 to 3	2.62	2.69

304 Stainless Steel STHE Samples

<u>Property</u>	<u>304 SS, wt%</u>	<u>STHE B-39, wt%</u>	<u>STHE B-40, wt%</u>
Sulfur	0.025, max	0.026	0.027
Phosphorous	0.025, max	0.020	0.022
Manganese	2.0, max	1.68	1.67
Silica	1.0, max	0.61	0.62
Chrome	18 to 20	18.36	18.58
Nickel	8 to 12	10.04	10.07
Molybdenum	0	0.39	0.37

D. Carbon Burnoff Procedure

All analyses were conducted on Control Equipment Corporation Model 240XA Elemental Analyzer. Specially constructed quartz sample boats were used to inject the test specimen into the furnace of the analyzer. The combustion tube section of the analyzer is set at 950 to 975°C, and the reduction tube section is set at 600 to 625°C. Calibration of the instrument is conducted using squalane and n-hexadecane. Analysis time is 250 seconds. Results are reported in micrograms of carbon ($\mu\text{g C}$).

E. Test Fuels

TABLE 2 provides fuel chemical and physical properties.

TABLE 2. Chemical and Physical Properties of Test Fuels

Property	Test Method	West Coast	Jet A-1	Reference No. 2	MIL-F-46162C
		Jet A AL-19471-F	AL-19546-F	(Cat 1-H) AL-19540-F	1% Sulfur Reference Fuel w/o Additives AL-19854-F
API Gravity	D 1298	40.8	50.4	33.6	31.1
Density, kg/L	D 1298	0.8212	0.7776	0.8566	0.8698
Flash Point, °C	D 93	46	48	87	49
Cloud Point, °C	D 2500	--	--	-8	<-45
Pour Point, °C	D 97	--	--	-9	<-45
Freeze Point, °C	D 2386	-42	-57	--	--
K Vis. at 40°C, cSt	D 445	--	--	2.84	3.36
Distillation, °C	D 86				
Initial Boiling Point		153	163	208	180
10% Recovered		183	171	233	228
50% Recovered		214	181	263	274
90% Recovered		241	204	302	326
End Point		261	232	349	372
Residue, vol%		0.5	0.8	1.4	0.5
Ash, wt%	D 482	--	--	0.01	0.03
Carbon Residue, 10%					
Bottoms, wt%	D 524	--	--	0.12	0.12
Particulate Contamination, mg/L	D 2276	1.2	0.8	1.5	1.7
Accelerated Stability, mg/100 mL	D 2274	--	--	0.5	1.3
TAN, mg KOH/g	D 974	0.001	0.009	0.08	0.16
Copper Strip Corrosion	D 130	1a	1b	1a	1a
Hydrogen, wt%		13.49	--	--	12.96
Sulfur, wt%		0.04	0.008	0.39	1.02
Net Heat of Combustion					
MJ/kg	D 240	42.8	43.4	42.5	42.1
BTU/lb	D 240	18406	18671	18260	18119
Aromatics, wt%	D 1319	21.7	11.8	41.1	33.1
Cetane Number	D 613	--	--	48.6	44.5
Cetane Index	D 976	--	--	44.8	43.0
Free Water and Particulate Contamination	D 4176	Sed/Bright	Clean/Bright	Sed/Bright	Sed/Bright
Mercaptan Sulfur, wt%	D 3227	0.0004	--	--	0.2086

IV. RESULTS

The data generated using the HLPS and the STHE are summarized in Appendices A and B, respectively.

V. DISCUSSION OF RESULTS

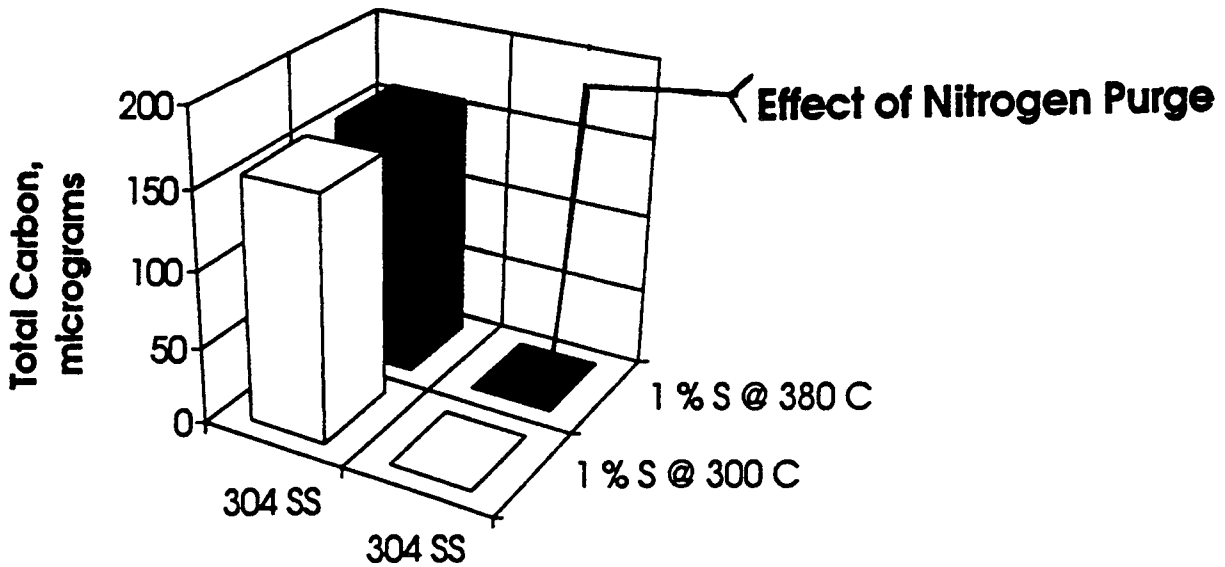
Data in Fig. 3, obtained using the HLPS at 380°C, compares the Jet A fuel with three additional fuels: a very stable Jet A-1, a Reference No. 2 D diesel, and a Referee 1% Sulfur Diesel No. 2. The test tube metallurgy included 316 SS, 304 SS aluminum plated on 304 SS, and magnesium plated on 304 SS. Note that for all the fuels except the Jet A, lower deposit levels were observed on the hot magnesium surface. Deposit levels are known to vary with fuel type and surface metallurgy.⁽¹²⁾

At both 300°C and 380°C (Fig. 4), deposit formation is dramatically reduced to essentially no deposit when the 1% Sulfur diesel fuel was purged with nitrogen as opposed to air, which showed significant deposit carbon burnoff values (also in Fig. 4).

By measuring oxygen and methane in the test fuel, sampled as it exited the reactor, oxygen was depleted at 300 to 340°C, and methane generation (indicative of pyrolysis) generally started at about 380°C, depending on the fuel type (Fig. 5). No methane was observed for the Reference No. 2 D fuel, even at the upper test temperature of 460°C.

The STHE gave more consistent and definitive results in that the three fuels reacted with all the available oxygen below a 260°C bath temperature and formed methane in the temperature range of 400 to 445°C, as shown in Fig. 6.

Deposit levels were measured as carbon burnoff values for both 304 SS and 316 SS test tubes in the STHE apparatus. This data is summarized in Fig. 7.



Test Tube Metal

Figure 4. Fuel nitrogen purge effect on deposit level on HLPS metal tubes

- Higher deposit levels were observed for Reference No. 2 D on 304 SS compared to 316 SS.
- Deposits formed by the 1% Sulfur fuel at pyrolysis temperatures on both 316 SS and 304 SS, but at higher tube locations. Deposits observed at lower tube locations in lower bath temperature experiments were not present at the higher test temperatures.
- Deposits from the Jet A-1 were significantly higher on 316 SS, especially at the higher test temperatures.

Data for particulates, summarized in Fig. 8, were measured by filtering reacted test fuel (at room temperature) through porous membrane filters having a nominal pore size of 0.8 micrometer. The particulate level tended to be lower at the higher pyrolysis temperatures, and were not formed at all for the very stable Jet A-1.

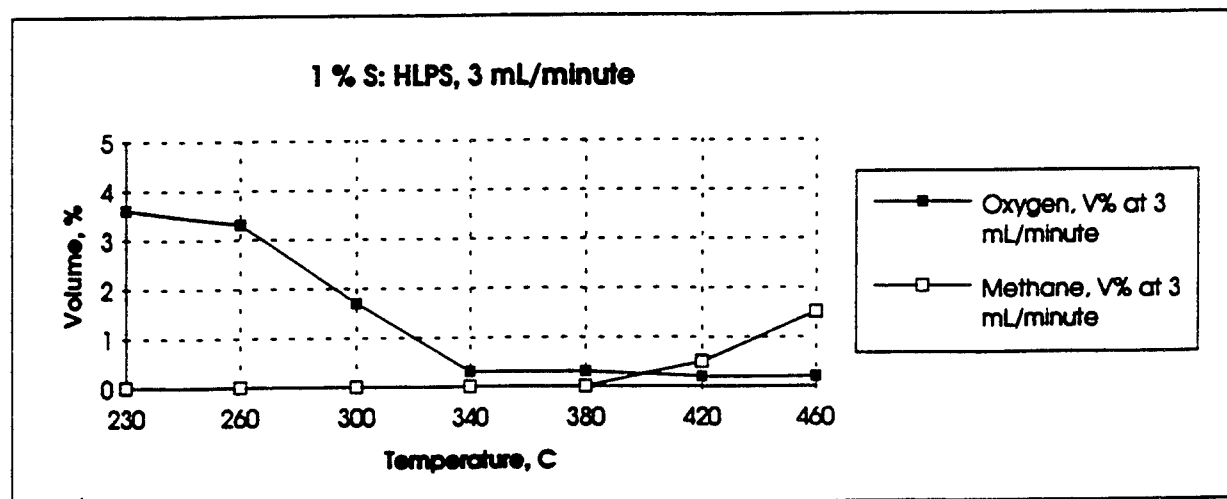
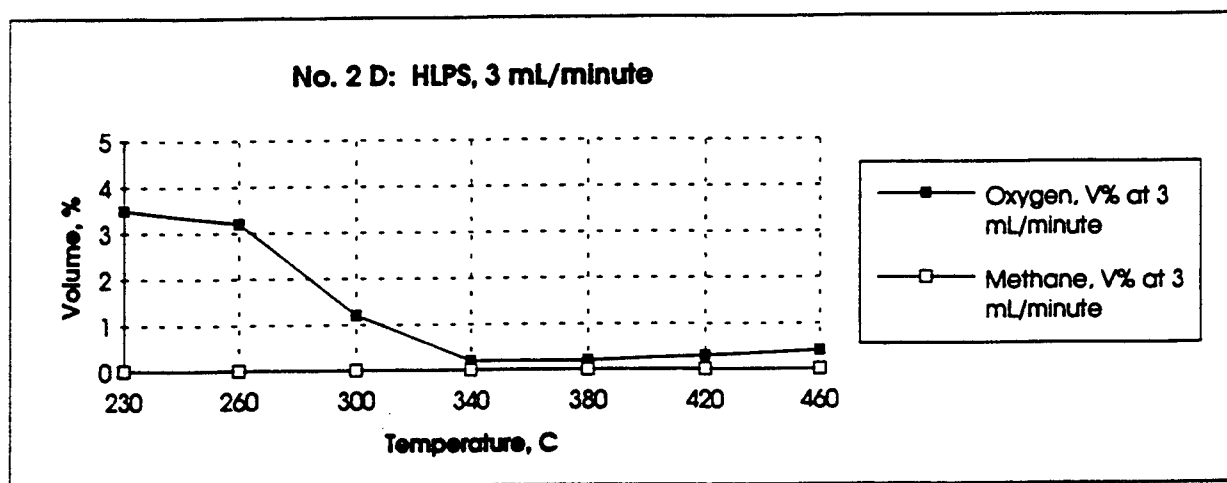
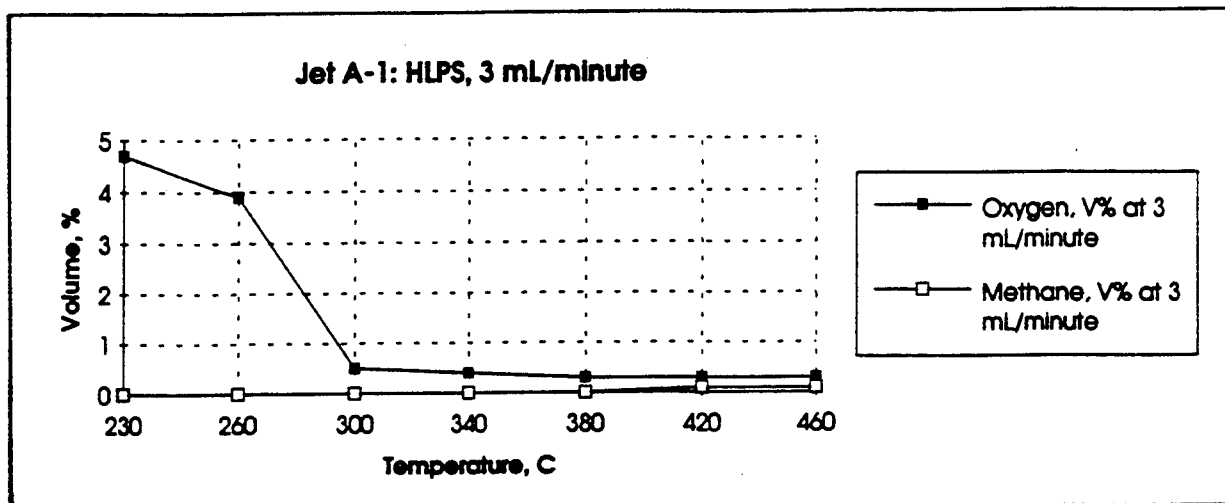


Figure 5. HLPS: Temperature effects on oxygen and methane

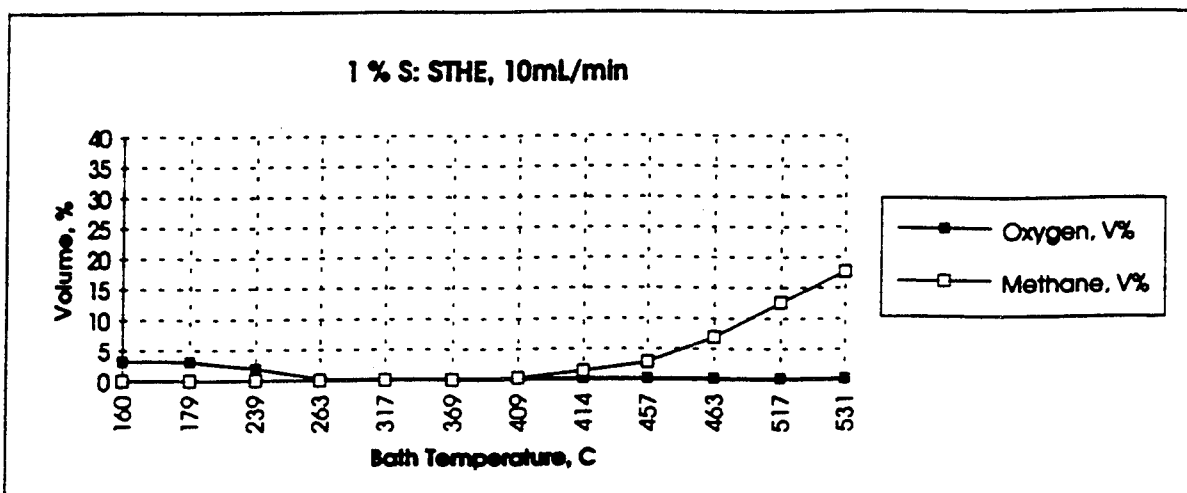
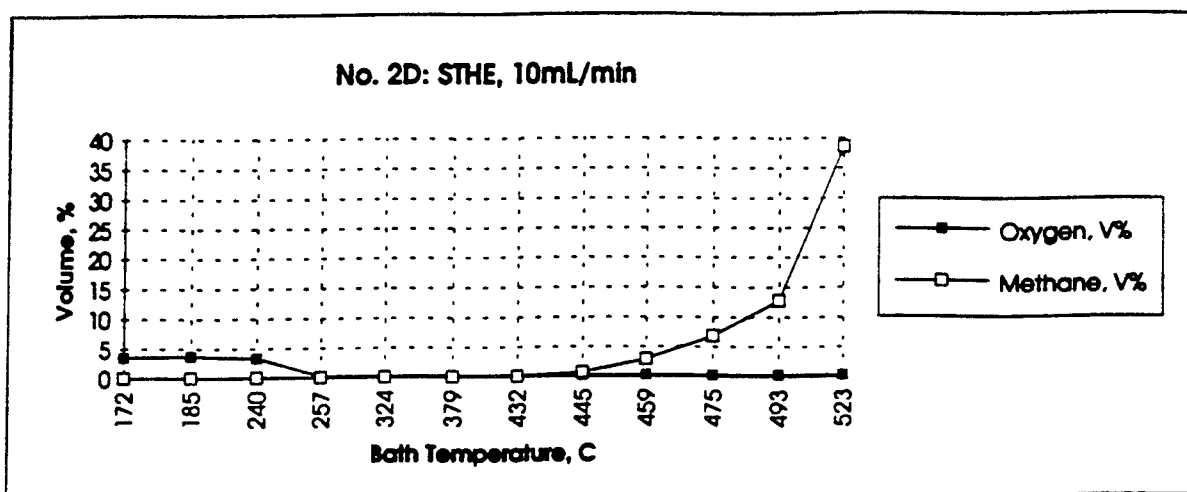
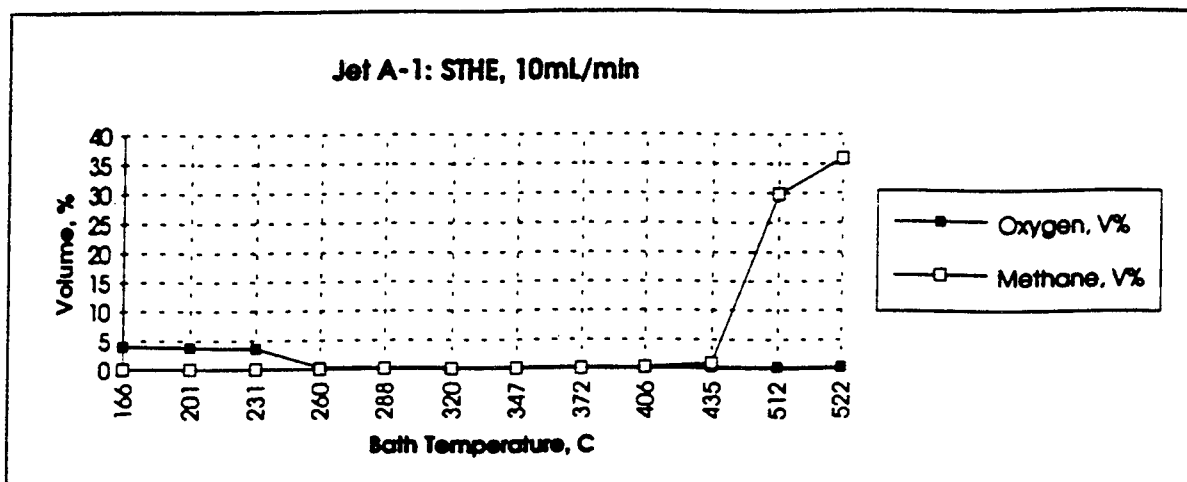


Figure 6. STHE: Temperature effects on oxygen and methane

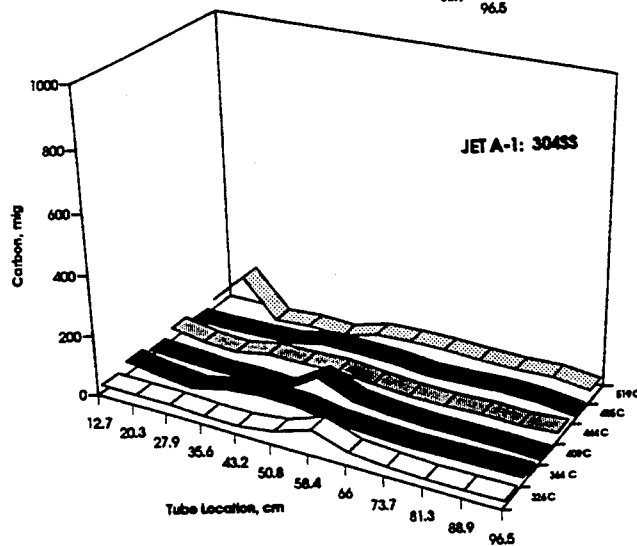
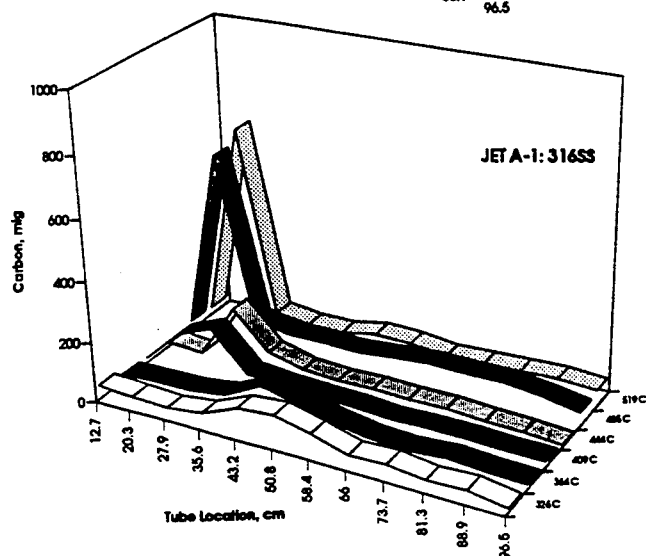
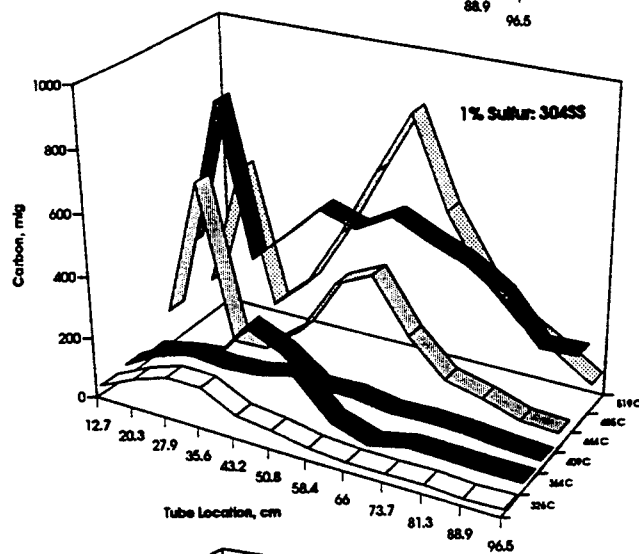
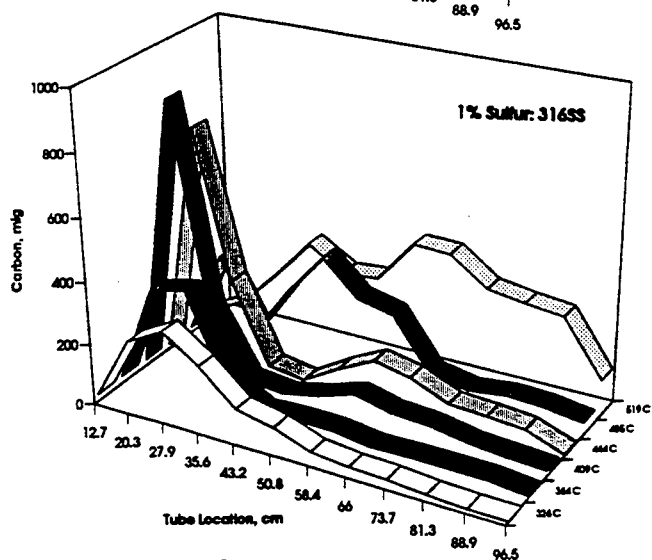
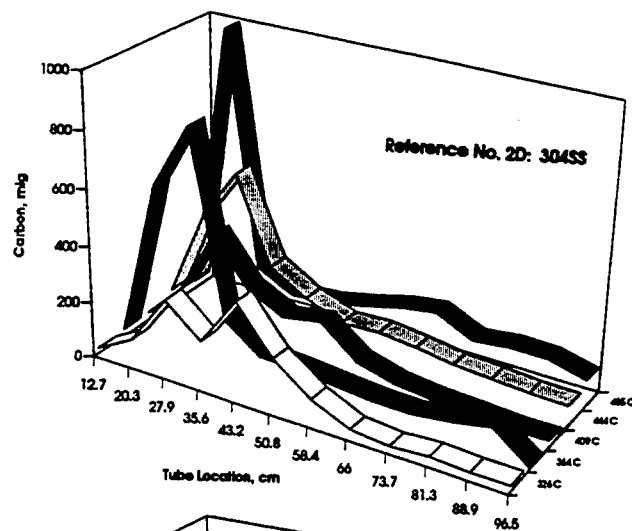
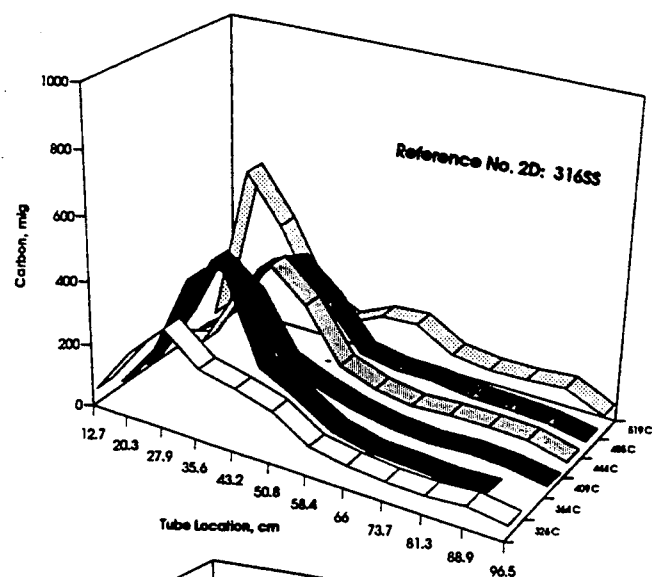


Figure 7. Carbon data for three fuels at various STHE bath temperatures

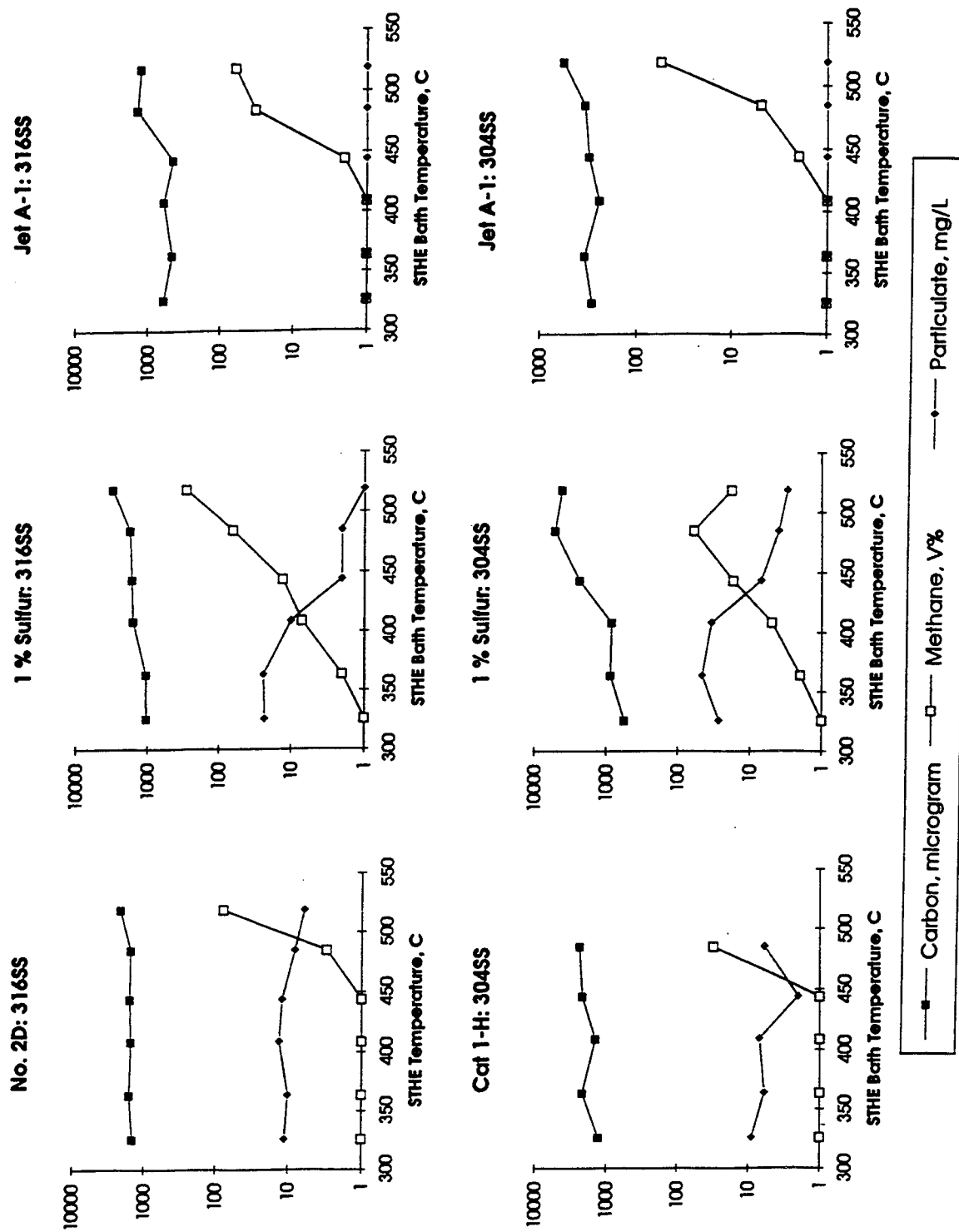


Figure 8. Fuel microparticulate levels after STHE stressing at various temperatures using 304 SS and 316 SS test tubes

When the 1% Sulfur test fuel was passed through filters of various pore sizes as the hot fuel exited the test tube, data was obtained using a 17-micrometer stainless steel filter, a 5-micrometer silver filter, and a 1.2-micrometer silver filter in separate tests (Fig. 9). While no deposits were found on the 17-micrometer filter, significant quantities were observed on both the 5- and 1.2-micrometer filters. Removal of the particulates during high temperature filtration was not reflected in the room temperature particulate values. Small size particulates formed in the fuel at high temperatures may not cause equipment distress, compared to large particles which would plug both injector filters and closely rubbing, highly loaded surfaces.

When the 1% Sulfur fuel was purged with nitrogen, deposit levels (Fig. 10) were significantly reduced from the aerated sample deposit level at 364°C.

When two test tubes were used in series, very low deposit levels were observed on the second tube using the 1% Sulfur and the Reference No. 2 D fuels. Figure 11 provides comparative data for the Reference No. 2 D fuel in both 316 SS and 304 SS test tubes, at 364 °C.

Figure 12 summarizes Arrhenius activation energy values for each of the three fuels corresponding to two sections of each test tube and the complete length of the test tube, respectively: 5.6 to 35.6 cm, 35.6 to 96.5 cm, and 5.6 to 95.6 cm. As would be expected, the values generally reflected the change in deposit quantity with temperature. Knowing that the oxygen was depleted at about 260°C, increases in deposit level with increases in temperature would not be expected to occur until pyrolysis temperatures were reached, and even then deposit levels would probably be lower as any deposit formed on the surface may subsequently pyrolyze.

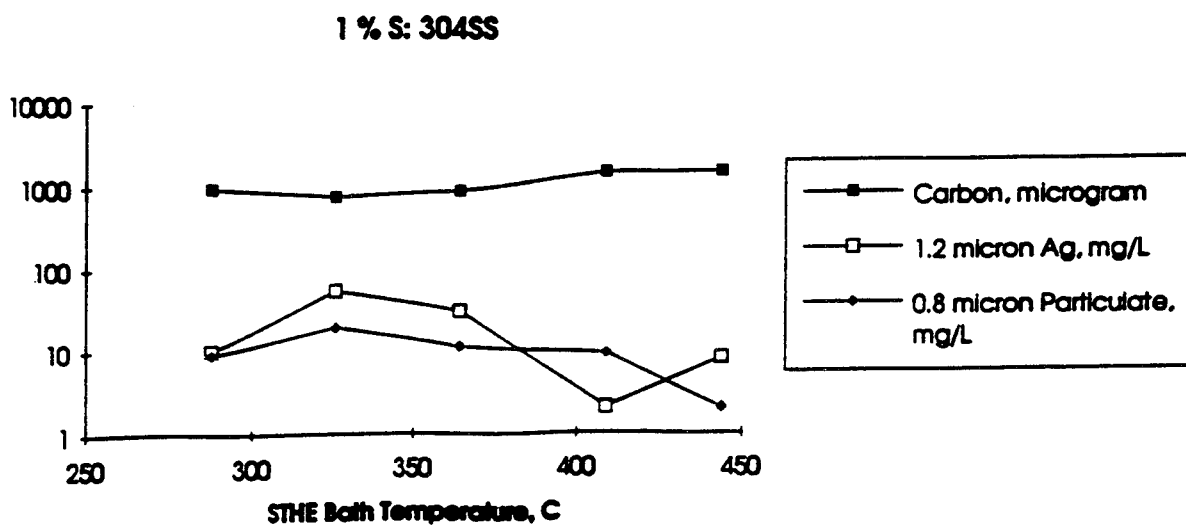
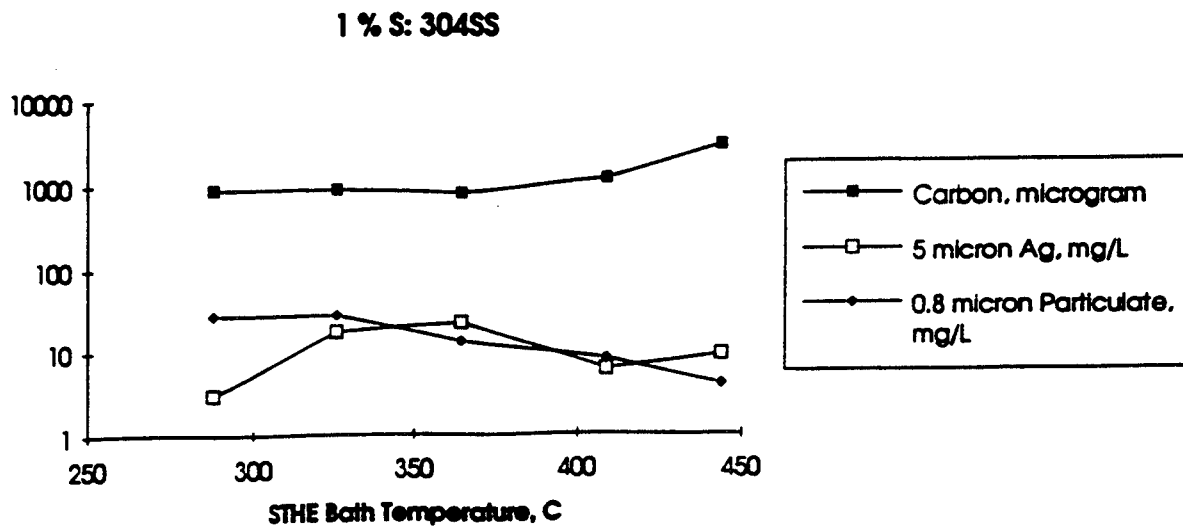
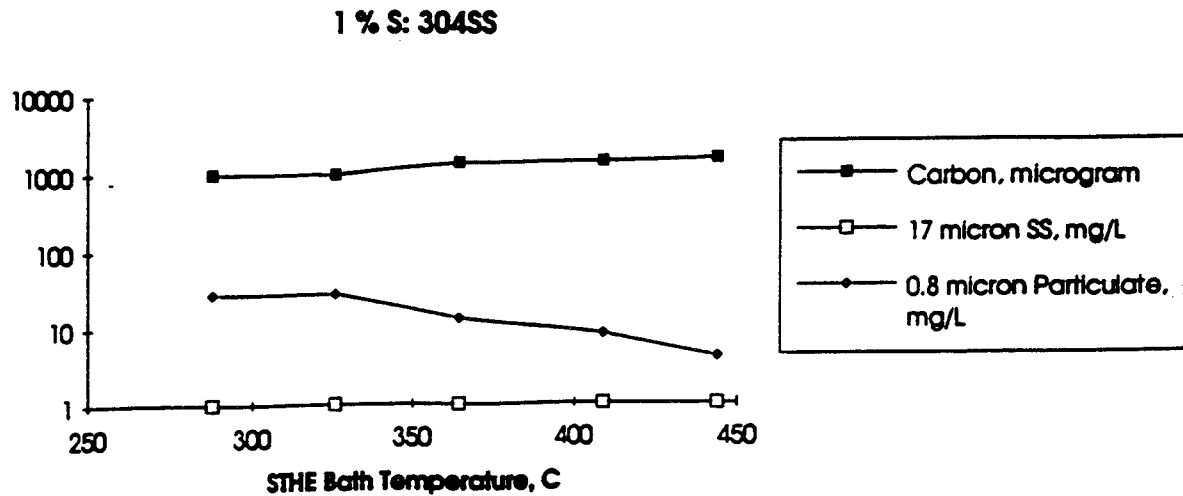


Figure 9. 1% S fuel microparticulate levels at room temperature after STHE stressing at various temperatures and flowing through in-line metal filters

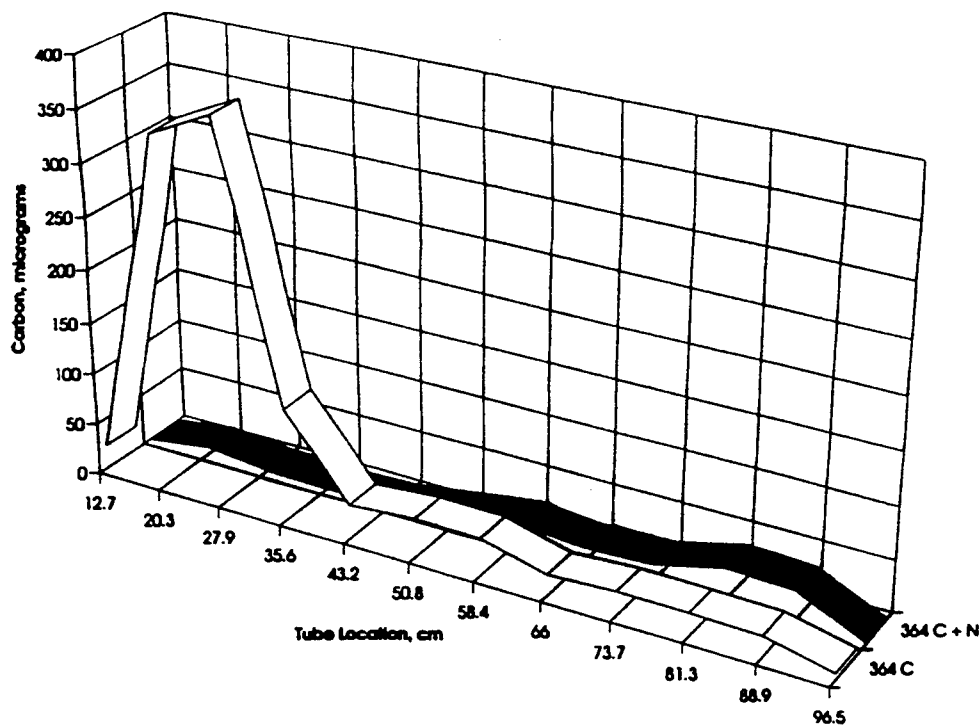


Figure 10. Nitrogen purge effect on 1% S fuel deposit level in STHE 316 SS metal tubes at 364°C

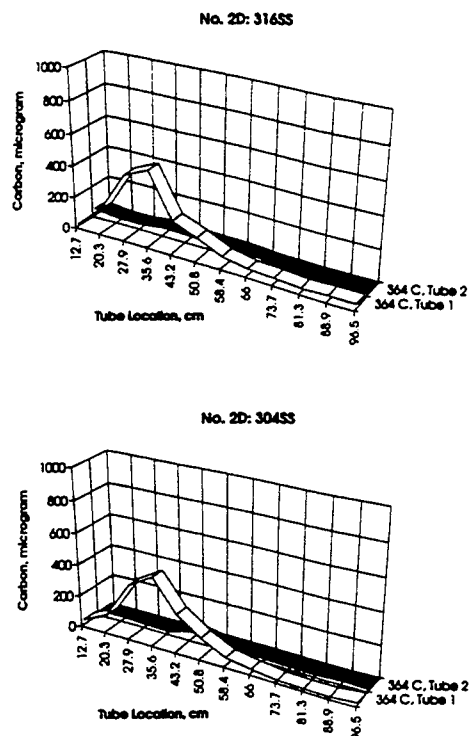


Figure 11. Reference No. 2 diesel fuel deposit level on STHE 316 SS and 304 SS serial metal tubes at 364°C

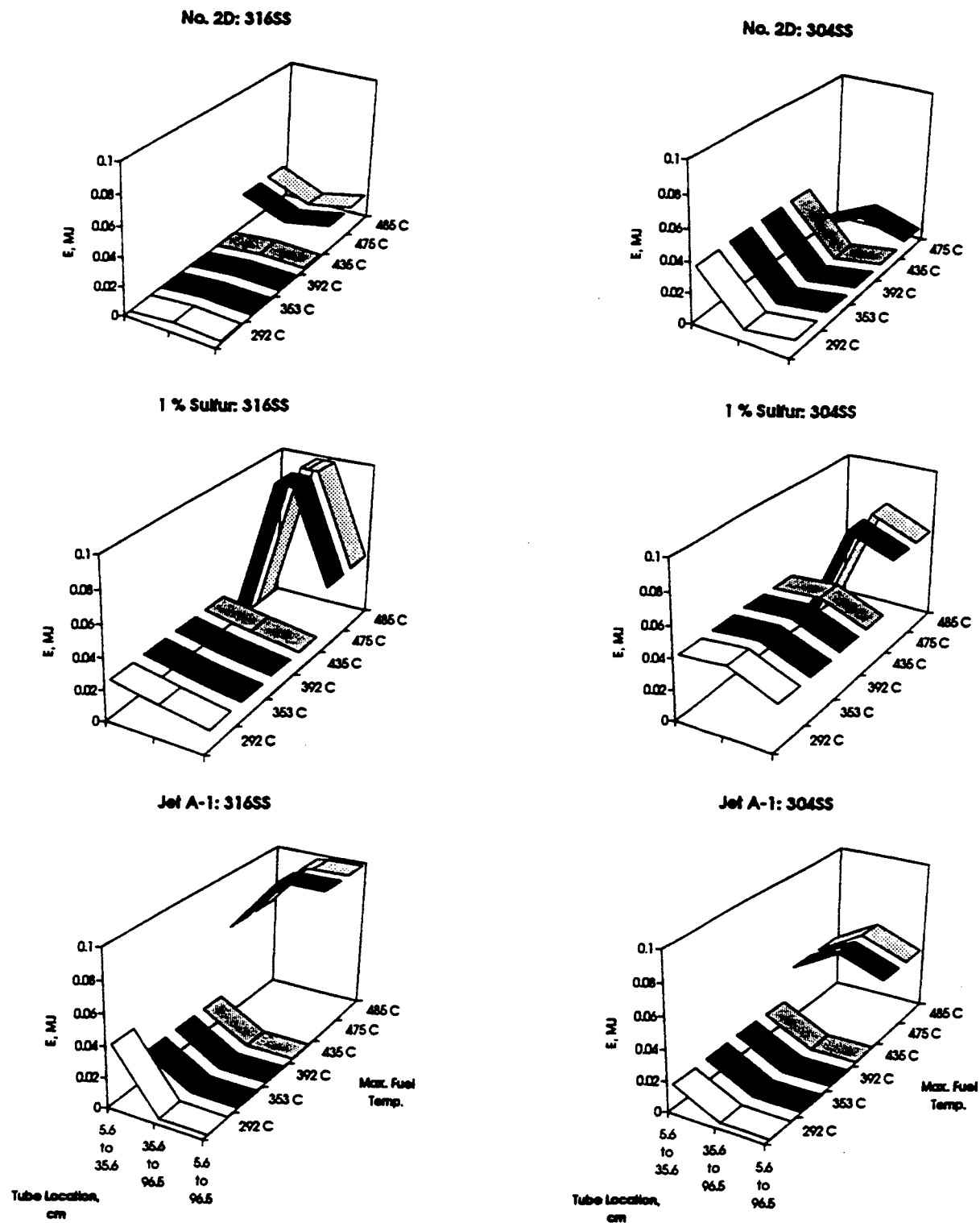


Figure 12. Arrhenius energies of activation for three fuels on 304 SS and 316 SS STHE metal tubes using carbon levels for the whole tube and two sections of the tube

VI. CONCLUSIONS

- The mechanism of deposit formation on fuel-wetted, hot metal surfaces involves thermal-oxidation reactions which are limited by the available oxygen. Different fuels contain different amounts of reactive species capable of oxidizing and subsequently agglomerating to form fuel insolubles which attach to the hot surfaces. Formation of non-deleterious thermal-oxidative products can effectively deplete the available oxygen, thus preventing deleterious oxidation. Metal surface composition effects the quantity of surface deposition, depending on fuel composition and whether the temperature is high enough for pyrolysis to occur.
- At higher pyrolysis temperatures, deposit levels are influenced by both the fuel composition and the surface composition.
- The STHE is a viable procedure for evaluating deposit formation from fuels at high temperatures.
- While the HLPS is a viable tool for evaluating the relative stability of fuels, the temperatures of the test tube are less effective than the bath temperature of the STHE, which more accurately reflects the bulk fuel temperature as it passes out of the heated section of the test tube. This is particularly true at STHE temperatures that caused fuel formation of methane, but no methane was observed at similar tube temperatures in the HLPS for at least one of the test fuels.
- Reduction of deposit can be accomplished by reducing oxygen or heat-pretreating the fuel.

VII. RECOMMENDATIONS

The Army Fuel System Design Guide in The Standard Army Refueling System (13) should address reducing the replenishment of oxygen in the fuel as this relates to the design of the tank venting system. Reduction of oxygen in fuel could reduce fuel-insoluble microparticulate, sediment, and harmful deposit formation on hot fuel handling surfaces in current and future engine systems. Quantitation of deposit reduction in adiabatic engine injectors and AGT-1500 turbine nozzles should be evaluated in vehicles with non-breathing fuel systems.

An expanded test matrix, including both tube size and test time, should be evaluated to support conclusions reached in this report related to the mechanism of deposit formation in hot-fuel flowing systems. Test fuels should include additives, especially deposit modifiers, oxidation inhibitors, and detergent/dispersants.

Fuel prestressing/cleanup systems and oxygen-reduction additives should be evaluated for eliminating thermal-oxidative deposits in hot fuel systems.

VIII. LIST OF ABBREVIATIONS

Å	Angstrom
ACS	American Chemical Society
ADMD	Automated Deposit Measuring Device
AES	Atomic Emission Spectroscopy
ASME	American Society of Mechanical Engineers
AMC	Army Material Command
ASTM	American Society for Testing and Materials
BFLRF	Belvoir Fuels and Lubricants Research Facility
BPT	Breakpoint Temperature
CRC	Coordinating Research Council
DF-2	Diesel Fuel No. 2
DMD	Deposit Measuring Device
ESCA	Electron Spectroscopy for Chemical Analysis
HLPS	Hot Liquid Process Simulator
HPLC	High Performance Liquid Chromatography
ILIR	In-House Laboratory Independent Research
ISD	Induction System Deposits
JFTOT	Jet Fuel Thermal Oxidation Tester
mL	milliliter
MTCB	Mobility Technology Center-Belvoir
ND	Not Determined
NES	Not Enough Sample
NT	Not Tested
No. 2 D	Reference No. 2 Diesel Fuel
ppb	parts per billion
psig	Pounds Per Square Inch
Ref. No. 2	Reference No. 2
S	Sulfur
SAE	Society of Automotive Engineers
SEM	Scanning Electron Microscopy
SS	Stainless Steel
STP	Special Technical Publication
STHE	Single Tube Heat Exchanger
SwRI	Southwest Research Institute
TDR	Tube Deposit Rater

IX. LIST OF REFERENCES

1. Cuellar, Jr., J.P. and Russell, J.A., "Additive Depletion and Thermal Stability Degradation of JP-5 Fuel Shipboard Samples," Report No. NAPC-PE-141C.
2. CRC Literature Survey on the Thermal Oxidation Stability of Jet Fuel, CRC Report No. 509, April 1979.
3. Uri, N., *ACS Advances in Chemistry Series*, **36**, Ch. 10, 1962, p. 102.
4. Hazell, L.B., Baker, C., David, P., and Fackereel, A.D., "An AES Depth Profiling Study of the Deposits on Aluminum During the Jet Fuel Thermal Oxidation Test," *Surface and Interface Analysis*, **1**, 1986, pp. 507-513.
5. Clark, R.H., "The Role of a Metal Deactivator in Improving the Thermal Stability of Aviation Kerosines," 3rd International Conference on Stability and Handling of Liquid Fuels, London, UK, 13-16 September 1988.
6. Schreifels, J.A., Morris, R.E., Turner, N.H., and Mowery, R.L., "The Interaction of a Metal Deactivator With Metal Surfaces," *American Chemical Society, Division of Fuel Chemistry, Preprints*, **35**, No. 2, 22-27 April 1990, pp. 555-562.
7. Morris, R.E. and Hazlett, R.N., "Methods for Quantifying JFTOT Heater Tube Deposits Produced From Jet Fuels," *Energy & Fuels*, **3**, No. 2, 1989, pp. 263-267.
8. ASTM Thermal Oxidation Stability of Aviation Turbine Fuels (JFTOT Procedure), in Annual Book of ASTM Standards, ASTM, Philadelphia, PA, 1989; Part 5.02, ASTM D 3241-88a.
9. Stavinocha, L.L., Westbrook, S.R., Naegeli, D.W., and Lestz, S.J., "Quantitation of Fuel Deposition on Hot Metal Surfaces," Proceedings of 4th International Conference on Stability and Handling of Liquid Fuels, Orlando, FL, 19-22 November 1991, pp. 272-286, edited by H.N. Giles, published by U.S. Department of Energy, Washington, D.C.
10. U.S. Patent No. 4,791,811, "Deposit Thickness Measurement," J.G. Barbee, Southwest Research Institute, Granted December 20, 1988.
11. Stavinocha, L.L., Barbee, J.G., and Buckingham, J.P., "Thermal Stability Deposit Measuring Device," Proceedings of 2nd International Conference on Long-Term Storage Stabilities of Liquid Fuels, San Antonio, TX, 29 July-August 1986.
12. Hazlett, Robert N., "Thermal Stability of Aviation Turbine Fuels," Monograph 1, December 1991, *American Society for Testing and Materials*, Philadelphia, PA.

13. Research, Development, and Acquisition Implementation of the Standard Army Refueling System, AMC Regulation No. 70-17, 20 July 1989, DOA, Hdq. U.S. Army Materiel Command, 5001 Eisenhower Avenue, Alexandria, VA 22333.
14. Strauss, K.H., "Thermal Stability Specification Testing of Jet Fuel - A Critical Review," SAE Paper No. 881532, 1988.
15. Schirmer, R.M., "Morphology of Deposits in Aircraft and Engine Fuel Systems," SAE Paper No. 700258, presented at the National Air Transportation Meeting, New York, NY, April 1970.

APPENDIX A

Summary of Hot Liquid Process Simulator (HLPS) Data

**TABLE A-1. Summary of Deposit Measuring Device (DMD) and Carbon Burnoff Evaluation
of JFTOT Tubes Along With Standard ASTM D 3241 Ratings**

D 3241 Ratings												
Test Fuel	Test No.	Date	Tube Metal	Test Temp., °C	Test Time, hr.	Pressure		Visual Rating	Max. Thickness, DMD, at Station, micrometers	Volume of Deposit, DMD, cubic mm	Total Carbon, micrograms	Calculated Density, g/cc
						Drop, mm of Hg. in min.	Max. TDR at Station No.					
AL-19471-F West Coast Jet A	280-H	08/01/90	304 SS	300	1.5	125	in 84.5	50+ at 46-58	>4 P ⁽¹⁾	0.977 at 56	289	3.2
	281-H	08/02/90	304 SS	300	1.5	125	in 62.9	50+ at 45-58	>4 P	0.617 at 54	223	3.2
	282-H	08/03/90	304 SS	340	1.5	125	in 48.3	50+ at 34-48	>4	1.745 at 42	206	1.3
	283-H	08/07/90	304 SS	340	1.5	125	in 44.3	50+ at 32-48	>4 P	2.031 at 40	283	1.4
	284-H	08/08/90	304 SS	380	1.5	125	in 39.5	50+ at 32-48	>4 P	2.080 at 32	271	1.4
	285-H	08/09/90	304 SS	380	1.5	125	in 34.9	50+ at 26-40	>4 P	2.028 at 34	249	1.3
	276-T	11/02/90	304 SS	380	1.5	125	in 59.4	50+ at 24-36	>4	1.882 at 30	217	1.4
	287-H	08/30/90	304 SS	420	1.5	125	in 59.4	50+ at 18-34	>4 P	2.120 at 24	334	1.8
	290-H	10/08/90	304 SS	420	1.5	125	in 59.1	50+ at 20-48	>4	1.780 at 26	289	2.1
	288-H	09/26/90	304 SS	460	1.5	125	in 37.0	50+ at 14-58	>4 P	1.928 at 20	326	1.9
	289-H	10/05/90	304 SS	460	1.5	125	in 47.4	50+ at 14-54	>4 P	2.100 at 20	205	1.5
	304-H	10/29/91	Al	300	1.5	125	in 80.5	38 at 42	4 P	0.700 at 38	NT ⁽⁴⁾	NT
	299-H	10/11/91	316 SS	300	1.5	125	in 47.8	50+ at 50-58	>4 P	2.142 at 54	201	1.1
	300-H	10/16/91	316 SS	380	1.5	125	in 46.5	50+ at 30-58	>4 P	1.548 at 34	131	0.8
	263-H	08/21/89	Al/304 SS	300	1.5	125	in 56.0	36 at 54	4 P	1.168 at 52	52	0.4
	273-H	09/13/89	Al/304 SS	380	1.5	125	in 48.1	50+ at 32-36	>4 P	1.805 at 34	143	0.9
	266-H	08/24/89	Mg/304 SS	300	1.5	125	in 52.1	Too Dark ⁽³⁾	4	1.082 at 54	118	0.5
	275-H	09/18/89	Mg/304 SS	380	1.5	125	in 58.3	Too Dark ⁽³⁾	>4	1.237 at 36	376	2.1
AL-19540-F Reference No. 2 Fuel	271-T	10/09/90	304 SS	300	1.5	125	in 34.3	50+ at 42-58	>4 P	1.011 at 50	364	3.1
	70-B	10/24/90	304 SS	340	1.5	125	in 31.7	50+ at 28-58	>4 P	2.188 at 34	210	1.3
	274-T ⁽²⁾	10/18/91	304 SS	340	1.5	125	in 19.9	50+ at 32-46	>4 P	1.842 at 38	157	1.1
	275-T	10/22/90	304 SS	380	1.5	125	in 33.5	50+ at 24-34	>4	1.702 at 30	216	1.7
	71-B	10/24/90	304 SS	380	1.5	125	in 38.5	50+ at 12-28	>4	1.548 at 16	170	1.5
	329-H	03/05/92	304 SS	380	1.5	125	in 23.5	48 at 32-40	>4 P	0.508 at 32	92	1.1
	330-H	03/09/92	304 SS	380	1.5	125	in 27.2	49 at 32-40	>4 P	0.711 at 30	87	1.1
	272-T	10/15/90	304 SS	340	2.5	125	in 30.6	50+ at 32-58	>4 P	2.648 at 36	424	1.7
	273-T	10/16/90	304 SS	340	3.5	125	in 28.1	50+ at 30-52	>4 P	2.871 at 36	655	1.9
	72-B	11/01/90	304 SS	380	3.5	125	in 35.6	50+ at 22-58	>4	3.037 at 28	570	1.7
	305-H	10/30/91	Al	300	1.5	125	in 14.1	33 at 40	>4 P	0.337 at 36	NT	NT

(1) P = Peacock

(2) 4X tube holder

(3) TDR cannot discriminate between dark gray color of tube and tube deposits.

(4) NT = Not Tested

**TABLE A-1. Summary of Deposit Measuring Device (DMD) and Carbon Burnoff Evaluation
of JFTOT Tubes Along With Standard ASTM D 3241 Ratings (Cont'd)**

D 3241 Ratings												
Test Fuel	Test No.	Date	Tube Metal	Test Temp., °C	Test Time, hr.	Pressure		Visual Rating	Max. Thickness, DMD, at Station, micrometers	Volume of Deposit, DMD, cubic mm	Total Carbon, micrograms	Calculated Density, g/cc
						Drop, mm of Hg, in min.	Max. TDR at Station No.					
AL-15542-F 1 wt% sulfur w/o additives (Drum 8 of 12)	301-H	10/17/91	316 SS	300	1.5	125 in 11.9	42 at 52	>4 P (1)	0.674 at 52	0.0472	59	1.2
	302-H	10/18/91	316 SS	380	1.5	125 in 26.0	49 at 50	>4 P	0.520 at 32	0.0689	95	1.4
	326-H	02/27/92	316 SS	380	1.5	125 in 22.8	50+ at 48-56	>4 P	1.142 at 30	0.0965	115	1.2
	327-H	03/02/92	316 SS	380	1.5	125 in 25.1	50+ at 48-56	>4 P	0.568 at 32	0.0851	110	1.3
	310-H	12/05/91	Al/304 SS	300	1.5	125 in 12.0	44 at 50	4 P	0.302 at 50	0.0372	35	0.9
	315-H	12/27/91	Al/304 SS	380	1.5	125 in 29.0	50+ at 26-28	>4 P	0.457 at 32	0.0408	91	2.2
	324-H	02/20/92	Al/304 SS	380	1.5	125 in 28.0	47 at 32-42	>4 P	0.482 at 30	0.0581	100	1.7
	316-H	01/03/92	Mg/304 SS	300	1.5	125 in 12.5	Too Dark (3)	4 P	0.137 at 50	0.0193	29	1.5
	319-H	01/15/92	Mg/304 SS	380	1.5	125 in 27.9	Too Dark (3)	>4 P	0.602 at 34	0.0909	61	0.7
	322-H	02/18/92	Mg/304 SS	380	1.5	125 in 34.1	Too Dark (3)	>4 P	0.408 at 32	0.0593	57	1.1
	284-T	05/20/91	304 SS	300	1.5	125 in 12.1	50+ at 44-50	4 P	2.117 at 40	0.2588	325	1.3
	336-H (5)	05/14/92	304 SS	300	1.5	23.6 in 90	37 at 52	3	<0.050	<0.0050	0	0
	285-T	05/21/91	304 SS	340	1.5	125 in 20.2	50+ at 26-42	>4 P	1.851 at 34	0.1817	299	1.6
	286-T	05/21/91	304 SS	380	1.5	125 in 19.9	50+ at 22-54	>4 P	2.574 at 24	0.2356	302	1.3
	331-H	03/10/92	304 SS	380	1.5	125 in 66.5	50+ at 22-52	>4 P	1.905 at 28	0.1562	158	1.2
	337-H (5)	05/22/92	304 SS	380	1.5	18.5 in 90	50 at 48-52	4	<0.050	<0.0050	0	0
	291-T	10/24/91	304 SS	340	2.5	125 in 93.6	50+ at 24-54	>4 P	2.748 at 30	0.2729	380	1.4
	292-T	10/25/91	304 SS	340	3.5	125 in 93.4	50+ at 24-54	>4 P	3.851 at 32	0.3487	554	1.6
	294-T	10/31/91	304 SS	380	3.5	125 in 135.3	50+ at 22-54	>4 P	3.991 at 26	0.3679	615	1.7
	307-H	11/08/91	Al	300	1.5	125 in 51.5	50+ at 32-36	>4 P	1.305 at 34	0.1295	NT (4)	NT
	297-H	10/09/91	316 SS	300	1.5	125 in 26.1	50+ at 44-58	>4 P	0.788 at 48	0.1077	174	1.6
	298-H	10/10/91	316 SS	380	1.5	83.5 in 90	50+ at 26-54	>4 P	2.208 at 30	0.1709	191	1.1
	328-H	03/04/92	316 SS	380	1.5	125 in 54.5	50+ at 24-34	>4 P	1.965 at 28	0.1539	179	1.2
	311-H	12/10/91	Al/304 SS	300	1.5	125 in 33.2	50+ at 46-50	4 P	0.911 at 46	0.0894	96	1.1
312-H	12/10/91	Al/304 SS	380	1.5	125 in 53.7	50+ at 26-34	>4 P	1.388 at 28	0.1036	132	1.3	
325-H	02/21/92	Al/304 SS	380	1.5	125 in 57.5	50+ at 26-32	>4 P	1.694 at 30	0.1167	143	1.2	
317-H	01/06/92	Mg/304 SS	300	1.5	125 in 15.0	Too Dark (3)	4 P	0.311 at 46	0.0502	20	0.4	
318-H	01/07/92	Mg/304 SS	380	1.5	125 in 56.3	Too Dark (3)	>4	0.388 at 30	0.0494	21	0.4	
323-H	02/19/92	Mg/304 SS	380	1.5	125 in 41.2	Too Dark (3)	>4 P	0.545 at 28	0.0454	53	1.2	

(1) P = Peacock

(2) 4X tube holder

(3) TDR cannot discriminate between dark gray color of tube and tube deposits.

(4) NT = Not Tested

(5) Fuel is nitrogen purged before test.

TABLE A-1. Summary of Deposit Measuring Device (DMD) and Carbon Burnoff Evaluation of JFTOT Tubes Along With Standard ASTM D 3241 Ratings (Cont'd)

Test Fuel	Test No.	Date	Tube Metal	Test Temp., °C	Test Time, hr.	Pressure		Max. TDR at Station No.	Visual Rating	Max. Thickness, DMD, at Station, micrometers	Volume of Deposit, DMD, cubic mm	Total Carbon, micrograms	Calculated Density, g/cc
						Drop, mm of Hg, in min.	Drop, mm of Hg, in min.						
AL-19554-F Jet A-1, w/o Additives	292-H	06/07/91	304 SS	300	1.5	3.6	in 90	30 at 54	3	<0.050	<0.005	NT (4)	NT
	293-H	06/10/91	304 SS	340	1.5	8.3	in 90	38 at 50	>4 P (1)	0.228 at 48	0.0168	NT	NT
	294-H	06/11/91	304 SS	380	1.5	12.2	in 90	49 at 52	>4 P	0.271 at 38	0.019	NT	NT
	290-T	10/23/91	304 SS	340	2.5	0		38 at 46	4	<0.050	0.009	7	0.8
	293-T	10/29/91	304 SS	340	3.5	56	in 210	46 at 50	4	0.051 at 50	0.0063	0	0
	300-T	11/27/91	304 SS	380	3.5	27	in 210	44 at 42	>4 P	0.091 at 34	0.0125	21	1.7
	314-H	12/17/91	304 SS	380	3.5	4.5	in 210	47 at 32-42	4	0.228 at 30	0.0174	11	0.6
	334-H	03/18/92	304 SS	380	3.5	2.7	in 210	42 at 38	4	0.205 at 30	0.0217	5	0.2
	308-H	11/15/91	304 SS	420	1.5	4.0	in 90	37 at 32	3	<0.050	0.0055	0	0
	309-H	11/18/91	304 SS	460	1.5	4.0	in 90	32 at 46	3	0.122 at 46	0.0113	0	0
	306-H	11/04/91	Al	300	1.5	3.5	in 90	7 at 40	2	<0.050	<0.005	NT	NT
	295-H	10/08/91	316 SS	300	1.5	3.2	in 90	24 at 50-58	3	<0.050	<0.005	0	0
	296-H	10/08/91	316 SS	380	1.5	3.2	in 90	41 at 50	4	<0.050	<0.005	0	0
	321-H	02/12/92	316 SS	380	3.5	3.3	in 210	49 at 50	4	0.248 at 30	0.0171	0	0
	333-H	03/17/92	316 SS	380	3.5	3.7	in 210	50+ at 44-56	4	0.188 at 30	0.0188	18	0.9
	313-H	12/12/91	Al/304 SS	380	3.5	5.3	in 210	47 at 32	>4	0.477 at 30	0.0293	30	1.1
	332-H	03/11/92	Al/304 SS	380	3.5	11.9	in 210	44 at 34	4	0.085 at 38	0.0106	29	2.7
	320-H	01/22/92	Mg/304 SS	380	3.5	4.1	in 210	Too Dark (3)	3	0.408 at 36	0.0674	0	0
	335-H	03/31/92	Mg/304 SS	380	3.5	3.2	in 210	Too Dark (3)	3	0.525 at 50	0.0754	2	0
	302-T	01/30/92	Al	355	5.0	0		50+ at 26-32	>4	0.648 at 26	0.0296	NT	NT
	308-T	05/21/92	Al	300	5.0	0		27 at 40	3 P	<0.050	<0.005	NT	NT

(1) P = Peacock

(2) 4X tube holder

(3) TDR cannot discriminate between dark gray color of tube and tube deposits.

(4) NT = Not Tested

TABLE A-2. Summary of Duplicate Evaluations of Deposit Measuring Device (DMD) and Carbon Burnoff of JFTOT Tubes Along With Standard ASTM D 3241 Ratings

D 3241 Ratings													
Test Fuel	Test No.	Date	Tube Metal	Test Temp., °C	Test Time, hr.	Pressure		Visual Rating	Max. Thickness, DMD, at Station, micrometers	Volume of Deposit, DMD, cubic mm	Total Carbon, micrograms	Calculated Density, g/cc	
						Drop, mm of Hg. in min.	Max. TDR at Station No.						
AL-19540-F Reference No. 2 Fuel	329-H	03/05/92	304 SS	380	1.5	125 in 23.5	48 at 32-40	>4 P (1)	0.508 at 32	0.0825	92	1.1	
	330-H	03/09/92	304 SS	380	1.5	125 in 27.2	49 at 32-40	>4 P	0.711 at 30	0.0909	87	1.1	
	326-H	02/27/92	316 SS	380	1.5	125 in 22.8	50+ at 48-56	>4 P	1.142 at 30	0.0965	115	1.2	
	327-H	03/02/92	316 SS	380	1.5	125 in 25.1	50+ at 48-54	>4 P	0.568 at 32	0.0851	110	1.3	
	315-H	12/27/91	Al/304 SS	380	1.5	125 in 29.0	50+ at 26-28	>4 P	0.457 at 32	0.0408	91	2.2	
	324-H	02/20/92	Al/304 SS	380	1.5	125 in 28.0	47 at 32-42	>4 P	0.482 at 30	0.0581	100	1.7	
	319-H	01/15/92	Mg/304 SS	380	1.5	125 in 27.9	Too Dark (2)	>4 P	0.602 at 34	0.0909	61	0.7	
	322-H	02/18/92	Mg/304 SS	380	1.5	125 in 34.1	Too Dark (2)	>4 P	0.408 at 32	0.0593	57	1.1	
	275-T	10/22/90	304 SS	380	1.5	125 in 33.5	50+ at 24-34	>4	1.702 at 30	0.1279	216	1.7	
	71-B	10/24/90	304 SS	380	1.5	125 in 38.5	50+ at 12-28	>4	1.548 at 16	0.1106	170	1.1	
	AL-15542-F 1 wt% sulfur w/o additives (Drum 8 of 12)	286-T	05/21/91	304 SS	380	1.5	125 in 19.9	50+ at 22-54	>4 P	2.574 at 24	0.2356	302	1.3
331-H		03/10/92	304 SS	380	1.5	125 in 66.5	50+ at 22-52	>4 P	1.905 at 28	0.1562	158	1.1	
298-H		10/10/91	316 SS	380	1.5	83.5 in 90	50+ at 26-54	>4 P	2.208 at 30	0.1709	191	1.1	
328-H		03/04/92	316 SS	380	1.5	125 in 54.5	50+ at 24-34	>4 P	1.965 at 28	0.1539	179	1.2	
312-H		12/10/91	Al/304 SS	380	1.5	125 in 53.7	50+ at 26-34	>4 P	1.388 at 28	0.1036	132	1.3	
325-H		02/21/92	Al/304 SS	380	1.5	125 in 57.5	50+ at 26-32	>4 P	1.694 at 30	0.1167	143	1.2	
318-H		01/07/92	Mg/304 SS	380	1.5	125 in 56.3	Too Dark (2)	>4	0.388 at 30	0.0494	21	0.4	
323-H		02/19/92	Mg/304 SS	380	1.5	125 in 41.2	Too Dark (2)	>4 P	0.545 at 28	0.0454	53	1.2	
AL-19554-F Jet A-1, w/o Additives		314-H	12/17/91	304 SS	380	3.5	4.5 in 210	47 at 32-42	4	0.228 at 30	0.0174	11	0.6
		334-H	03/18/92	304 SS	380	3.5	2.7 in 210	42 at 48	4	0.205 at 30	0.0217	5	0.2
		321-H	02/12/92	316 SS	380	3.5	3.3 in 210	49 at 50	4	0.248 at 30	0.0171	0	0
	333-H	03/18/92	316 SS	380	3.5	3.7 in 210	50+ at 44-56	4	0.188 at 30	0.0188	18	0.9	
	313-H	12/12/91	Al/304 SS	380	3.5	5.3 in 210	47 at 32	>4	0.477 at 30	0.0293	30	1	
	332-H	03/11/92	Al/304 SS	380	3.5	11.9 in 210	44 at 34	4	0.085 at 38	0.0106	29	2.7	
	320-H	01/22/92	Mg/304 SS	380	3.5	4.1 in 210	Too Dark (2)	3	0.408 at 36	0.0674	0	0	
335-H	03/31/92	Mg/304 SS	380	3.5	3.2 in 210	Too Dark (2)	3	0.525 at 50	0.0754	2	0		

(1) P = Peacock

(2) TDR cannot discriminate between dark gray color of tube and tube deposits.

TABLE A-3. Hot Liquid Process Simulator (HLPS) Average Oxygen/Methane Data at Standard Fuel Flow of 3.0 mL/min

Temperature, °C	AL-19554-F (Jet A-1)		AL-19540-F (Cat 1-H)		AL-19854-F (1 wt% S)	
	Oxygen, Avg., vol%	Methane, Avg., vol%	Oxygen, Avg., vol%	Methane, Avg., vol%	Oxygen, Avg., vol%	Methane, Avg., vol%
230	4.7	0	3.5	0	3.6	0
260	3.9	0	3.2	0	3.3	0
300	0.5	0	1.2	0	1.7	0
340	0.4	0	0.2	0	0.3	0
380	0.3	0	0.2	0	0.3	0
420	0.3	0.1	0.3	0	0.2	0.5
460	0.3	0.1	0.4	0	0.2	1.5

TABLE A-4. Hot Liquid Process Simulator (HLPS) Average Oxygen/Methane Data at Fuel Flow of 1.5 mL/min

Temperature, °C	AL-19554-F (Jet A-1)		AL-19540-F (Cat 1-H)		AL-19854-F (1 wt% S)	
	Oxygen, Avg., vol%	Methane, Avg., vol%	Oxygen, Avg., vol%	Methane, Avg., vol%	Oxygen, Avg., vol%	Methane, Avg., vol%
230	3.5	0	2.6	0	2.8	0
260	3.9	0	1.5	0	0.8	0
300	0.7	0	2.5	0	0.5	0
340	0.7	0	0.5	0	0.4	0
380	0.6	0.3	0.4	0	0.4	0
420	0.7	0.5	0.4	0	0.2	1.2
460	0.5	0.7	0.3	0	0.3	4.2

TABLE A-5. Hot Liquid Process Simulator (HLPS) Average Oxygen/Methane Data at Fuel Flow of 4.5 mL/min

Temperature, °C	AL-19554-F (Jet A-1)		AL-19540-F (Cat 1-H)		AL-19854-F (1 wt% S)	
	Oxygen, Avg., vol%	Methane, Avg., vol%	Oxygen, Avg., vol%	Methane, Avg., vol%	Oxygen, Avg., vol%	Methane, Avg., vol%
260	2.1	0	2.7	0	3.5	0
300	0.3	0	1.4	0	2.8	0
340	0.3	0	0.2	0	1.0	0
380	0.3	0.1	0.2	0	0.3	0
420	0.3	0.5	0.2	0	0.2	0
460	0.3	0.6	0.2	0	0.2	0.8

TABLE A-6. Summary of Oxygen/Methane Results of No. 2 Reference Fuel Evaluated by HLPS at Fuel Flow of 1.0 mL/min

Fuel Code No.	Fuel Description	Date	Test Temp., °C	Test Time, min.	Oxygen, vol%	Methane, vol%
AL-19540-F	No. 2 Reference Fuel	08/09/91	380	Pre-Test:	4.1	0
				10	1.1	0
				20	1.1	0
				30	0.4	0
				Test Average:	0.9	0
		08/09/91	420	Pre-Test:	1.9	0
				10	0.3	0
				20	0.3	0
				30	0.3	0
				Test Average:	0.3	0
		08/09/91	460	Pre-Test:	1.7	0
				10	0.3	0.3
				20	0.4	0.4
				30	0.2	0.4
				Test Average:	0.3	0.4
		08/07/91	480	Pre-Test:	3.4	0
				10	0.2	1.7
				20	0.2	1.9
				30	0.2	1.9
				Test Average:	0.2	1.8

**TABLE A-7. Summary of Oxygen/Methane Results of Jet A Fuel Evaluated
by HLPS at Fuel Flow of 1.0 mL/min**

Fuel Code No.	Fuel Description	Date	Test Temp., °C	Test Time, min.	Oxygen, vol%	Methane, vol%
AL-19471-F	West Coast Jet A	08/20/91	380	Pre-Test:	4.7	0
				10	0.8	0
				20	0.6	0
				30	0.6	0
				Test Average:	0.7	0
		08/20/91	420	Pre-Test:	1.4	0
				10	0.8	0
				20	0.3	0
				30	0.3	0
				Test Average:	0.5	0
		08/21/91	460	Pre-Test:	0.4	0
				10	0.3	0
				20	0.3	Trace
				30	0.3	0.5
				Test Average:	0.3	0.5
		08/21/91	480	Pre-Test:	0.4	0
				10	0.3	0.4
				20	0.3	1.6
				30	0.3	2.1
				Test Average:	0.3	1.6

**TABLE A-8. Summary of Oxygen/Methane Results of Jet A-1 Fuel Evaluated
by HLPS at Fuel Flow of 3.0 mL/min**

Fuel Code No.	Fuel Description	Date	Test Temp., °C	Test Time, min.	Oxygen, vol%	Methane, vol%
AL-19554-F	Jet A-1, w/o Additives	06/18/91	230	Pre-Test:	4.7	0
				10	4.7	0
				20	4.7	0
				30	4.7	0
				Test Average:	4.7	0
		06/20/91	260	Pre-Test:	4.8	0
				10	3.7	0
				20	4.0	0
				30	4.2	0
				40	3.8	0
				Test Average:	3.9	0
		06/18/91	300	Pre-Test:	3.9	0
				10	0.6	0
				20	0.3	0
				Test Average:	0.5	0
		06/18/91	320	Pre-Test:	3.3	0
				10	0.6	0
				20	0.3	0
				Test Average:	0.5	0
		06/19/91	340	Pre-Test:	4.8	0
				10	0.6	0
				20	0.3	0
				30	0.3	0
				Test Average:	0.4	0
		06/19/91	380	Pre-Test:	4.4	0
				10	0.3	0
				20	0.3	0
				30	0.3	0
				Test Average:	0.3	0
		06/19/91	420	Pre-Test:	4.4	0
				10	0.3	Trace
				20	0.3	Trace
				30	0.3	Trace
				Test Average:	0.3	Trace

**TABLE A-8. Summary of Oxygen/Methane Results of Jet A-1 Fuel Evaluated
by HLPS at Fuel Flow of 3.0 mL/min (Cont'd)**

<u>Fuel Code No.</u>	<u>Fuel Description</u>	<u>Date</u>	<u>Test Temp., °C</u>	<u>Test Time, min.</u>	<u>Oxygen, vol%</u>	<u>Methane, vol%</u>
		06/20/91	460	Pre-Test:	4.7	0
				10	0.3	Trace
				30	0.3	Trace
				Test Average:	0.3	Trace
		06/20/91	480	Pre-Test:	2.2	0
				10	0.3	Trace
				20	0.2	Trace
				30	0.3	Trace
				40	0.3	Trace
				Test Average:	0.3	Trace

**TABLE A-9. Summary of Oxygen/Methane Results of 1 wt% Sulfur Fuel Evaluated
by HLPS at Fuel Flow of 3.0 mL/min**

<u>Fuel Code No.</u>	<u>Fuel Description</u>	<u>Date</u>	<u>Test Temp., °C</u>	<u>Test Time, min.</u>	<u>Oxygen, vol%</u>	<u>Methane, vol%</u>
AL-15542-F	1 wt% Sulfur, w/o Additives	07/01/91	230	Pre-Test:	4.4	0
				10	3.7	0
				20	3.6	0
				30	3.6	0
				Test Average:	3.6	0
		07/01/91	260	Pre-Test:	3.6	0
				10	3.3	0
				20	3.3	0
				30	3.3	0
				Test Average:	3.3	0
		07/01/91	300	Pre-Test:	3.3	0
				10	1.8	0
				20	1.7	0
				30	1.5	0
				Test Average:	1.7	0
		07/02/91	340	Pre-Test:	3.9	0
				10	0.5	0
				20	0.3	0
				30	0.2	0
				Test Average:	0.3	0
		07/02/91	380	Pre-Test:	3.3	0
				10	0.4	0
				20	0.3	0
				30	0.2	0
				Test Average:	0.3	0
		07/03/91	420	Pre-Test:	3.8	0
				10	0.3	Trace
				20	0.2	0.5
				30	0.2	0.5
				40	0.2	0.4
				Test Average:	0.2	0.5
		07/03/91	460	Pre-Test:	3.4	0
				10	0.3	1.4
				20	0.2	1.5
				30	0.2	1.5
				40	0.2	1.5
				Test Average:	0.2	1.5

TABLE A-10. Summary of Oxygen/Methane Results of No. 2 Reference Fuel Evaluated by HLPS at Fuel Flow of 3.0 mL/min

Fuel Code No.	Fuel Description	Date	Test Temp., °C	Test Time, min.	Oxygen, vol%	Methane, vol%
AL-19540-F	No. 2 Reference Fuel	06/24/91	230	Pre-Test:	3.8	0
				10	3.5	0
				20	3.5	0
				30	3.5	0
				Test Average:	3.5	0
		06/24/91	260	Pre-Test:	3.5	0
				10	3.1	0
				20	3.2	0
				30	3.2	0
				Test Average:	3.2	0
		06/24/91	300	Pre-Test:	3.2	0
				10	1.3	0
				20	1.2	0
				30	1.2	0
				Test Average:	1.2	0
		06/24/91	340	Pre-Test:	2.1	0
				10	0.3	0
				20	0.2	0
				30	0.2	0
				Test Average:	0.2	0
		06/27/91	380	Pre-Test:	4.4	0
				10	0.3	0
				20	0.2	0
				30	0.2	0
				Test Average:	0.2	0
		06/27/91	420	Pre-Test:	3.9	0
				10	0.4	0
				20	0.2	0
				30	0.2	0
				Test Average:	0.3	0
		06/28/91	460	Pre-Test:	4.1	0
				10	0.6	0
				20	0.2	0
				Test Average:	0.4	0

TABLE A-10. Summary of Oxygen/Methane Results of No. 2 Reference Fuel Evaluated by HLPS at Fuel Flow of 3.0 mL/min (Cont'd)

<u>Fuel Code No.</u>	<u>Fuel Description</u>	<u>Date</u>	<u>Test Temp., °C</u>	<u>Test Time, min.</u>	<u>Oxygen, vol%</u>	<u>Methane, vol%</u>
		06/28/91	480	Pre-Test:	3.9	0
				10	0.4	0
				20	0.3	0
				30	0.2	0
				Test Average:	0.3	0

**TABLE A-11. Summary of Oxygen/Methane Results of Jet A Fuel Evaluated
by HLPS at Fuel Flow of 3.0 mL/min**

Fuel Code No.	Fuel Description	Date	Test Temp., °C	Test Time, min.	Oxygen, vol%	Methane, vol%
AL-19471-F	West Coast Jet A	08/16/91	260	Pre-Test:	4.6	0
				10	2.5	0
				20	2.7	0
				30	2.7	0
				Test Average:	2.6	0
		08/16/91	300	Pre-Test:	2.8	0
				10	0.4	0
				20	0.3	0
				30	0.3	0
				Test Average:	0.3	0
		08/16/91	340	Pre-Test:	1.3	0
				10	0.3	0
				20	0.3	0
				30	0.3	0
				Test Average:	0.3	0
		08/19/91	380	Pre-Test:	4.5	0
				10	0.4	0
				20	0.3	0
				30	0.3	0
				Test Average:	0.3	0
		08/19/91	420	Pre-Test:	0.3	0
				10	0.3	0
				20	0.3	0
				30	0.3	0
				Test Average:	0.3	0
		08/19/91	460	Pre-Test:	0.3	0
				10	0.3	Trace
				20	0.3	0.3
				30	0.3	0.4
				Test Average:	0.3	0.4
		08/19/91	480	Pre-Test:	0.3	0
				10	0.3	Trace
				20	0.3	0.4
				30	0.3	0.5
				Test Average:	0.3	0.5

**TABLE A-12. Summary of Oxygen/Methane Results of Jet A-1 Fuel Evaluated
by HLPS at Fuel Flow of 1.5 mL/min**

Fuel Code No.	Fuel Description	Date	Test Temp., °C	Test Time, min.	Oxygen, vol%	Methane, vol%
AL-19554-F	Jet A-1, w/o Additives	07/23/91	230	Pre-Test:	5.3	0
				10	4.0	0
				20	3.4	0
				30	3.2	0
				Test Average:	3.5	0
		07/23/91	260	Pre-Test:	4.7	0
				10	4.3	0
				20	3.7	0
				30	3.7	0
				Test Average:	3.9	0
		07/22/91	300	Pre-Test:	3.1	0
				10	1.4	0
				20	0.3	0
				30	0.3	0
				Test Average:	0.7	0
		07/22/91	340	Pre-Test:	5.8	0
				10	1.7	0
				20	0.5	0
				30	0.3	0
				40	0.3	0
				Test Average:	0.7	0
		07/22/91	380	Pre-Test:	3.0	0
				10	1.3	0
				20	0.4	0.3
				30	0.3	0.3
				40	0.3	0.3
				Test Average:	0.6	0.3
		07/23/91	420	Pre-Test:	5.3	0
				10	1.5	Trace
				20	0.5	0.5
				30	0.4	0.4
				40	0.4	0.5
				Test Average:	0.7	0.5

**TABLE A-12. Summary of Oxygen/Methane Results of Jet A-1 Fuel Evaluated
by HLPS at Fuel Flow of 1.5 mL/min (Cont'd)**

<u>Fuel Code No.</u>	<u>Fuel Description</u>	<u>Date</u>	<u>Test Temp., °C</u>	<u>Test Time, min.</u>	<u>Oxygen, vol%</u>	<u>Methane, vol%</u>
		07/23/91	460	Pre-Test:	4.1	0
				10	0.6	0.8
				20	0.4	0.6
				30	0.4	0.7
				Test Average:	0.5	0.7

**TABLE A-13. Summary of Oxygen/Methane Results of 1 wt% Sulfur Fuel Evaluated
by HLPS at Fuel Flow of 1.5 mL/min**

<u>Fuel Code No.</u>	<u>Fuel Description</u>	<u>Date</u>	<u>Test Temp., °C</u>	<u>Test Time, min.</u>	<u>Oxygen, vol%</u>	<u>Methane, vol%</u>
AL-15542-F	1 wt% Sulfur, w/o Additives	07/11/91	230	Pre-Test:	3.9	0
				10	2.7	0
				20	2.8	0
				30	2.9	0
				Test Average:	2.8	0
		07/11/91	260	Pre-Test:	2.9	0
				10	1.3	0
				20	0.8	0
				30	0.4	0
				Test Average:	0.8	0
		07/11/91	300	Pre-Test:	2.9	0
				10	0.9	0
				20	0.3	0
				30	0.2	0
				Test Average:	0.5	0
		07/15/91	340	Pre-Test:	3.8	0
				10	0.8	0
				20	0.3	0
				30	0.2	0
				Test Average:	0.4	0
		07/15/91	380	Pre-Test:	3.5	0
				10	0.7	0
				20	0.3	Trace
				30	0.2	Trace
				Test Average:	0.4	Trace
		07/15/91	420	Pre-Test:	2.7	0
				10	0.2	1.0
				20	0.2	1.2
				30	0.2	1.3
				40	0.2	1.3
				Test Average:	0.2	1.2
		07/16/91	460	Pre-Test:	2.6	0
				10	0.5	3.7
				20	0.2	4.4
				30	0.2	4.6
				Test Average:	0.3	4.2

TABLE A-14. Summary of Oxygen/Methane Results of No. 2 Reference Fuel Evaluated by HLPS at Fuel Flow of 1.5 mL/min

Fuel Code No.	Fuel Description	Date	Test Temp., °C	Test Time, min.	Oxygen, vol%	Methane, vol%
AL-19540-F	No. 2 Reference Fuel	07/30/91	230	Pre-Test:	3.0	0
				10	2.7	0
				20	2.7	0
				30	2.5	0
				Test Average:	2.6	0
		07/30/91	260	Pre-Test:	2.3	0
				10	1.7	0
				20	1.4	0
				30	1.5	0
				Test Average:	1.5	0
		07/19/91	300	Pre-Test:	3.9	0
				10	3.0	0
				20	2.7	0
				30	1.9	0
				Test Average:	2.5	0
		07/18/91	340	Pre-Test:	3.9	0
				10	1.0	0
				20	0.3	0
				30	0.2	0
				Test Average:	0.5	0
		07/18/91	380	Pre-Test:	3.8	0
				10	0.9	0
				20	0.2	0
				30	0.2	0
				Test Average:	0.4	0
		07/19/91	420	Pre-Test:	3.9	0
				10	0.9	0
				20	0.2	0
				30	0.2	0
				Test Average:	0.4	0
		07/19/91	460	Pre-Test:	3.4	0
				10	0.7	0
				20	0.2	0
				30	0.2	Trace
				40	0.2	0
				Test Average:	0.3	0

TABLE A-14. Summary of Oxygen/Methane Results of No. 2 Reference Fuel Evaluated by HLPS at Fuel Flow of 1.5 mL/min (Cont'd)

<u>Fuel Code No.</u>	<u>Fuel Description</u>	<u>Date</u>	<u>Test Temp., °C</u>	<u>Test Time, min.</u>	<u>Oxygen, vol%</u>	<u>Methane, vol%</u>
		08/07/91	480	Pre-Test:	3.4	0
				10	0.2	1.0
				20	0.2	1.5
				30	0.2	1.0
				Test Average:	0.2	1.2

**TABLE A-15. Summary of Oxygen/Methane Results of Jet A Fuel Evaluated
by HLPS at Fuel Flow of 1.5 mL/min**

<u>Fuel Code No.</u>	<u>Fuel Description</u>	<u>Date</u>	<u>Test Temp., °C</u>	<u>Test Time, min.</u>	<u>Oxygen, vol%</u>	<u>Methane, vol%</u>
AL-19471-F	West Coast Jet A	08/20/91	380	Pre-Test:	4.7	0
				10	0.9	0
				20	0.7	0
				Test Average:	0.8	0
		08/20/91	420	Pre-Test:	0.3	0
				10	0.3	0
				20	0.3	0
				Test Average:	0.3	0
		08/20/91	460	Pre-Test:	0.7	0
				10	0.3	0
				20	0.3	0.4
				30	0.3	0.5
				Test Average:	0.3	0.5
		08/21/91	480	Pre-Test:	0.8	0
				10	0.3	Trace
				20	0.3	0.5
				30	0.3	0.5
				Test Average:	0.3	0.5

**TABLE A-16. Summary of Oxygen/Methane Results of Jet A-1 Fuel Evaluated
by HLPS at Fuel Flow of 4.5 mL/min**

<u>Fuel Code No.</u>	<u>Fuel Description</u>	<u>Date</u>	<u>Test Temp., °C</u>	<u>Test Time, min.</u>	<u>Oxygen, vol%</u>	<u>Methane, vol%</u>
AL-19554-F	Jet A-1, w/o Additives	08/01/91	260	Pre-Test:	3.5	0
				10	2.3	0
				20	2.0	0
				30	1.8	0
				Test Average:	2.1	0
		08/01/91	300	Pre-Test:	2.9	0
				10	0.3	0
				20	0.3	0
				30	0.3	0
				Test Average:	0.3	0
		08/01/91	340	Pre-Test:	2.3	0
				10	0.3	0
				20	0.3	0
				30	0.3	0
				Test Average:	0.3	0
		08/06/91	380	Pre-Test:	4.5	0
				10	0.3	Trace
				20	0.3	Trace
				30	0.3	Trace
				Test Average:	0.3	Trace
		08/06/91	420	Pre-Test:	1.4	0
				10	0.3	0.5
				20	0.3	0.5
				30	0.3	0.5
				Test Average:	0.3	0.5
		07/23/91	460	Pre-Test:	1.7	0
				10	0.3	0.6
				20	0.3	0.6
				30	0.3	0.7
				Test Average:	0.3	0.6

TABLE A-17. Summary of Oxygen/Methane Results of 1 wt% Sulfur Fuel Evaluated by HLPS at Fuel Flow of 4.5 mL/min

Fuel Code No.	Fuel Description	Date	Test Temp., °C	Test Time, min.	Oxygen, vol%	Methane, vol%
AL-15542-F	1 wt% Sulfur, w/o Additives	07/25/91	260	Pre-Test:	3.8	0
				10	3.5	0
				20	3.5	0
				30	3.5	0
				Test Average:	3.5	0
		07/25/91	300	Pre-Test:	3.6	0
				10	2.7	0
				20	2.7	0
				30	2.9	0
				Test Average:	2.8	0
		07/25/91	340	Pre-Test:	3.3	0
				10	1.1	0
				20	1.0	0
				30	1.0	0
				Test Average:	1.0	0
		07/26/91	380	Pre-Test:	3.7	0
				10	0.2	0
				20	0.2	0
				30	0.6	0
				Test Average:	0.3	0
		07/26/91	420	Pre-Test:	3.5	0
				10	0.2	0
				20	0.2	0
				30	0.2	0
				Test Average:	0.2	0
		07/26/91	460	Pre-Test:	2.5	0
				10	0.2	0.9
				20	0.2	1.2
				30	0.2	0.6
				40	0.2	0.6
				Test Average:	0.2	0.8

TABLE A-18. Summary of Oxygen/Methane Results of No. 2 Reference Fuel Evaluated by HLPS at Fuel Flow of 4.5 mL/min

<u>Fuel Code No.</u>	<u>Fuel Description</u>	<u>Date</u>	<u>Test Temp., °C</u>	<u>Test Time, min.</u>	<u>Oxygen, vol%</u>	<u>Methane, vol%</u>
AL-19540-F	No. 2 Reference Fuel	07/19/91	260	Pre-Test:	2.7	0
				10	2.7	0
				20	2.7	0
				30	2.7	0
				Test Average:	2.7	0
		07/19/91	300	Pre-Test:	2.8	0
				10	1.4	0
				20	1.4	0
				30	1.4	0
				Test Average:	1.4	0
		07/18/91	340	Pre-Test:	1.6	0
				10	0.2	0
				20	0.3	0
				30	0.2	0
				Test Average:	0.2	0
		07/18/91	380	Pre-Test:	3.4	0
				10	0.2	0
				20	0.2	0
				30	0.2	0
				Test Average:	0.2	0
		07/19/91	420	Pre-Test:	1.7	0
				10	0.2	0
				20	0.2	0
				30	0.2	0
				Test Average:	0.2	0
		07/19/91	460	Pre-Test:	0.9	0
				10	0.2	0
				20	0.2	0
				30	0.2	0
				Test Average:	0.2	0

APPENDIX B

Summary of Single-Tube Heat Exchanger (STHE) Data

TABLE B-1. Results of BFLRF Single-Tube Heat Exchanger (STHE) Tests

Test No.	Test Temp., °C	Test Metals	Time, minutes	Fuel AL-Code Number	Fuel Description	D 2276, mg/L	Section Length - (B through M) in centimeters, carbon weight in micrograms												Total
							B	C	D	E	F	G	H	I	J	K	L	M	
							12.7	20.3	27.9	35.6	43.2	50.8	58.4	66.0	73.7	81.3	88.9	96.5	
B-32	340	304 SS	240	19540-F	Cat 1-H	8.6	22	93	275	168	349	190	88	26	13	20	15	17	1276
B-1	380	304 SS	240	19540-F	Cat 1-H	6.2	27	583	819	182	89	82	68	56	53	71	98	*	2127
B-2	380	304 SS	240	19540-F	Cat 1-H	6.8	24	577	701	155	72	69	64	57	58	49	40	36	1902
B-3	420	304 SS	240	19540-F	Cat 1-H	NT	61	1089	539	191	174	191	163	143	125	116	114	115	3020
B-37	420	304 SS	240	19540-F	Cat 1-H	6.6	27	156	390	232	169	192	85	48	33	27	19	22	1400
B-7	460	304 SS	240	19540-F	Cat 1-H	2.0	53	373	558	254	177	127	131	116	97	87	79	76	2127
B-8	500	304 SS	240	19540-F	Cat 1-H	5.6	27	1002	157	91	100	128	161	179	119	135	134	100	2332
B-4	AMB to 540	304 SS	240	19540-F	Cat 1-H	NT	57	311	347	240	198	246	273	259	265	256	251	169	2872
B-28-(2) ^F	380	304 SS	240	19540-F	Cat 1-H	4.4	31	100	335	425	230	124	46	19	2	*	0	9	1320
B-28-(2) ^S	380	304 SS	240	19540-F	Cat 1-H	Same	19	15	8	3	45	13	13	3	1	1	10	0	130
B-11	340	316 SS	240	19540-F	Cat 1-H	11.4	47	197	308	218	192	156	82	61	50	47	56	38	1451
B-27-(2) ^F	380	316 SS	240	19540-F	Cat 1-H	10.2	13	153	410	477	201	140	69	39	34	25	31	28	1619
B-27-(2) ^S	380	316 SS	240	19540-F	Cat 1-H	Same	44	20	20	39	34	28	29	21	4	1	0	1	240
B-48	380	316 SS	240	19540-F	Cat 1-H	13.0	10	50	112	196	325	614	134	42	30	29	18	17	1577
B-16	420	316 SS	240	19540-F	Cat 1-H	13.2	14	909	448	108	45	37	40	42	31	29	29	17	1748
B-50	420	316 SS	240	19540-F	Cat 1-H	12.8	11	190	422	334	159	112	76	55	46	52	44	25	1327
B-54	460	316 SS	240	19540-F	Cat 1-H	11.6	39	69	263	386	289	129	87	69	75	74	69	40	1588
B-55	500	316 SS	240	19540-F	Cat 1-H	7.6	9	94	293	342	247	115	94	94	77	72	65	45	1546
B-51	540	316 SS	240	19540-F	Cat 1-H	6.4	28	537	387	185	127	181	188	122	107	109	120	65	2156
B-53	AMB to 540	316 SS	180	19554-F**	Jet A-1	NT	13	13	13	14	25	68	59	38	40	33	28	40	382
B-12	340	316 SS	240	19554-F	Jet A-1	0.2	47	37	30	46	95	102	74	40	43	29	33	13	590
B-13	380	316 SS	240	19554-F	Jet A-1	0.6	23	23	25	42	105	74	46	25	20	30	21	16	448
B-14	420	316 SS	240	19554-F	Jet A-1	1.2	16	128	175	50	39	36	32	23	27	26	19	19	589
B-15	460	316 SS	240	19554-F	Jet A-1	0.8	10	4	186	64	33	27	29	26	27	18	13	5	441
B-9	500	316 SS	240	19554-F	Jet A-1	0.8	29	629	90	68	68	64	76	86	83	84	70	47	1395
B-10	540	316 SS	240	19554-F	Jet A-1	0.6	25	672	56	44	45	68	65	52	54	59	65	56	1261
B-6	AMB to 540	304 SS	180	19554-F	Jet A-1	NT	55	82	176	126	100	105	97	70	70	82	72	52	1087
B-33	340	304 SS	240	19554-F	Jet A-1	0.4	24	20	19	14	16	30	70	30	19	13	14	15	284
B-34	380	304 SS	240	19554-F	Jet A-1	0.4	44	25	11	41	54	49	28	22	15	17	18	18	342
B-35	420	304 SS	240	19554-F	Jet A-1	0.6	23	16	10	13	7	83	32	20	12	12	9	4	242
B-36	460	304 SS	240	19554-F	Jet A-1	0.2	42	22	17	39	39	42	*	21	18	23	18	26	307
B-30	500	304 SS	240	19554-F	Jet A-1	1.0	15	15	18	22	46	44	41	27	30	36	31	16	341
B-31	540	304 SS	240	19554-F	Jet A-1	0.8	32	141	14	21	15	49	54	54	50	47	51	38	566

* Sample contaminated.
 ** AL-19554-F; without additives.
 NT = Not Tested.

(2) = Test used two tubes.
 F = First tube in series.
 S = Second tube in series.

TABLE B-1. Results of BFLRF Single-Tube Heat Exchanger (STHE) Tests (Cont'd)

Test No.	Test Temp., °C	Test Metals	Time, minutes	Fuel AL-Code Number	Fuel Description	D 227/6, mg/L	Carbon Burnoff												
							Section Length - (B through M) in centimeters, carbon weight in micrograms												
							B	C	D	E	F	G	H	I	J	K	L	M	Total
B-17	340	316 SS	240	15542-F	1 wt% Sulfur	23.4	24	230	292	211	1106	78	35	22	18	8	2	1	2026
B-18	380	316 SS	240	15542-F	1 wt% Sulfur	24.2	23	337	366	109	33	38	37	21	24	23	21	7	1040
B-19	420	316 SS	240	15542-F	1 wt% Sulfur	9.6	19	896	246	46	31	56	97	67	60	37	26	17	1597
B-20	460	316 SS	240	15542-F	1 wt% Sulfur	2.2	16	764	290	34	16	87	146	122	68	61	50	2	1656
B-21	500	316 SS	240	15542-F	1 wt% Sulfur	2.4	17	292	69	234	369	264	238	77	52	67	61	42	1780
B-22	540	316 SS	240	15542-F	1 wt% Sulfur	1.4	23	84	206	336	266	276	415	411	327	309	297	121	3070
B-23	340	316 SS	240	15542-F	1 wt% Sulfur	27.8	26	492	417	108	54	58	46	28	28	22	23	9	1310
B-24	380	316 SS	240	15542-F	1 wt% Sulfur	NT	23	187	147	74	99	61	0	24	24	26	22	4	691
B-25	380	316 SS	240	Stressed B-24	1 wt% Sulfur	1.2	8	52	0	0	2	13	26	17	21	26	27	9	201
B-26-(2) ^F	380	316 SS	240	15542-F	1 wt% Sulfur	14.0	2	11	24	126	233	384	90	9	7	3	9	0	898
B-26-(2) ^S	380	316 SS	240	15542-F	1 wt% Sulfur	Same	10	7	8	9	11	27	35	22	20	16	10	10	187
B-29-(2) ^F	380	304 SS	240	15542-F	1 wt% Sulfur	21.0	28	170	196	83	28	16	3	17	15	8	6	0	570
B-29-(2) ^S	380	304 SS	240	15542-F	1 wt% Sulfur	Same	1	0	0	4	3	22	18	12	7	0	0	0	66
B-5	AMB to 540	304 SS	180	15542-F*	1 wt% Sulfur	NT	40	124	146	81	62	896	708	165	200	203	158	61	2843
B-38	340	304 SS	240	15542-F	1 wt% Sulfur	4.8	30	85	123	122	64	50	26	16	14	16	9	13	568
B-39	380	304 SS	240	15542-F	1 wt% Sulfur	46.0	43	104	139	129	137	168	47	5	33	30	26	25	886
B-40	420	304 SS	240	15542-F	1 wt% Sulfur	23.8	26	50	66	206	156	67	69	49	52	48	35	27	852
B-41	460	304 SS	240	15542-F	1 wt% Sulfur	7.4	114	576	72	78	169	353	409	240	128	100	59	52	2348
B-42	500	304 SS	240	15542-F	1 wt% Sulfur	4.4	289	802	296	402	517	478	547	492	447	371	237	243	5122
B-43	540	304 SS	240	15542-F	1 wt% Sulfur	3.0	115	527	88	191	386	617	833	537	350	232	165	88	4128
B-45	380	304 SS	240	15542-F	1 wt% Sulfur	NT	20	102	147	156	81	58	43	30	20	16	15	16	702
B-46	380	304 SS	240	Stressed B-45	1 wt% Sulfur	8.4	37	40	142	17	26	44	49	39	35	39	20	22	508
B-47-(2) ^F	380	304 SS	240	15542-F	1 wt% Sulfur	13.6	20	350	173	52	29	14	47	38	36	36	30	36	860
B-47-(2) ^S	380	304 SS	240	15542-F	1 wt% Sulfur	13.6	9	6	6	8	9	34	40	27	25	17	9	0	190
B-52	AMB to 540	316 SS	150	15542-F	1 wt% Sulfur	NT	2	32	57	36	25	101	91	50	56	59	58	13	580
B-56-1	380	316 SS	240	15542-F	1 wt% Sulfur	22.6	47	108	127	63	55	44	12	32	25	29	15	2	557
B-56-2	380	316 SS	240	Stressed B-56	1 wt% Sulfur	NT	24	41	40	43	38	35	33	10	5	0	0	0	270
B-56-3	380	316 SS	240	Stressed B-56	1 wt% Sulfur	NT	26	50	57	60	53	103	61	14	11	9	10	13	466
B-56-4	380	316 SS	240	Stressed B-56	1 wt% Sulfur	NT	36	106	54	52	71	61	57	40	41	36	35	29	618
B-56-5	380	316 SS	240	Stressed B-56	1 wt% Sulfur	NT	31	91	50	28	24	25	45	36	34	29	27	38	457
B-57**	380	316 SS	300	15542-F	1 wt% Sulfur	0.8	--	--	--	--	--	--	--	--	--	--	--	--	--
B-58	300	316 SS	240	15542-F	1 wt% Sulfur ^(N)	6.2	5	1	2	0	0	10	1	0	0	0	0	0	19
B-59	380	316 SS	240	15542-F	1 wt% Sulfur ^(N)	7.4	0	8	2	0	2	11	20	15	17	33	30	0	138

* AL-15542-F: without additives.

** Fuel stressed for makeup fuel for repeat runs of B-56 (R-1) through (R-5). No carbon burnoff analysis.

NT = Not Tested.

(2) = Test used two tubes.

F = First tube in series.

S = Second tube in series.

(N) = Nitrogen purged prior to test.

TABLE B-1. Results of BFLRF Single-Tube Heat Exchanger (STHE) Tests (Cont'd)

Test No.	Test Temp., °C	Test Metals	Time, minutes	Fuel AL-Code Number	Fuel Description	D 2276, mg/L	Carbon Burnoff												
							Section Length - (B through M) in centimeters, carbon weight in micrograms												
							B	C	D	E	F	G	H	I	J	K	L	M	Total
B-60 ^(ST)	300	Al-Shim	240	19854-F*	1 wt% Sulfur	8.2	12.7	20.3	27.9	35.6	43.2	50.8	58.4	66.0	73.7	81.3	88.9	96.5	185
B-61 ^(ST)	340	Al-Shim	240	19854-F	1 wt% Sulfur	4.2	--	--	--	--	20	53	33	13	10	15	28	13	185
B-62	380	Al-Shim	240	19854-F	1 wt% Sulfur	2.0	--	--	--	--	31	39	48	50	44	39	24	7	283
B-63	420	Al-Shim	240	19854-F	1 wt% Sulfur	2.2	--	--	--	--	27	67	78	64	87	49	50	31	453
B-64	460	Al-Shim	240	19854-F	1 wt% Sulfur	0.8	--	--	--	--	71	45	60	53	71	76	46	23	446
B-65	300	Cu-Shim	240	19854-F	1 wt% Sulfur	15.4	--	--	--	--	31	38	35	28	24	21	22	31	230
B-66	340	Cu-Shim	240	19854-F	1 wt% Sulfur	3.6	--	--	--	--	36	32	26	18	12	9	7	14	153
B-67	260	Cu-Shim	240	19854-F	1 wt% Sulfur	12.2	--	--	--	--	31	42	27	11	5	8	12	33	169
B-68	300	304 SS**	240	19854-F	1 wt% Sulfur	27.0	13	209	209	127	91	153	54	31	20	18	17	28	970
B-69	340	304 SS**	240	19854-F	1 wt% Sulfur	27.4	29	273	219	117	78	105	46	23	15	11	10	8	934
B-70	380	304 SS**	240	19854-F	1 wt% Sulfur	12.8	25	696	222	82	40	49	47	43	42	33	29	13	1321
B-71	420	304 SS**	240	19854-F	1 wt% Sulfur	8.2	23	643	283	65	24	41	61	54	40	34	40	13	1321
B-72	460	304 SS**	240	19854-F	1 wt% Sulfur	4.0	33	525	49	63	138	177	150	130	85	57	37	8	1452
B-73	300	304-Shim	240	19854-F	1 wt% Sulfur	15.2	--	--	--	--	124	160	72	36	22	23	47	63	547
B-74	340	304-Shim	240	19854-F	1 wt% Sulfur	15.6	--	--	--	--	28	30	26	20	12	13	14	10	153
B-75	380	304-Shim	240	19854-F	1 wt% Sulfur	7.0	--	--	--	--	29	35	39	39	519	29	28	12	730
B-76	420	304-Shim	240	19854-F	1 wt% Sulfur	7.2	--	--	--	--	37	42	36	47	56	50	29	13	310
B-77	460	304-Shim	240	19854-F	1 wt% Sulfur	4.8	--	--	--	--	50	79	99	83	89	78	46	27	551
B-78	300	304 SS†	240	19854-F	1 wt% Sulfur	23.2	0	167	215	149	102	168	42	14	10	4	0	2	873
B-79	340	304 SS†	240	19854-F	1 wt% Sulfur	33.0	17	303	223	91	74	83	31	22	10	4	5	2	865
B-80 ^(A)	380	304 SS†	195	19854-F	1 wt% Sulfur	28.4	13	176	167	104	89	103	42	24	23	21	18	11	791
B-81	420	304 SS†	240	19854-F	1 wt% Sulfur	8.4	33	686	72	21	35	61	71	47	31	37	26	17	1137
B-82	460	304 SS†	240	19854-F	1 wt% Sulfur	1.8	78	467	195	241	402	485	379	177	156	134	86	48	2848
B-83 ^(A)	300	304 SS†	150	19854-F	1 wt% Sulfur	8.6	23	30	32	47	46	378	216	0	58	42	29	38	939
B-84 ^(A) (B)	340	304 SS†	60	19854-F	1 wt% Sulfur	19.4	35	75	83	67	64	70	60	65	58	59	51	42	729
B-85 ^(A)	380	304 SS†	100	19854-F	1 wt% Sulfur	11.4	62	171	102	61	69	90	78	65	54	41	31	29	853
B-86	420	304 SS†	240	19854-F	1 wt% Sulfur	8.6	87	443	77	72	107	153	164	86	67	44	45	30	1375
B-87	460	304 SS†	240	19854-F	1 wt% Sulfur	1.8	61	162	59	94	162	237	201	166	81	68	94	40	1425
B-88 ^(C)	420	304 SS†	240	19854-F	1 wt% Sulfur	7.8	112	825	239	94	72	73	106	119	116	100	77	87	2020
B-95	420	304 SS	240	19854-F ^(D)	1 wt% Sulfur	19.6	47	128	76	45	46	72	95	44	31	30	16	11	641
B-96	500	304 SS	240	19854-F ^(D)	1 wt% Sulfur	12.6	41	475	91	103	95	(PF)	185	169	62	43	46	49	1359
B-97	420	304 SS	240	19854-F ^(E)	1 wt% Sulfur	10.2	79	572	57	24	51	75	83	59	39	30	19	17	1105
B-98	500	304 SS	240	19854-F ^(E)	1 wt% Sulfur	8.2	63	225	160	182	118	307	280	198	51	57	72	35	1748

(B) 1.2 micron filter plugged at 150 mL; D 2276 value is calculated.

(C) Repeat of B-86.

(D) Treated with MIL-S-53021.

(E) Treated with 24 mg/L AO29.

(PF) Power Failure.

* AL-19854-F: without additives.

** Tested with a Stainless Steel, 17 micron filter in the system, to reduce particulates.

† Tested with a 5 micron silver metal membrane filter in the system, to reduce particulates.

‡ Tested with a 1.2 micron silver metal filter in the system, to reduce particulates.

(ST) B-60 and B-61 were tested at the same time in the carbon burnoff analyzer.

(A) Filter plugged, test terminated.

TABLE B-2. Results of BFLRF Single-Tube Heat Exchanger (STHE)
Evaluation of Various Metal Filters
 1 wt% Sulfur Fuel (AL-19854-F) Without Additives
 304 SS U-Tube

<u>STHE Test No.</u>	<u>Test Temp., °C</u>	<u>Filter Metal</u>	<u>Test Time, minute</u>	<u>Metal Filter Size, microns</u>	<u>Deposit, mg/L</u>	<u>D 2276, mg/L</u>
B-68	300	Stainless	240	17	ND	27.0
B-69	340	Stainless	240	17	ND	27.4
B-70	380	Stainless	240	17	ND	12.8
B-71	420	Stainless	240	17	ND	8.2
B-72	460	Stainless	240	17	ND	4.0
B-78	300	Silver	240	5	3.2	23.2
B-79	340	Silver	240	5	16.8	33.0
B-80 ^(A)	380	Silver	195	5	21.8	28.4
B-81	420	Silver	240	5	5.6	8.4
B-82	460	Silver	240	5	8.8	1.8
B-83 ^(A)	300	Silver	150	1.2	10.4	8.6
B-84 ^{(A) (B)}	340	Silver	60	1.2	52.8	19.4
B-85 ^(A)	380	Silver	100	1.2	29.6	11.4
B-86	420	Silver	240	1.2	2.2	8.6
B-87	460	Silver	240	1.2	8.0	1.8
B-88 ^(C)	420	Silver	240	1.2	4.0	7.8

ND = Not Detected.

^(A) Filter plugged, test terminated.

^(B) During filtration, the filter plugged at 150 mL; value is calculated.

^(C) Repeat of B-86.

TABLE B-3. Results of STHE Monitor of Oxygen and Methane

Heat on 10 minutes before first analysis

Test B-4 03-28-91					Test B-5 04-01-91					Test B-6 04-05-91				
Cat 1-H: Ambient to 540°C 304 SS					1 wt% Sulfur: Ambient to 540°C 304 SS					Jet A-1: Ambient to 540°C 304 SS				
Time	Time, min	Bath Temp., °C	Oxygen, vol%	Methane, vol%	Time	Time, min	Bath Temp., °C	Oxygen, vol%	Methane, vol%	Time	Time, min	Bath Temp., °C	Oxygen, vol%	Methane, vol%
Initial	0	29	4.5	0	Initial	0	29	3.3	0	Initial	0	26	4.0	0
12:55	10	92	3.6	0	12:35	10	94	3.2	0	10:20	10	88	3.8	0
1:05	20	172	3.5	0	12:45	20	160	3.2	0	10:30	20	166	3.9	0
1:15	30	185	3.7	0	12:55	30	179	3.1	0	10:40	30	201	3.7	0
1:25	40	240	3.3	0	1:05	40	239	1.9	0	10:50	40	231	3.6	0
1:35	50	257	0.2	0	1:15	50	263	0.2	0	11:00	50	260	0.3	0
1:45	60	294	0.2	0	1:25	60	317	0.2	0	11:10	60	288	0.2	0
1:55	70	324	0.2	0	1:35	70	369	0.2	0	11:20	70	320	0.2	0
2:05	80	352	0.2	0	1:45	80	409	0.2	0.3	11:30	80	347	0.2	0
2:15	90	379	0.2	0	1:55	90	414	0.2	1.4	11:40	90	372	0.2	0
2:35	110	432	0.2	0	2:05	100	457	0.2	2.8	11:50	100	406	0.2	0.2
2:45	120	445	0.2	0.7	2:15	110	463	0.2	6.9	12:00	110	435	Out of Calibration	0.9
2:55	130	459	0.2	2.9	2:35	130	517	0.2	12.6	12:50	160	512	0.2	29.9
3:05	140	475	0.2	6.9	2:45	140	531	0.2	17.7	1:00	170	522	0.2	35.9
3:15	150	493	0.2	12.8	2:55	150	531	0.2	16.5	1:10	180	510	0.2	39.1
3:25	160	384	0.2	36.6										
3:35	170	382	0.2	55.2										
3:45	180	523	0.2	38.5										
3:55	190	520	0.8	31.6										
4:05	200	522	0.2	36.9										
4:15	210	522	0.2	32.8										

Test B-7 04-10-92					Test B-8 04-12-91					Test B-9 04-17-91				
Cat 1-H at 460°C 304 SS					Cat 1-H at 500°C 304 SS					Jet A-1 at 500°C 316 SS				
Time	Time, min	Bath Temp., °C	Oxygen, vol%	Methane, vol%	Time	Time, min	Bath Temp., °C	Oxygen, vol%	Methane, vol%	Time	Time, min	Bath Temp., °C	Oxygen, vol%	Methane, vol%
Initial	0	22	3.6	0	Initial	0	23	5.0	0	Initial	0	23	5.1	0
9:55	10	410	2.3	0	10:10	10	486	0.8	16.2	10:10	10	491	0.5	14.7
10:05	20	430	0.2	0	10:20	20	487	0.2	30.8	10:20	20	494	0.3	31.6
10:15	30	436	0.2	0.5	10:30	30	486	0.2	32.4	10:30	30	492	0.3	32.8
10:25	40	434	0.2	0.6	10:40	40	486	0.2	30.3	10:40	40	493	0.4	30.9
10:35	50	420	0.2	0	10:50	50	486	0.2	29.0	10:50	50	494	0.3	29.5
11:00	75	420	0.2	0.3	11:00	60	488	0.6	33.4	11:00	60	492	0.3	31.6
11:30	105	424	0.2	0	11:30	90	489	0.2	28.7	11:30	90	493	1.9	27.8
12:00	135	437	0.2	0	12:00	120	487	0.2	31.5	12:00	120	495	0.3	33.9
12:30	165	400	0.2	0.4	12:30	150	488	0.2	29.2	12:30	150	495	0.4	27.9
1:00	185	430	0.2	0	1:00	180	487	0.4	26.5	1:00	180	494	0.3	27.1
1:30	215	410	0.2	0	1:30	210	489	0.4	30.9	1:30	210	497	0.3	30.5
					2:00	240	487	0.2	28.0	2:00	240	495	0.3	33.4

TABLE B-3. Results of STHE Monitor of Oxygen and Methane (Cont'd)

Test B-10 04-18-91 Jet A-1 at 540°C 304 SS					Test B-11 04-19-91 Cat 1-H at 340°C 316 SS					Test B-12 04-24-91 Jet A-1 at 340°C 316 SS				
Time	Time, min	Bath Temp., °C	Oxygen, vol%	Methane, vol%	Time	Time, min	Bath Temp., °C	Oxygen, vol%	Methane, vol%	Time	Time, min	Bath Temp., °C	Oxygen, vol%	Methane, vol%
Initial	0	23	4.9	0	Initial	0	23	3.8	0	Initial	0	22	6.6	0
10:10	10	515	0.4	45.7	10:10	10	331	0.7	0	10:10	10	333	2.1	0
10:20	20	514	0.3	61.9	10:20	20	331	0.2	0	10:20	20	335	0.3	0
10:30	30	516	0.3	60.4	10:30	30	332	0.2	0	10:30	30	337	0.3	0
10:40	40	517	0.2	59.8	10:40	40	333	0.2	0	10:40	40	334	0.3	0
10:50	50	519	0.3	56.8	11:00	60	334	0.2	0	10:50	50	334	0.3	0
11:00	60	517	0.4	64.5	11:10	70	334	0.3	0	11:00	60	335	0.3	0
11:30	90	519	0.4	60.1	11:30	90	333	0.2	0	11:30	90	335	0.3	0
12:00	120	518	0.6	58.8	12:00	120	330	0.2	0	12:00	120	334	0.3	0
12:30	150	519	0.2	69.7	12:30	150	332	0.2	0	12:30	150	334	0.3	0
1:00	180	517	0.3	58.2	1:00	180	332	0.2	0	1:00	180	334	0.3	0
1:30	210	517	0.6	66.1	1:30	210	331	0.2	0	1:30	210	332	0.3	0
2:00	240	518	0.3	61.1	2:00	240	330	0.2	0	2:00	240	333	0.3	0

Test B-13 04-25-91 Jet A-1 at 380°C 316 SS					Test B-14 04-26-91 Jet A-1 at 420°C 316 SS					Test B-15 04-30-91 Jet A-1 at 460°C 316 SS				
Time	Time, min	Bath Temp., °C	Oxygen, vol%	Methane, vol%	Time	Time, min	Bath Temp., °C	Oxygen, vol%	Methane, vol%	Time	Time, min	Bath Temp., °C	Oxygen, vol%	Methane, vol%
Initial	0	23	4.7	0	Initial	0	24	4.8	0	Initial	0	23	4.7	0
10:10	10	367	1.1	0	10:10	10	405	GC Noise	GC Noise	10:10	10	443	0.5	0.9
10:20	20	364	0.2	0	10:20	20	406	0.3	0.9	10:20	20	437	0.2	1.9
10:30	30	369	0.2	0	10:30	30	407	0.3	0.3	10:30	30	442	0.2	1.6
10:40	40	371	0.2	0	10:40	40	407	0.3	GC Noise	10:40	40	445	0.2	1.6
11:00	60	371	0.4	0	11:00	60	408	0.3	GC Noise	11:00	60	444	0.2	1.2
11:30	90	370	0.2	0	11:30	90	409	0.3	0.2	11:30	90	444	0.2	1.5
12:00	120	375	0.3	0	12:00	120	408	0.2	0.9	12:00	120	442	0.2	1.1
12:30	150	372	0.3	0	12:30	150	410	GC Noise	GC Noise	12:30	150	444	0.2	1.9
1:00	180	374	0.3	0	1:00	180	409	1.1	0.9	1:00	180	443	0.2	1.7
1:30	210	375	0.3	0	1:30	210	411	GC Noise	GC Noise	1:30	210	442	0.2	1.8
2:00	240	374	0.2	0	2:00	240	412	GC Noise	GC Noise	2:00	240	441	0.2	1.9

TABLE B-3. Results of STHE Monitor of Oxygen and Methane (Cont'd)

Test B-16					Test B-17					Test B-18				
Cat 1-H at 420°C					1 wt% Sulfur at 340°C					1 wt% Sulfur at 380°C				
05-01-91					05-08-91					05-09-91				
316 SS					316 SS					316 SS				
Time	Time, min	Bath Temp., °C	Oxygen, vol%	Methane, vol%	Time	Time, min	Bath Temp., °C	Oxygen, vol%	Methane, vol%	Time	Time, min	Bath Temp., °C	Oxygen, vol%	Methane, vol%
Initial	0	23	3.7	0	Initial	0	19	4.2	0	Initial	0	23	3.8	0
10:10	10	404	0.9	0	10:10	10	330	1.3	0	10:30	10	363	1.7	0
10:20	20	403	0.2	0	10:20	20	330	0.2	0	10:40	20	363	0.2	1.9
10:30	30	404	0.2	0	10:30	30	331	0.2	0	10:50	30	366	0.2	2.1
10:40	40	404	0.3	0	10:40	40	331	0.2	0	11:00	40	365	0.2	2.3
10:50	50	405	0.2	0	10:50	50	328	0.2	0	11:10	50	368	0.2	1.8
11:00	60	405	0.2	0	11:00	60	329	0.2	0	11:20	60	363	0.2	1.8
12:00	120	402	0.2	0	11:30	90	327	0.2	0	11:30	70	364	0.2	1.7
12:30	150	405	0.2	0	12:00	120	329	0.2	0	12:00	100	362	0.2	1.2
1:00	180	404	0.2	0	12:30	150	331	0.2	0	12:30	130	360	0.2	1.8
1:30	210	403	0.2	0	1:00	180	330	0.2	0	1:00	160	364	0.2	1.6
2:00	240	404	0.2	0	1:30	210	327	0.2	0	1:30	190	361	0.2	1.3
					2:00	240	329	0.2	0	2:00	220	368	0.2	1.5

Test B-19					Test B-20					Test B-21				
1 wt% Sulfur at 420°C					1 wt% Sulfur at 460°C					1 wt% Sulfur at 500°C				
05-10-91					05-13-91					05-14-91				
316 SS					316 SS					316 SS				
Time	Time, min	Bath Temp., °C	Oxygen, vol%	Methane, vol%	Time	Time, min	Bath Temp., °C	Oxygen, vol%	Methane, vol%	Time	Time, min	Bath Temp., °C	Oxygen, vol%	Methane, vol%
Initial	0	24	3.4	0	Initial	0	23	4.7	0	Initial	0	24	3.6	0
10:10	10	397	0.7	4.7	10:10	10	442	1.2	6.1	10:40	10	486	0.4	56.4
10:20	20	406	0.2	6.7	10:20	20	451	0.2	9.8	10:50	20	486	0.3	80.8
10:30	30	402	0.2	6.6	10:30	30	444	0.2	10.4	11:00	30	486	0.3	75.9
10:40	40	417	0.2	6.3	10:40	40	448	0.2	10.4	11:10	40	488	0.2	75.4
10:50	50	398	0.2	6.2	10:50	50	447	0.2	11.0	11:20	50	489	0.2	74.9
11:00	60	404	0.2	6.3	11:00	60	443	0.2	11.4	11:30	60	490	0.2	63.6
11:30	90	408	0.2	6.7	11:30	90	442	0.2	12.3	12:00	90	488	0.2	67.4
12:00	120	403	0.2	6.9	12:00	120	437	0.2	13.0	12:30	120	486	0.3	52.1
12:30	150	409	0.2	7.7	12:30	150	436	0.2	12.5	1:00	150	487	0.2	54.8
1:00	180	404	0.2	7.5	1:00	180	443	0.2	12.4	1:30	180	486	0.2	42.8
1:30	210	405	0.2	7.6	1:30	210	442	0.2	13.3	2:00	210	486	0.2	55.0
2:00	240	400	0.2	7.4	2:00	240	442	0.2	13.2	2:30	240	484	0.2	47.9

TABLE B-3. Results of STHE Monitor of Oxygen and Methane (Cont'd)

Test B-22 05-15-91					Test B-23 05-21-91					Test B-30 08-28-91				
1 wt% Sulfur at 540°C 316 SS					1 wt% Sulfur at 340°C 316 SS					Repeat of B-9: With 304 SS Jet A-1 at 500°C				
Time	Time, min	Bath Temp., °C	Oxygen, vol%	Methane, vol%	Time	Time, min	Bath Temp., °C	Oxygen, vol%	Methane, vol%	Time	Time, min	Bath Temp., °C	Oxygen, vol%	Methane, vol%
Initial	0	24	2.8	0	Initial	0	24	2.9	0	Initial	0	25	5.1	0
10:40	10	518	0.4	151.7	10:10	10	336	0.7	0	10:10	10	424	1.3	0
10:50	20	521	0.2	275.0	10:20	20	336	0.2	0	10:20	20	440	0.3	1.2
11:00	30	522	0.1	295.1	10:30	30	331	0.2	0	10:30	30	441	0.3	2.1
11:10	40	522	0.1	293.8	10:40	40	332	0.2	0	10:40	40	447	0.3	3.0
11:20	50	522	0.1	276.1	10:50	50	332	0.2	0	10:50	50	459	0.3	4.2
11:30	60	522	1.4	264.6	11:00	60	329	0.3	0	11:00	60	458	0.3	4.0
12:00	90	520	*	253.8	11:30	90	334	0.2	0	11:30	90	463	0.3	4.1
12:30	120	520	*	248.3	12:00	120	333	0.2	0	12:00	120	457	0.3	3.0
12:45	135	519	*	245.1	12:30	150	330	0.2	0	12:30	150	472	0.3	2.1
1:00	150	519	*	243.6	1:00	180	333	0.2	0	1:00	180	482	0.3	9.4
1:30	180	519	*	266.1	1:30	210	332	0.2	0	1:15	195	484	0.3	7.9
2:00	210	518	*	278.7	2:00	240	330	0.2	0	1:30	210	489	0.3	4.4
2:30	240	521	*	279.1						1:45	225	483	0.4	3.7
										2:00	240	476	0.3	3.1
* Lost Baseline.														
Test B-31 08-29-91					Test B-32 08-29-91					Test B-33 09-03-91				
Repeat of B-10: With 304 SS Jet A-1 at 540°C					Repeat of B-11: With 304 SS Cat 1-H at 340°C					Repeat of B-12: With 304 SS Jet A-1 at 340°C				
Time	Time, min	Bath Temp., °C	Oxygen, vol%	Methane, vol%	Time	Time, min	Bath Temp., °C	Oxygen, vol%	Methane, vol%	Time	Time, min	Bath Temp., °C	Oxygen, vol%	Methane, vol%
Initial	0	26	5.2	0	Initial	0	25	3.7	0	Initial	0	25	4.9	0
10:10	10	494	0.5	14.3	10:10	10	321	2.1	0	10:10	10	327	0.4	0
10:20	20	508	0.3	46.9	10:20	20	330	0.2	0	10:20	20	315	0.3	0
10:30	30	540	0.3	20.7	10:30	30	333	0.2	0	10:30	30	326	0.3	0
10:40	40	520	0.3	22.0	10:40	40	321	0.2	0	10:40	40	328	0.3	0
10:50	50	516	0.3	43.0	10:50	50	322	0.2	0	10:50	50	329	0.3	0
11:00	60	516	0.3	53.9	11:00	60	325	0.2	0	11:00	60	327	0.3	0
11:30	90	522	0.3	67.5	11:30	60	326	0.2	0	11:30	90	328	0.3	0
12:00	120	508	0.3	75.7	12:00	120	323	0.2	0	12:00	120	330	0.3	0
12:30	150	511	0.3	69.0	12:30	150	327	0.2	0	12:30	150	331	0.3	0
1:00	180	530	0.3	38.0	1:00	180	324	0.2	0	1:00	180	333	0.3	0
1:30	210	501	0.3	62.6	1:30	210	330	0.2	0	1:30	210	330	0.3	0
2:00	240	515	0.3	42.4	2:00	240	327	0.2	0	2:00	240	332	0.3	0

TABLE B-3. Results of STHE Monitor of Oxygen and Methane (Cont'd)

Test B-34 09-04-91					Test B-35 09-05-91					Test B-36 09-06-91				
Repeat of B-13: With 304 SS Jet A-1 at 380°C					Repeat of B-14: With 304 SS Jet A-1 at 420°C					Repeat of B-15: With 304 SS Jet A-1 at 460°C				
Time	Time, min	Bath Temp., °C	Oxygen, vol%	Methane, vol%	Time	Time, min	Bath Temp., °C	Oxygen, vol%	Methane, vol%	Time	Time, min	Bath Temp., °C	Oxygen, vol%	Methane, vol%
Initial	0	26	5.0	0	Initial	0	25	3.4	0	Initial	0	25	3.9	0
10:10	10	364	0.5	0	10:10	10	368	2.0	0	10:10	10	414	0.3	0.7
10:20	20	365	0.3	0	10:20	20	397	0.3	0	10:20	20	425	0.3	1.4
10:35	35	365	0.3	0	10:30	30	397	0.3	0.4	10:30	30	432	0.3	1.5
10:50	50	368	0.3	0	10:40	40	402	0.3	0.5	10:40	40	435	0.3	2.3
11:00	60	368	0.3	0	10:50	50	401	0.4	0.4	10:50	50	433	0.3	2.2
11:30	90	373	0.3	0	11:00	60	399	0.3	0.5	11:00	60	422	0.3	2.0
12:00	120	370	0.3	0	11:30	90	404	0.3	0.4	11:30	90	430	0.3	1.7
12:30	150	370	0.3	0	12:00	120	411	0.3	0	12:00	120	438	0.3	1.9
1:00	180	370	0.3	0	12:30	150	409	0.3	0.4	12:30	150	437	0.3	1.8
1:30	210	371	0.3	0	1:00	180	406	0.3	0.4	1:00	180	439	0.3	1.8
					1:30	210	410	0.3	0	1:30	210	435	0.3	1.8
					2:00	240	408	0.3	0.5	2:00	240	437	0.3	1.3

Test B-37 10-08-91					Test B-38 10-08-91					Test B-39 10-10-91				
Repeat of B-16: With 304 SS Cat 1-H at 420°C					Repeat of B-17: With 304 SS 1 wt% Sulfur at 340°C					Repeat of B-18: With 304 SS 1 wt% Sulfur at 380°C				
Time	Time, min	Bath Temp., °C	Oxygen, vol%	Methane, vol%	Time	Time, min	Bath Temp., °C	Oxygen, vol%	Methane, vol%	Time	Time, min	Bath Temp., °C	Oxygen, vol%	Methane, vol%
10:10	10	361	0.2	0	Initial	0	20	4.5	0	Initial	0	21	4.3	0
10:20	20	393	0.2	0	10:10	10	314	1.1	0	10:10	10	361	0.9	0
10:30	30	372	0.2	0	10:20	20	327	0.2	0	10:20	20	367	0.2	1.2
10:40	40	401	0.2	0	10:30	30	322	0.2	0	10:30	30	369	0.2	1.1
10:50	50	405	0.2	0	10:40	40	326	0.2	0	10:40	40	365	0.2	0.8
11:00	60	387	0.2	0	10:50	50	322	0.2	0	10:50	50	362	0.2	0.8
11:30	90	396	0.2	0	11:00	60	325	0.2	0	11:00	60	365	0.2	1.1
12:00	120	399	0.2	0	11:30	90	333	0.2	0	11:30	90	359	0.2	1.0
12:30	150	394	0.2	0	12:00	120	330	0.2	0	12:00	120	369	0.2	1.3
1:00	180	401	0.2	0	12:30	150	327	0.2	0	12:30	150	370	0.2	1.7
1:30	210	401	0.2	0	1:00	180	330	0.2	0	1:00	180	364	0.2	1.7
					1:30	210	332	0.2	0	1:30	210	362	0.2	1.2
										2:00	240	367	0.2	1.6

TABLE B-3. Results of STHE Monitor of Oxygen and Methane (Cont'd)

Test B-40 10-11-91					Test B-41 10-14-91					Test B-42 10-15-91				
Repeat of B-19: With 304 SS 1 wt% Sulfur at 420°C					Repeat of B-20: With 304 SS 1 wt% Sulfur at 460°C					Repeat of B-21: With 304 SS 1 wt% Sulfur at 500°C				
Time	Time, min	Bath Temp., °C	Oxygen, vol%	Methane, vol%	Time	Time, min	Bath Temp., °C	Oxygen, vol%	Methane, vol%	Time	Time, min	Bath Temp., °C	Oxygen, vol%	Methane, vol%
Initial	0	21	4.0	0	Initial	0	23	4.4	0	Initial	0	22	3.8	0
10:10	10	375	0.7	3.5	10:10	10	380	0.8	1.0	10:10	10	474	1.2	24.4
10:20	20	397	0.2	3.9	10:20	20	393	0.2	6.8	10:20	20	474	0.2	29.5
10:30	30	401	0.2	3.3	10:30	30	415	0.2	9.5	10:30	30	485	0.2	23.6
10:40	40	403	0.2	4.1	10:40	40	425	0.3	12.8	10:40	40	479	0.2	23.1
10:50	50	405	0.2	4.9	10:50	50	420	0.2	13.7	10:50	50	478	0.2	22.1
11:00	60	402	0.2	4.8	11:00	60	432	0.2	14.4	11:00	60	481	0.3	60.9
11:30	90	401	0.2	4.6	11:30	90	430	0.2	17.2	11:30	90	481	0.2	69.0
12:00	120	407	0.2	5.0	12:00	120	431	0.3	16.4	12:00	120	478	0.3	67.4
12:30	150	408	0.2	4.9	12:30	150	428	0.3	17.9	12:30	150	484	0.3	71.6
1:00	180	406	0.3	4.6	1:00	180	433	0.2	18.7	1:00	180	481	0.2	62.1
1:30	210	406	0.2	4.7	1:30	210	430	0.2	17.7	1:30	210	484	0.2	63.3
2:00	240	407	0.2	5.8	2:00	240	433	0.2	18.1	2:00	240	485	0.2	66.3

Test B-43 10-16-91					Test B-45 10-17-91					Test B-46 10-18-91				
Repeat of B-22: With 304 SS 1 wt% Sulfur at 540°C					Repeat of B-24: With 304 SS 1 wt% Sulfur at 380°C					Repeat of B-25: With 304 SS: Fuel Stressed in B-45 1 wt% Sulfur at 380°C				
Time	Time, min	Bath Temp., °C	Oxygen, vol%	Methane, vol%	Time	Time, min	Bath Temp., °C	Oxygen, vol%	Methane, vol%	Time	Time, min	Bath Temp., °C	Oxygen, vol%	Methane, vol%
Initial	0	21	3.5	0	Initial	0	22	4.0	0	Initial	0	22	0.2	0
10:10	10	501	Bad Start	Bad Start	10:10	10	336	0.8	0	10:10	10	354	0.2	0.5
10:20	20	500	0.2	11.5	10:20	20	358	0.3	0.8	10:20	20	353	0.2	1.2
10:30	30	502	0.2	18.4	10:30	30	352	0.2	1.5	10:30	30	361	0.2	0.9
10:40	40	512	0.2	17.5	10:40	40	353	0.2	1.0	10:40	40	356	0.2	1.9
11:00	60	513	0.2	20.0	10:50	50	352	0.2	0.8	10:50	50	359	0.2	1.8
11:30	90	514	0.2	17.2	11:00	60	359	0.2	0.7	11:00	60	359	0.2	3.7
12:00	120	511	0.2	15.7	11:30	90	368	0.2	0.7	11:30	90	357	0.2	1.3
12:30	150	516	0.2	18.5	12:00	120	367	0.2	1.3	12:00	120	351	0.2	2.2
1:00	180	518	0.3	12.2	12:30	150	366	0.3	0.9	12:30	150	360	0.2	2.6
1:30	210	515	0.2	18.1	1:00	180	369	0.2	1.3	1:00	180	359	0.2	2.0
					1:30	210	368	0.2	1.3	1:30	210	364	0.2	2.1
					2:00	240	368	0.2	1.0					

TABLE B-3. Results of STHE Monitor of Oxygen and Methane (Cont'd)

Test B-47 10-22-91					Test B-48 10-23-91					Test B-50 10-24-91				
Repeat of B-26-1 and B-26-2: With 304 SS 1 wt% Sulfur at 380°C					Repeat of B-1: With 316 SS Cat 1-H at 380°C					Repeat of B-3: With 316 SS Cat 1-H at 420°C				
Time	Time, min	Bath Temp., °C	Oxygen, vol%	Methane, vol%	Time	Time, min	Bath Temp., °C	Oxygen, vol%	Methane, vol%	Time	Time, min	Bath Temp., °C	Oxygen, vol%	Methane, vol%
Initial	0	22	4.1	0	Initial	0	24	3.7	0	Initial	0	24	3.9	0
10:10	10	368	0.9	1.2	10:10	10	349	0.7	0	10:10	10	376	1.0	0
10:20	20	365	0.2	5.2	10:20	20	357	0.2	0	10:20	20	395	0.2	0
10:30	30	366	0.2	5.2	10:30	30	360	0.2	0	10:30	30	402	0.2	0
10:40	40	367	0.2	5.1	10:40	40	357	0.2	0	10:40	40	405	0.2	0
10:50	50	367	0.2	5.0	10:50	50	361	0.2	0	10:50	50	401	0.2	0
11:00	60	363	0.2	5.8	11:00	60	360	0.2	0	11:00	60	407	0.2	0
11:30	90	367	0.3	5.8	11:30	90	360	0.2	0	11:30	90	408	0.2	0
12:00	120	367	0.2	5.4	12:00	120	365	0.2	0	12:00	120	409	0.2	0
12:30	150	368	0.2	5.2	12:30	150	358	0.2	0	12:30	150	409	0.2	0
1:00	180	365	0.2	5.2	1:00	180	364	0.2	0	1:00	180	409	0.2	0
1:30	210	367	0.2	5.0	1:30	210	360	0.2	0	1:30	210	411	0.2	0
2:00	240	366	0.2	4.9	2:00	240	364	0.2	0					

Test B-51 10-25-91					Test B-52 10-30-91					Test B-53 10-31-91				
Repeat of B-4: With 316 SS Cat 1-H at 540°C					Repeat of B-5: With 316 SS 1 wt% Sulfur: Ambient to 540°C					Repeat of B-6: With 316 SS Jet A-1: Ambient to 540°C				
Time	Time, min	Bath Temp., °C	Oxygen, vol%	Methane, vol%	Time	Time, min	Bath Temp., °C	Oxygen, vol%	Methane, vol%	Time	Time, min	Bath Temp., °C	Oxygen, vol%	Methane, vol%
Initial	0	24	4.1	0	Initial	0	18	3.9	0	Initial	0	19	5.0	0
10:10	10	450	0.4	1.3	10:10	10	47	3.9	0	10:10	10	39	5.1	0
10:20	20	469	0.2	9.9	10:20	20	90	3.9	0	10:20	20	69	5.5	0
10:30	30	509	0.2	45.7	10:30	30	168	3.9	0	10:30	30	200	5.3	0
10:40	40	511	0.2	71.6	10:40	40	230	3.4	0	10:40	40	236	4.3	0
10:50	50	506	0.2	65.7	10:50	50	262	1.4	0	10:50	50	263	0.5	0
11:00	60	497	0.2	57.9	11:00	60	292	0.2	0	11:00	60	276	0.3	0
11:30	90	504	0.3	32.0	11:10	70	302	0.2	0	11:10	70	319	0.3	0
12:00	120	510	0.2	64.0	11:20	80	317	0.2	0	11:20	80	340	0.3	0
12:30	150	516	0.2	35.2	11:30	90	368	0.2	1.7	11:30	90	358	0.4	0
1:00	180	515	0.2	16.0	11:40	100	370	0.2	4.9	11:40	100	385	0.4	0
1:30	210	512	0.2	105.0	11:50	110	383	0.2	7.2	11:50	110	387	0.3	0.6
2:00	240	518	0.2	125.0	12:00	120	432	0.2	9.6	12:00	120	427	0.3	1.1
					12:10	130	425	0.2	13.9	12:10	130	442	0.4	2.6
					12:20	140	454	0.2	36.1	12:20	140	486	0.3	6.5
					12:30	150	443	0.2	33.3	12:30	150	466	0.3	14.3
										12:40	160	469	0.3	8.0
										12:50	170	484	0.3	10.1
										1:00	180	490	0.3	13.7

TABLE B-3. Results of STHE Monitor of Oxygen and Methane (Cont'd)

Test B-54 10-28-91					Test B-55 10-29-91					Test B-56-1 11-07-91				
Repeat of B-7: With 316 SS					Repeat of B-8: With 316 SS					1 wt% Sulfur at 380°C				
Cat 1-H at 460°C					Cat 1-H at 500°C					316 SS				
Time	Time, min	Bath Temp., °C	Oxygen, vol%	Methane, vol%	Time	Time, min	Bath Temp., °C	Oxygen, vol%	Methane, vol%	Time	Time, min	Bath Temp., °C	Oxygen, vol%	Methane, vol%
Initial	0	24	4.2	0	Initial	0	24	3.9	0	Initial	0	24	3.9	0
10:10	10	435	0.9	0	10:10	10	370	0.8	0	10:10	10	367	1.0	0.6
10:20	20	443	0.2	0	10:20	20	390	0.2	0.3	10:20	20	367	0.2	0.6
10:30	30	444	0.2	0	10:30	30	401	0.2	0.8	10:30	30	368	0.2	2.0
10:40	40	443	0.2	0	10:50	50	438	0.2	2.6	10:40	40	369	0.2	1.9
10:50	50	445	0.2	0	11:00	60	438	0.2	1.7	10:50	50	369	0.3	3.4
11:00	60	444	0.2	0	11:30	90	443	0.2	1.2	11:00	60	370	0.4	2.4
11:30	90	445	0.3	0	12:00	120	468	0.2	3.3	11:30	90	371	0.2	2.2
12:00	120	447	0.3	0	12:30	150	466	0.2	3.1	12:00	120	368	0.3	2.1
12:30	150	442	0.2	0.4	1:00	180	469	0.2	3.3	12:30	150	367	0.2	2.8
1:00	180	444	0.2	0.8	1:30	210	473	0.2	2.7	1:00	180	371	0.2	1.9
1:30	210	444	0.2	0	2:00	240	473	0.2	2.7	1:30	210	366	0.2	2.2
2:00	240	442	0.3	0						2:00	240	368	0.2	1.8

Test B-57 11-08-91					Test B-56-2 11-12-91					Test B-56-3 11-13-91				
Stressed Fuel for B-56, Make-Up					Second Test of B-56 Fuel*					Test Fuel From B-56-2*				
1 wt% Sulfur at 380°C					1 wt% Sulfur at 380°C					1 wt% Sulfur at 380°C				
316 SS					316 SS					316 SS				
Time	Time, min	Bath Temp., °C	Oxygen, vol%	Methane, vol%	Time	Time, min	Bath Temp., °C	Oxygen, vol%	Methane, vol%	Time	Time, min	Bath Temp., °C	Oxygen, vol%	Methane, vol%
Initial	0	25	3.3	0	Initial	0	20	3.4	0	Initial	0	20	3.1	0
10:10	10	343	0.5	0	10:10	10	378	0.5	0.4	10:10	10	367	0.5	2.7
10:20	20	365	0.2	1.0	10:20	20	363	0.2	0.6	10:20	20	365	0.2	2.6
10:30	30	370	0.2	0.7	10:30	30	361	0.2	0.7	10:30	30	365	0.2	2.5
10:40	40	367	0.2	0.6	10:40	40	363	0.2	0.7	10:40	40	364	0.2	1.8
10:50	50	368	0.2	0.9	10:50	50	367	0.2	1.1	10:50	50	362	0.2	1.3
11:00	60	372	0.2	1.5	11:00	60	368	0.2	0.6	11:00	60	364	0.2	1.3
11:30	90	367	0.2	1.4	11:15	75	374	0.2	0.7	11:30	90	360	0.2	1.1
12:00	120	364	0.2	0.8	12:00	90	371	0.2	1.7	12:00	120	363	0.2	0.8
12:30	150	367	0.2	0.8	1:00	150	360	0.2	0.5	12:30	150	366	0.2	1.6
1:00	180	367	0.2	1.2	1:15	165	364	0.2	1.3	1:00	180	365	0.2	1.6
1:30	210	368	0.2	0.9	1:30	180	373	0.2	0.8	1:30	210	366	0.2	2.0
2:00	240	372	0.2	0.8						2:00	240	363	0.2	1.7

* Added 1000 mL from B-57.

* Added 400 mL from B-57.

TABLE B-3. Results of STHE Monitor of Oxygen and Methane (Cont'd)

New Batch of 1 wt% Sulfur Without
Additives: AL-19854-F

Test B-56-4					Test B-56-5					Test B-58				
11-14-91					11-18-91					05-12-92				
Test Fuel From B-56-3*					Test Fuel From B-56-4					1 wt% Sulfur at 300°C*				
316 SS					316 SS					316 SS				
1 wt% Sulfur at 380°C					1 wt% Sulfur at 380°C									
Time	Time, min	Bath Temp., °C	Oxygen, vol%	Methane, vol%	Time	Time, min	Bath Temp., °C	Oxygen, vol%	Methane, vol%	Time	Time, min	Bath Temp., °C	Oxygen, vol%	Methane, vol%
Initial	0	22	3.5	0	Initial	0	23	3.4	0	10:10	10	295	0.2	0
10:10	10	364	1.3	0.5	10:10	10	363	1.0	0.9	10:20	20	293	0	0
10:20	20	366	0.2	1.9	10:20	20	364	0.2	1.7	10:30	30	296	0	0
10:30	30	364	0.2	2.0	10:30	30	366	0.2	1.6	10:40	40	294	0	0
10:40	40	365	0.2	2.0	10:40	40	363	0.2	1.5	10:50	50	293	0	0
10:50	50	367	0.2	2.3	10:50	50	364	0.2	1.7	11:00	60	292	0	0
11:00	60	364	0.2	2.1	11:00	60	361	0.2	1.5	11:30	90	292	0	0
11:30	90	364	0.2	1.6	12:00	120	359	0.2	3.3	12:00	120	294	0	0
12:00	120	361	0.2	1.6	12:30	150	362	0.2	1.7	12:30	150	292	0	0
12:30	150	363	0.2	1.5	1:00	180	362	0.2	1.8	1:00	180	292	0	0
1:00	180	367	0.2	1.9	1:30	210	359	0.3	0.6	1:30	210	292	0	0
1:30	210	363	0.2	1.8	2:00	240	363	0.2	2.3					
2:00	240	362	0.2	2.0										

* Added 400 mL from B-57.

* Aerated with Zero Nitrogen.

Test B-59					Test B-61					Test B-62				
05-13-92					06-26-92					06-30-92				
1 wt% Sulfur at 380°C*					Aluminum Shim Stock					Aluminum Shim Stock				
316 SS					304 SS					304 SS				
					1 wt% Sulfur at 340°C					1 wt% Sulfur at 380°C				
Time	Time, min	Bath Temp., °C	Oxygen, vol%	Methane, vol%	Time	Time, min	Bath Temp., °C	Oxygen, vol%	Methane, vol%	Time	Time, min	Bath Temp., °C	Oxygen, vol%	Methane, vol%
10:10	10	363	0.1	0.7	10:10	10	329	0.9	0	10:10	10	353	0.7	0
10:20	20	366	0	3.2	10:20	20	335	0.1	0	10:20	20	364	0.2	0.9
10:30	30	366	0	3.6	10:30	30	334	0.1	0	10:30	30	364	0.2	0.9
10:40	40	368	0	3.8	10:40	40	334	0.1	0	10:40	40	366	0.2	1.0
10:50	50	367	0	4.2	10:50	50	332	0.1	0	10:50	50	372	0.3	1.0
11:00	60	365	0	3.9	11:00	60	333	0.1	0	11:00	60	368	0.3	0.8
11:30	90	369	0	4.8	11:30	90	332	0.1	0	11:30	90	365	0.3	0.6
12:00	120	368	0	4.4	12:00	120	334	0.1	0	12:00	120	364	0.3	1.0
12:30	150	365	0	4.1	12:30	150	332	0.1	0	12:30	150	365	0.2	1.1
1:00	180	366	0	4.3	1:00	180	332	0.1	0	1:00	180	367	0.2	1.1
1:30	210	366	0	4.2	1:30	210	332	0.1	0	1:30	210	364	0.2	1.1
										2:00	240	369	0.2	1.1

* Aerated with Zero Nitrogen.

TABLE B-3. Results of STHE Monitor of Oxygen and Methane (Cont'd)

Test B-63					Test B-64					Test B-65				
07-01-92					07-02-92					07-08-92				
Aluminum Shim Stock					Aluminum Shim Stock					Aluminum Shim Stock				
1 wt% Sulfur at 420°C					1 wt% Sulfur at 460°C					1 wt% Sulfur at 300°C				
Time	Time, min	Bath Temp., °C	Oxygen, vol%	Methane, vol%	Time	Time, min	Bath Temp., °C	Oxygen, vol%	Methane, vol%	Time	Time, min	Bath Temp., °C	Oxygen, vol%	Methane vol%
10:10	10	401	0.7	1.6	10:10	10	435	0.3	4.6	10:10	10	297	0.8	0
10:20	20	401	0.3	2.4	10:20	20	441	0.2	11.6	10:20	20	300	0.2	0
10:30	30	407	0.2	2.2	10:30	30	440	0.3	13.2	10:30	30	299	0.2	0
10:40	40	406	0.2	2.1	10:40	40	443	0.2	13.4	10:40	40	299	0.2	0
10:50	50	404	0.2	2.2	10:50	50	443	0.2	13.2	10:50	50	295	0.3	0
11:00	60	406	0.2	2.1	11:00	60	443	0.2	13.9	11:00	60	295	0.3	0
11:30	90	411	0.2	2.2	11:30	90	445	0.4	11.9	11:30	90	290	0.2	0
12:00	120	404	0.2	2.4	12:00	120	443	0.2	12.2	12:00	120	294	0.2	0
12:30	150	403	0.2	2.5	12:30	150	444	0.2	11.5	12:30	150	294	0.2	0
1:00	180	395	0.2	2.5	1:00	180	444	0.2	13.2	1:00	180	295	0.2	0
1:30	210	407	0.2	2.5	1:30	210	445	0.2	8.3	1:30	210	295	0.3	0
					2:00	240	446	0.2	5.7					

Test B-66					Test B-67					Test B-68				
07-09-92					07-10-92					07-21-92				
Copper Shim Stock					Copper Shim Stock					Stainless Steel Filter in System				
1 wt% Sulfur at 340°C					1 wt% Sulfur at 260°C					1 wt% Sulfur at 340°C at 380°C				
Time	Time, min	Bath Temp., °C	Oxygen, vol%	Methane, vol%	Time	Time, min	Bath Temp., °C	Oxygen, vol%	Methane, vol%	Time	Time, min	Bath Temp., °C	Oxygen, vol%	Methane vol%
10:10	10	334	0.8	0	10:10	10	259	0.5	0	10:10	10	280	3.6	0
10:20	20	336	0.2	0	10:20	20	258	0.2	0	10:20	20	291	0.3	0
10:30	30	336	0.2	0	10:30	30	259	0.2	0	10:30	30	294	0.3	0
10:40	40	338	0.2	0	10:40	40	259	0.2	0	10:50	50	296	0.2	0
10:50	50	337	0.2	0	10:50	50	259	0.2	0	11:00	60	296	0.2	0
11:00	60	337	0.2	0	11:00	60	260	0.2	0	11:30	90	296	0.2	0
11:30	90	336	0.2	0	11:30	90	261	0.3	0	12:00	120	296	0.2	0
12:00	120	337	0.2	0	12:00	120	260	0.2	0	12:30	150	297	0.2	0
12:30	150	337	0.2	0	12:30	150	259	0.3	0	1:00	180	297	0.2	0
1:00	180	338	0.2	0	1:00	180	261	0.3	0	1:30	210	296	0.2	0
1:30	210	334	0.3	0	1:30	210	269	0.2	0					

TABLE B-3. Results of STHE Monitor of Oxygen and Methane (Cont'd)

Test B-69 07-22-92					Test B-70 07-23-92					Test B-71 07-28-92				
Stainless Steel Filter in System 304 SS					Stainless Steel Filter in System 304 SS					Stainless Steel Filter in System 304 SS				
1 wt% Sulfur at 340°C					1 wt% Sulfur at 380°C					1 wt% Sulfur at 420°C				
Time	Time, min	Bath Temp., °C	Oxygen, vol%	Methane, vol%	Time	Time, min	Bath Temp., °C	Oxygen, vol%	Methane, vol%	Time	Time, min	Bath Temp., °C	Oxygen, vol%	Methane, vol%
10:10	10	324	2.5	0	10:10	10	370	2.7	0.6	10:10	10	392	3.3	0
10:20	20	328	0.3	0	10:20	20	372	0.2	1.2	10:20	20	395	0.2	1.4
10:30	30	331	0.2	0	10:30	30	372	0.2	1.3	10:30	30	396	0.2	1.5
10:40	40	322	0.2	0	10:40	40	371	0.2	1.2	10:40	40	398	0.2	1.7
10:50	50	324	0.2	0	10:50	50	370	0.2	1.2	10:50	50	398	0.2	1.8
11:00	60	322	0.3	0	11:00	60	371	0.2	1.1	11:00	60	402	0.2	1.8
11:30	90	330	0.2	0	11:30	90	369	0.2	1.1	11:30	90	405	0.2	1.9
12:00	120	330	0.2	0	12:00	120	372	0.2	1.0	12:00	120	398	0.2	2.0
12:30	150	327	0.2	0	12:30	150	370	0.3	1.0	12:30	150	402	0.3	1.9
1:00	180	328	0.2	0	1:00	180	370	0.3	1.0	1:00	180	403	0.2	2.1
1:30	210	330	0.2	0	1:30	210	370	0.2	1.1	1:30	210	400	0.2	1.9

Test B-72 07-29-92					Test B-74 08-10-92					Test B-75 08-11-92				
Stainless Steel Filter in System 304 SS					304 SS Shim Stock 304 SS					304 SS Shim Stock 304 SS				
1 wt% Sulfur at 460°C					1 wt% Sulfur at 340°C					1 wt% Sulfur at 380°C				
Time	Time, min	Bath Temp., °C	Oxygen, vol%	Methane, vol%	Time	Time, min	Bath Temp., °C	Oxygen, vol%	Methane, vol%	Time	Time, min	Bath Temp., °C	Oxygen, vol%	Methane, vol%
10:10	10	445	2.4	4.1	10:10	10	335	0.6	0	10:10	10	369	0.5	1.1
10:20	20	447	0.3	13.2	10:20	20	333	0.2	0	10:20	20	369	0.3	1.7
10:30	30	448	0.3	13.2	10:30	30	333	0.2	0	10:30	30	369	0.3	1.7
10:40	40	447	0.3	13.6	10:40	40	334	0.2	0	10:40	40	367	0.2	1.5
10:50	50	447	0.2	12.6	10:50	50	333	0.2	0	10:50	50	368	0.2	1.7
11:00	60	448	0.3	13.1	11:00	60	333	0.2	0	11:00	60	368	0.4	1.8
11:30	90	447	0.4	12.6	11:30	90	333	0.2	0	11:30	90	367	0.3	1.7
12:00	120	446	0.3	12.6	12:00	120	334	0.2	0	12:00	120	368	0.3	1.7
12:30	150	445	0.3	12.3	12:30	150	333	0.3	0	12:30	150	370	0.3	2.2
1:00	180	446	0.3	12.5	1:00	180	330	0.2	0	1:00	180	368	0.3	1.7
1:30	210	445	0.3	10.8	1:30	210	330	0.2	0	1:30	210	368	0.4	2.1

TABLE B-3. Results of STHE Monitor of Oxygen and Methane (Cont'd)

Test B-76					Test B-77				
08-12-92					08-13-92				
304 SS Shim Stock					304 SS Shim Stock				
1 wt% Sulfur at 420°C					1 wt% Sulfur at 460°C				
Bath					Bath				
Time	Time, min	Temp., °C	Oxygen, vol%	Methane, vol%	Time	Time, min	Temp., °C	Oxygen, vol%	Methane, vol%
10:10	10	409	0.5	1.9	10:10	10	446	0.3	5.7
10:20	20	410	0.2	3.1	10:20	20	446	0.3	10.4
10:30	30	410	0.2	3.0	10:30	30	445	0.2	9.9
10:40	40	408	0.2	3.0	10:40	40	444	0.2	8.3
10:50	50	410	0.2	2.7	10:50	50	442	0.3	6.9
11:00	60	412	0.2	2.9	11:00	60	443	0.3	6.3
11:30	90	408	0.2	2.9	11:30	90	454	0.3	5.7
12:00	120	411	0.2	3.0	12:00	120	446	0.3	6.2
12:30	150	410	0.2	2.8	12:30	150	449	0.3	4.4
1:00	180	411	0.2	3.1	1:00	180	452	0.3	4.8
1:30	210	409	0.2	3.1	1:30	210	453	0.2	3.6

APPENDIX C

Quantitation of Fuel Deposition on Hot Metal Surfaces

**4TH INTERNATIONAL CONFERENCE ON
STABILITY AND HANDLING OF LIQUID FUELS
Orlando, Florida, November 19-22, 1991**

QUANTITATION OF FUEL DEPOSITION ON HOT METAL SURFACES

L.L. Stavinoha
S.R. Westbrook
D.W. Naegeli
S.J. Lestz

Belvoir Fuels and Lubricants Research Facility (SwRI)
Southwest Research Institute
San Antonio, Texas

ABSTRACT

Experiments were performed in a Hot Liquid Process Simulator (HLPS) configured and operated such that it performed under conditions similar to Jet Fuel Thermal Oxidation Tester (JFTOT) ASTM D 3241 requirements. The JFTOT heater tubes used were 1018 mild steel, 304 stainless steel(SS), and 304 SS tubes coated with aluminum, magnesium, gold, and copper. A low sulfur Jet A fuel with a breakpoint temperature of 254°C was used to create deposits on the heater tubes at temperatures of 300, 340 and 380°C. Deposit thickness was measured by dielectric breakdown voltage and Auger ion milling. Auger ion milling of the deposits showed the order of deposition to be copper > Mild Steel > gold > aluminum > magnesium. The dielectric strength method indicated deposit thickness ranking of Mild Steel > 304 SS > gold > magnesium = aluminum = copper. The pronounced differences between the deposit thickness measuring techniques suggested that both the Auger milling rate and the dielectric strength of the deposit may be affected by deposit morphology/composition (such as metal ions that may have become included in the bulk of the deposit). Carbon burn-off data have been obtained as a means of judging the validity of DMD derived deposit evaluations. ESCA data had suggested that the thinnest deposit was on the magnesium coated test tube. The SEM photographs showed marked variations in the deposit morphology and the results suggested that surface composition has a significant effect on the mechanism of deposition. Aside from variations in the thickness of deposits due to metallurgy, the most dramatic effect observed was that the bulk of deposits moved to tube locations of lower temperature as the maximum temperature of the tube was increased from 300 to 380°C, also verified in a single tube heat exchanger. The results indicate that the deposition rate is highly temperature dependent and may be limited by the concentration of dissolved oxygen or reactive components in the fuel. The overall results show that the surface temperature and composition play an important role in deposition.

INTRODUCTION

The effect of fuel system metallurgy on fuel stability is an important concern in the development of high efficiency/advanced engine technology such as adiabatic, low-heat rejection engines. Several studies have shown that trace metals adversely affect the thermal stability of hydrocarbon fuels.^{1,2} Metal concentrations as low as 15 ppb of copper, 25 ppb of iron, 100 ppb of zinc, and about 200 ppb of lead have been found to cause significant change in the thermal stability of jet fuels. These studies suggest that the slightest metallic contamination could cause a significant change in the thermal oxidative stability of hydrocarbon fuels. In fact, the theory has been

advanced that all hydrocarbon autoxidations are trace metal catalyzed.³ Recent work,⁴ in which only limited data are available, suggests that aluminum tubes with magnesium-enriched surfaces tend to have lower deposit buildups than the standard aluminum tubes. If such minor changes in surface metallurgy cause significant differences in the rate of deposit formation, major changes in surface composition could dramatically effect processes such as deposit adherence and oxidation catalysis.⁵ Experiments with metal deactivator in dodecane using JFTOT equipment suggest that the effect on deposit reduction may be a consequence of interactions in the liquid-phase rather than a reduced adherence to the hot metal surface.⁶

One measure of the thermal stability of aviation fuels is the quantity of deposits formed on heated metal surfaces.⁷ In accelerated stability tests conducted in accordance with the JFTOT procedure (ASTM D 3241),⁸ the rating methods currently employed involve either visual comparisons or measurements of reflected light by the tube deposit rater (TDR), both of which are sensitive to deposit color and surface texture. Morris and Hazlett⁷ examined deposits formed on stainless-steel JFTOT heater tubes in several ways including TDR, gravimetric carbon combustion, and two new nondestructive techniques for determining deposit volumes based on dielectric strength and optical interference. Measurements of total carbon content by combustion were used as a reference. They found that the dielectric and interference methods correlated well with the combustion analyses and each other, while the total TDR often gave misleading results. In the present study, the purpose was to investigate the role of metal composition in the formation of deposits on fuel wetted hot surfaces. This report emphasizes methods of quantitation of fuel deposits on hot metal surfaces.

EXPERIMENTAL

HLPS. Experiments were performed in an Alcor model HLPS300 Hot Liquid Process Simulator (HLPS), which is a modular version of the JFTOT apparatus used for the ASTM D 3241 method. The HLPS was operated to give conditions equivalent to D 3241 requirements except that Triton-treated fuel prefilters were not used. The results in Fig. 1 show the longitudinal temperature profile of the heater tubes at controlled maximum temperatures of 300, 340, and 380°C. In Fig. 1, station 0 is the fuel inlet and station 60 is where the fuel leaves the JFTOT heater tube jacket. Preparation of JFTOT tubes for carbon burn-off involved removing both of the tube end grips using a fine tooth jeweler's saw. Special care is taken not to handle the test section of the tube. After SEM evaluation, the test section is then placed in a pre-labeled test tube and cleaned with toluene followed by n-hexane. After descanting the solvents, the test tube is placed in a vacuum oven and dried at 75°C for approximately one hour. The specimens are now ready for carbon burn-off analysis.

STHE. Fig. 2 is a schematic description of the single tube heat exchanger (STHE). The upper diagram depicts the full STHE, while the lower diagram is an enlarged view of the heater and heat exchanger tube portion. Fig. 3 are fuel temperature profiles at various bath temperatures. Prior to a run the test fuel is filtered and aerated according to the procedures outlined in ASTM D 3241, the JFTOT test. Prior to beginning a run, test fuel is pumped through the system for 15 minutes to flush the lines of all residue from the previous run or cleanup. The pumping is done with a standard HPLC pump set to deliver 10 mL/min. The pressure in the system fluctuates (due to the pulsing action of the pump) between 800 and 950 psig with the help of a back pressure regulator. A safety pressure relief valve is set at 1000 psig. The flush is performed with no heat applied to the heat exchanger tube. Once the flush is complete, the heating bath, a Techne Fluidized Bath Model SBL-2D, is raised into position around the heat exchanger tube. This point is the beginning of the 4 hour run. At this point also, a zero hour oxygen/methane analysis is made using gas chromatography. Additional oxygen/methane analyses are conducted

throughout the run, once every 10 minutes for the first hour and every 30 minutes thereafter. An end of test analysis, at ambient temperature, is also made for comparison purposes. At the end of a STHE run the heating bath is lowered away from the U-tube. Fuel is allowed to flow through the tube for approximately 10 more minutes to cool the tube. The pressure is released and the U-tube is removed from the STHE. Next the U-tube is rinsed with heptane and air dried. The tube is then clamped in a bench vise and straightened. The longitudinal center of the tube is marked. Measuring from the center point, marks are made at 3 inch (7.6 cm.) intervals along the entire length of the tube. Beginning at the inlet end of the tube, inscribe each marked-off section with a letter; starting with "A" and ending with "N." Cut the tube at each of the 3 inch scribe marks using a tubing cutter. Since the tubing cutter will tend to close the openings at each end of the 3 inch sections, use a 1/4" drill bit to open the holes to original diameter. The sections (B through M) are now ready for carbon burn-off analysis.

Procedure for Coating HLPS Heater Tubes. Aluminum, gold, carbon, magnesium, and copper were deposited on sets of three each 304 SS heater tubes. Basically, the objective was to make coatings on the heater tubes thick enough to cover the surface completely yet thin enough to minimize possible effects of both electrical and thermal conductivity. The coatings were accomplished with a Denton model DV-502 vacuum deposition apparatus that was set up to produce a thin layer of the test element onto standard 304 SS JFTOT heater tubes. In developing the procedure for coating the tubes, it was found that the success of the method depended greatly on the cleanliness of the heater tube surface. Quality adherence of the coatings was achieved when the heater tubes were cleaned with trichloroethane in a sonic bath for about 2 minutes and dried in a laboratory specimen dryer.

Deposit Measurement Device. The deposit thickness measurement device (DMD) determines the thickness of a deposit on a conductive surface by applying a voltage across the deposit while measuring the dielectric breakdown of the layer at various points.⁹ The DMD used in this work was first reported in Reference 10. The DMD voltage measurements were shown to relate thickness of deposits with 350 volts equal to 1 micrometer.¹⁰ Methods for calculating deposit volume on JFTOT heater tubes were also discussed in Reference 10. This procedure was used to develop DMD data correlations to carbon burn-off values reported in Reference 7.

Auger Milling Technique. The raw data from Auger ion milling are given in units of time. To determine thickness repeatably, it is necessary to make the appropriate calibration. For the deposit thickness measurements, a piece of tantalum foil with a layer of tantalum oxide of known thickness was ion-milled at a given rate until the oxide was removed. For a given milling rate, it was then possible to measure thickness in terms of time. JFTOT deposit thicknesses were determined assuming that the rates of material removal from the deposit and the tantalum oxide standard were equivalent. However, it was expected that the deposit would mill at a somewhat faster rate since it is primarily carbon and hydrogen, i.e., lighter elements than the oxygen and tantalum. Since the mass removal rate for the deposit could be faster than that of the standard, the actual deposit thicknesses may have been somewhat larger than those reported in this paper.

ESCA. Electron Spectroscopy for Chemical Analysis (ESCA) was performed by Surface Science Laboratories. ESCA is a surface-sensitive technique capable of obtaining elemental and chemical bonding information from the top 100 Å of a conductive or insulating material. ESCA measurements can detect elements with atomic number >2, with a sensitivity of roughly one atom percent.

SEM. The Scanning Electron Microscope (SEM) was used to examine the topography of the deposits formed on JFTOT tubes. In preparation for the SEM, the deposit samples were coated with platinum.

Carbon Burn-off Procedure. All analyses were conducted on Control Equipment Corporation Model 240XA Elemental Analyzer. Specially constructed quartz sample boats were used to inject the test

specimen into the furnace of the analyzer. The combustion tube section of the analyzer is set at 950-975°C and the reduction tube section is set at 600-625°C. Calibration of the instrument is conducted using squalane and n-hexadecane. Analysis time is 250 seconds. Results are reported in micrograms of carbon ($\mu\text{g C}$).

Test Fuel. The objective in choosing a test fuel was to find one that could provide assessable deposits on 304 SS heater tubes at test temperatures of 300, 340 and 380°C. After evaluating several fuels, a West Coast Jet A fuel was found to give acceptable levels of deposit on 304 SS heater tubes over the test temperature range. The fuel met ASTM D 1655 specification at the time of manufacture, and had a breakpoint temperature of 254°C when the tests reported here were initiated.

RESULTS AND DISCUSSION

The results in Fig. 1 show the longitudinal temperature profile of the heater tubes at controlled maximum temperatures of 300, 340, and 380°C. These data were used as a reference to determine the temperature at a particular heater tube station. Stainless steel (304) tubes were evaluated using the West Coast Jet A fuel and test durations of 0.5, 1.0, 1.5 and 2.5 hours at maximum heater tube temperatures of 300, 340, and 380°C. The 1.5-hour test period was selected for use in the metal surface evaluations because it produced a deposit that was relatively nascent, yet assessable by the DMD and Auger measuring techniques. The results of the JFTOT and the DMD measurements are given in Table 1. Figures 4 through 9 summarize the deposit thickness measurements by DMD and Auger for the West Coast Jet A using the Mild Steel heater tube, the 304 SS heater tube, and the 304 SS heater tubes coated with aluminum, magnesium, gold, and copper. Auger milling measurements of deposit thickness were made at several of the heater tube stations for the various surfaces. Note that Auger results were not available for the 304 stainless steel. General comparisons of the thickness measurements by Auger milling and DMD indicate Auger milling gives much greater thicknesses than DMD for deposits formed on copper-coated tubes. The two methods give similar deposit profiles and locations of maximum thickness. Magnesium-coated tube deposit values by Auger were increasingly higher than DMD values at higher heater tube temperatures. Note, however, that at 300°C, Auger deposit thickness values of 0.2, 0.2, and 3.8 micrometer were reported at stations 46, 50, and 52, respectively.

Mild Steel tube deposit values by Auger were higher than DMD values and the difference increased as the heater tube temperature was raised. Aluminum-coated tube deposit thickness by Auger was approximately one-half the DMD measurement. Gold-coated tube deposit thickness by Auger milling was essentially equal to the DMD measurement. Generally, the difference between Auger and DMD thickness values was greatest at the stations of thickest deposit and more closely agreed at stations of lower thickness.

In ASTM D 3241-88a, note 8 states: "Heater tubes should not be reused. Tests indicate that magnesium migrates to the heater tube surface under normal test conditions. The enriched magnesium surface may reduce adhesion of deposits to re-used heater tubes."^{8,11} Using the data in Figures 4 through 9, Auger ion milling of the deposits showed the order of deposition to be copper > Mild Steel > gold > aluminum > magnesium (using the 0.2 rather than the 3.8 micrometer value for magnesium) for the 300°C data. The dielectric strength method indicated deposit thickness ranking of Mild Steel 304 SS > gold > magnesium = aluminum = copper. Since all of these deposits are much thicker than the deposit would be to give a code 3 JFTOT visual deposit rating, these data do not directly differentiate between ability of either aluminum

or magnesium to reduce (or increase) deposit propensity at the standard test temperature of 260°C, which uses a standard aluminum tube containing a small amount of magnesium.

The pronounced differences between the deposit thickness measuring techniques suggest that both the Auger milling rate and the dielectric strength of the deposit may be affected by deposit morphology/composition (such as metal ions that may have become included in the bulk of the deposit or deposit geometry). This was especially true for copper and magnesium. While the DMD data are valuable for showing where the deposit is on the heater tube, this data must be augmented with the addition of carbon burn-off data for deposit quantitation. Carbon burn-off and ESCA results are summarized in Table 2. The ESCA results show a thick (>100 Å) aliphatic hydrocarbon film containing an abundance of ether, alcohol, ester and carboxylic acid groups. The elemental assay showed a preponderance of carbon (70 to 85 percent) and oxygen (16 to 24 percent), which is typical of gums and deposits resulting from fuel oxidation. The trace quantities of other heteroatoms are probably due to trace reactive compounds since the fuel was considered essentially free of sulfur and nitrogen. Aluminum in some of the deposits on magnesium, copper, and gold surfaces are attributed to contaminants at the point of ESCA analysis. The deposits on the magnesium surface showed magnesium in the deposit at 300 and 340°C. These relatively high concentrations of magnesium (approx. 7 percent) probably resulted because the sampling depth either exceeded the deposit thickness (thus allowing detection of the magnesium substrate) or contained dissolved magnesium in the deposit. It is important to note that ESCA is not expected to detect trace metal ions included in deposits since their concentrations are most probably much less than the detection limit of one percent. The carbon burn-off data tended to agree with the DMD data for comparing at the three temperatures and for the different tube metals. Using the carbon burn-off data at 340°C allowed an observation that the deposit magnitude essentially the same, except it seemed dramatically lower for aluminum. The highest value was 416 µg for Mg at 380°C. Note that no repeatability data is available yet.

The results (in Figures 4-9 and Table 1) show that the surface temperature as well as composition plays an important role in deposition. Other than for variation in the thickness of deposits formed during 1.5-hour tests, using various metal surfaces, the most dramatic effect observed was that the bulk of deposits moved to lower tube temperature as the maximum tube temperature was increased from 300 to 380°C. Compared to the other surface materials, the results in Table 3 indicate that copper causes an even greater shift of the deposit to lower temperature. These data show that the deposition rate is highly dependent on temperature and may be limited by the concentration of dissolved oxygen or possibly a reactive component in the fuel. If the rate of deposition is limited by the rate of autoxidation, copper may be catalytic; otherwise, as discussed below, it is probably involved in the deposition process.

Basically, there are two theories on the role of metals in fuel stability. When fuels are exposed to hot metal surfaces, it is believed that naphthenic acids react with surface oxides to produce fuel-soluble metal naphthenates. In solution, the trace metals may either initiate autoxidation reactions or enhance free radical concentrations by decomposing hydroperoxides. The other theory is that gums formed in the autoxidation process have different affinities for surface materials and thus adhere to some surfaces more than others. If it is simply the adherence of either fuel soluble or insoluble gums to the surface that matters, the effect would be expected to be important only in the formation of nascent deposits, and the composition of the deposit would

not be changed by the metal. If the mechanism is based solely on the dissolution of metals by acidic constituents in the fuel, one would not anticipate a change in the rate of deposition as the deposit builds up. Also, metal ions would probably become incorporated homogeneously in the deposit since metals tend to form chelates with the relatively polar gum and deposit forming molecules in the fuel.

To further explore this phenomenon, the deposits formed on the different heater tube surfaces were examined with a scanning electron microscope (SEM). Fig. 10 provides photographs taken with the SEM at a magnification of 2000; comparing the metal surface that is essentially free of deposit with the area having a maximum deposit thickness. The photographs show significant differences in the topographies of the deposits formed on the various surface materials. The topography of the deposit formed on the magnesium surface was particularly different than those formed on the other metals. The most striking feature is the multitude of large (1 to 3 μm) spheroids making up the deposit on the magnesium surface and possibly contributing to the large variation in Auger thickness values observed at the 46-, 50-, and 52-mm tube stations. Before the tests, the magnesium coatings showed no apparent abnormalities; all of the metal coatings were made with essentially the same thickness estimated at approximately 10 to 30 \AA . After the test, the deposit thickness profiles appeared to be similar to those formed on the other metal surfaces. The results indicated either adhesion of agglomerated insolubles or the formation of deposits from soluble gums at particular sites on the magnesium surface.

Spheroidal shapes in deposits are not that uncommon; Schirmer¹² found that deposits consisted of soft particles measuring about 1000 \AA in diameter. These microspheres form random three-dimensional structures on the deposit face, which become closely packed in the deposit substrate, and undergo fusion on heated surfaces. In the case of magnesium, however, the spheres are more than an order of magnitude larger in diameter than those observed by Schirmer. Fig. 11 provides SEM photographs taken of the thick portions of the deposits at a magnification of 7000. Under this much greater magnification (compared to Fig. 10), it is found that the large spheres formed on the magnesium surface are, in fact, composed of microspheres of about 1000 \AA in diameter. One possible explanation for this phenomenon is that the microspheres form in the fuel and tend to agglomerate into large spheroids before they reach the surface of the heater tube. The magnesium, no doubt, plays a role in the agglomeration mechanism. As noted above, the Auger deposit thickness measurements were higher than those with the DMD and the difference tended to increase with rising temperature. While not definitive, these results suggest that greater amounts of magnesium become incorporated into the structure of the deposit as the temperature is raised, and that dissolved magnesium has a significant effect on nucleation and the agglomeration of microspheres in the bulk fuel.

The deposits formed on copper-coated heater tubes also exhibited an unusually coarse structure. The surface shown in Fig. 11 appears as if globules or spheroids have partially coalesced and fused. It is well known that traces of copper in fuels cause premature plugging of the filter that passes the stressed fuel in the JFTOT. One theory is that copper causes enhanced agglomeration of insolubles (microspheres) in the bulk fuel because it tends to chelate with soluble gums. This appears to be consistent with the relatively coarse structure shown in Fig. 11 since the large agglomerates formed in the fuel could also precipitate onto the surface of the heater tube.

For mild steel and the 304 SS, the microspheres appear to agglomerate at particular sites on the

metal surface rather than in the bulk of the fuel. In the 340°C test, the deposit on the mild steel had a cauliflower appearance, indicating that the microspheres from the bulk fuel agglomerated at sites on the metal surface. When the test temperature was raised to 380°C, the agglomerated microspheres on the mild steel appeared to have fused because the deposit changed to a relatively smooth platelet-type structure. In the 300°C test on the 304 SS, the large spheroids appear to be in a partially fused condition, i.e., the fine structure seems to have disappeared due to melting and coalescence of the particles.

In view of the observations made by Schirmer¹², the deposits formed on the aluminum and gold surfaces appear to be normal, i.e., they appear to have a relatively smooth platelet-type structure. Under higher magnification, the microspherical structure previously observed by Schirmer is apparent.

Single Tube Heat Exchanger (STHE) carbon burn-off data are summarized in Fig. 12. The STHE test tubes were 0.64 cm O.D. 304 SS test tubes heated at 300, 340, and 380°C for four hours with a fuel flow of 10 mL/Minute. The position of the fuel deposit in the tube versus the fuel temperature (Fig. 3) at various bath set temperatures very closely approximates what was observed for HLPS heater tubes. This data supports the observation based on HLPS data that the depositing position on the tube is temperature dependent. Furthermore, the magnitude of the deposit is essentially the same at all three temperatures. Oxygen measurements for this fuel in both HLPS and STHE indicate that it is depleted at temperatures below 260°C. At higher temperatures (set temperature of 420°C) for the STHE, methane generation is observed due to pyrolysis of the fuel.

CONCLUSION

Under JFTOT D 3241 test conditions, thickness profiles of deposits formed on a variety of surfaces including mild steel, 304 SS, Al, Mg, Cu and Au, were compared using the DMD (dielectric breakdown voltage) and Auger milling. Except for gold and aluminum, the deposit thicknesses measured by DMD were substantially lower than those measured by Auger milling, and the disparity in the two methods seemed to grow with increased temperature and deposit thickness. The disparities in the thicknesses measured by DMD and Auger milling were most pronounced in the copper-coated heater tubes. Carbon burn-off data has been used to quantitate the temperature and metal effects on deposit formation. Using only the carbon burn-off data at 340°C allowed an observation that the deposit magnitude essentially the same, except it seemed dramatically lower for aluminum. The highest value was 416 µg for Mg at 380°C while the lowest value at 380°C was 153 µg C for aluminum. It was noted that no repeatability data for these experiments were yet available.

Aside from variations in the thickness of deposits due to metallurgy, the most dramatic effect observed was that the bulk of deposits moved to tube locations of lower temperature as the maximum temperature of the tube was increased from 300 to 380°C. This effect was somewhat greater on the copper-coated tubes. The results indicate that the deposition rate is highly temperature dependent and may be limited by the concentration of dissolved oxygen or reactive components in the fuel.

Surface analysis by ESCA showed that the deposits consisted of a highly oxygenated aliphatic

hydrocarbon film containing alcohol, ether, ester and carboxylic acid groups.

The SEM photographs showed marked variations in the deposit morphology among the surface materials tested. The results suggested that surface composition has a significant effect on the mechanism of deposition. In general, it appears that insolubles coalesce in the fuel to form microspheres less than 1000 Å in diameter. The microspheres then either deposit directly onto the surface, forming a relatively smooth platelet-type structure or they agglomerate into macrospheres (1- to 3 µm in diameter) before adhering to the surface. The former is observed on aluminum and gold, while the latter is particularly evident in deposits formed on magnesium. For copper, mild steel, and 304 SS, the deposits appear to form from several particle sizes ranging from micro to macrospheres.

Single Tube Heat Exchanger Experiments using 304 SS tubing has confirmed the temperature dependence of fuel deposits and limited depositing capacity (with oxygen starvation) for the Jet A fuel based on HLPS data.

(NOTE: This work was conducted under DOD Contract administered by the Fuels and Lubricants Division of the Materials, Fuels, and Lubricants Laboratory, U.S. Army Belvoir Research, Development and Engineering Center, Fort Belvoir, Virginia. This paper represents only the views of the authors.

REFERENCES

- (1) Cuellar, Jr., J.P., Russell, J.A.; "Additive Depletion and Thermal Stability Degradation of JP-5 Fuel Shipboard Samples," Report No. NAPC-PE-141C.
- (2) CRC Literature Survey on the Thermal Oxidation Stability of Jet Fuel, CRC Report NO.509, April 1979.
- (3) Uri, N., *ACS Advances in Chemistry Series*, 36, Chapt.10, 1962, p. 102.
- (4) Hazell, L.B.; Baker, C.; David, P.; and Fackerel, A.D., "An AES Depth Profiling Study of the Deposits on Aluminum During the Jet Fuel Thermal Oxidation Test," *Surface and Interface Analysis*, 1, 1986, pp. 507-513.
- (5) Clark, R.H., "The Role of a Metal Deactivator in Improving the Thermal Stability of Aviation Kerosines," 3rd International Conference on Stability and Handling of Liquid Fuels, London, UK, 13-16 September 1988.
- (6) Schreifels, J.A.; Morris, R.E.; Turner, N.H.; and Mowery, R.L., "The Interaction of a Metal Deactivator With Metal Surfaces," American Chemical Society, Division of Fuel Chemistry, Preprints, 35, No.2, 22-27 April 1990, pp. 555-562.
- (7) Morris, R.E.; and Hazlett, R.N., "Methods for Quantifying JFTOT Heater Tube Deposits Produced From Jet Fuels," *Energy and Fuels*, Vol. 3, No. 2, 1989, pp. 263-267.
- (8) ASTM Thermal Oxidation Stability of Aviation Turbine Fuels (JFTOT Procedure). In Annual Book of ASTM Standards; ASTM: Philadelphia, PA, 1989; Part 5.02, ASTM D 3241-88a.
- (9) U.S. Patent No. 4,791,811, "Deposit Thickness Measurement," J.G. Barbee, Southwest Research Institute, Granted December 20, 1988.
- (10) Stavinocha, L.L.; Barbee, J.G.; and Buckingham, J.P., "Thermal Stability Deposit Measuring Device," Proceedings of 2nd International Conference on Long-Term Storage Stabilities of Liquid Fuels, San Antonio, TX, 29 July-August 1986.
- (11) Strauss, K.H., "Thermal Stability Specification Testing of Jet Fuel-A Critical Review", SAE Paper No. 881532; 1988.
- (12) Schirmer, R.M., "Morphology of Deposits in Aircraft and Engine Fuel Systems," SAE Paper No. 700258, presented at the National Air Transportation Meeting, New York, NY, April 1970.

**Table 1. Summary of Deposit Measuring Device (DMD) Evaluation of JFTOT
Tubes Along With Standard ASTM D 3241 Ratings**

Test No.	Tube Metal	Total Test Time, hr	Prefilter	Temp, °C	Pressure Drop, mm of Hg at Time	TDR Spun Rating at Station, mm	Visual Rating	DMD, Max. Thickness, cm $\times 10^{-7}$ at Station, mm	DMD, Vol. of Deposit, cm ³ $\times 10^{-7}$
253-H	304 SS	2.5	No	300	125 at 46.5 min	50+ at 44-58	>4 Peacock	2394 at 54	3785
254-H	304 SS	2.5	No	340	125 at 38.1 min	50+ at 32-50	>4 Peacock	2277 at 40	2999
255-H	304 SS	2.5	No	380	125 at 52.1 min	50+ at 26-58	>4 Peacock	2005 at 32	3226
157-T	Al	2.5	Yes	260	2 at 148.7 min	12 at 38-45	<4	42 at 54	54
256-H	304 SS	1.5	No	340	125 at 36.0 min	50+ at 34-58	>4 Peacock	1862 at 40	2282
257-H	304 SS	1.5	No	300	125 at 31.2 min	50+ at 45-58	>4 Peacock	1968 at 50	2255
258-H	304 SS	3.5	No	300	125 at 63.3 min	50+ at 40-58	>4 Peacock	2742 at 54	2742
259-H	304 SS	0.5	No	300	5.3 at 30.0 min	47 at 50-52	4	345 at 54	439
260-H	304 SS	1.0	No	300	125 at 56.1 min	50+ at 45-58	>4	1811 at 54	1835
261-H	304 SS	0.5	No	340	19.5 at 30.0 min	50 at 38-42	>4	591 at 42	651
262-H	304 SS	1.0	No	340	125 at 48.0 min	50+ at 36-49	>4	1845 at 42	2091
257-H	304 SS	1.5	No	300	125 at 31.2 min	50+ at 45-58	>4 Peacock	1968 at 50	2255
263-H	Al/304 SS	1.5	No	300	125 at 56.0 min	36 at 54	4 Peacock	1168 at 52	1256
264-H	Au/304 SS	1.5	No	300	125 at 66.3 min	50+ at 50-56	>4 Peacock	1411 at 52	1294
266-H	Mg/304 SS	1.5	No	300	125 at 52.1 min	Too Dark to Rate	4	1082 at 54	1558
267-H	Cu/304 SS	1.5	No	300	125 at 18.5 min	50+ at 38-58	4 Peacock	862 at 46	1164
279-H	Mild Stl	1.5	No	300	125 at 58.2 min	50+ at 28-58	>4 Peacock	2211 at 54	2669
256-H	304 SS	1.5	No	340	125 at 36.0 min	50+ at 34-58	>4 Peacock	1862 at 40	2282
268-H	Al/304 SS	1.5	No	340	125 at 33.5 min	50+ at 40-45	>4 Peacock	1200 at 42	1649
269-H	Au/304 SS	1.5	No	340	125 at 31.5 min	50+ at 40-45	>4 Peacock	1917 at 42	2048
270-H	Mg/304 SS	1.5	No	340	125 at 40.5 min	Too Dark to Rate	>4	1297 at 42	1944
271-H	Cu/304 SS	1.5	No	340	125 at 30.0 min	50+ at 29-58	>4 Peacock	751 at 36	682
278-H	Mild Stl	1.5	No	340	125 at 40.9 min	50+ at 24-56	>4 Peacock	2668 at 40	2440
272-H	304 SS	1.5	No	380	125 at 52.4 min	50+ at 30-40, 49-54	>4 Peacock	2137 at 34	2191
273-H	Al/304 SS	1.5	No	380	125 at 48.1 min	50+ at 32-36	>4 Peacock	1805 at 34	1633
274-H	Au/304 SS	1.5	No	380	125 at 56.9 min	50+ at 32-36	>4 Peacock	2248 at 34	1824
275-H	Mg/304 SS	1.5	No	380	125 at 58.3 min	Too Dark to Rate	>4	1237 at 36	1782
276-H	Cu/304 SS	1.5	No	380	125 at 31.2 min	50+ at 24-58	>4	1148 at 30	812
277-H	Mild Stl	1.5	No	380	125 at 35.5 min	50+ at 18-58	>4 Peacock	2477 at 34	1757

Table 2. Summary of ESCA Results and Carbon Burnoff Data

Sample Description**	Bonding Atom Percentages*					Elemental Composition						Carbon Burnoff, ug C
	C ₁	C ₂	C ₃	O ₁	O ₂	C	O	N	S	Al	Mg	
Fe-380-32	66	11	5	6	12	80	18	2	<1	-	-	-
Fe-340-42	70	7	4	6	14	78	19	3	<1	-	-	-
Fe-300-48	69	10	5	5	11	83	17	1	<1	-	-	-
304-380-42	84	2	3	3	8	89	11	-	<1	-	-	293
304-340-40	63	11	5	7	13	80	20	-	-	-	-	286
304-300-48	64	11	6	7	13	78	19	-	<1	-	-	222
Al-380-32	65	9	6	7	13	78	20	1	-	-	-	153
Al-340-42	74	7	3	6	9	84	16	-	-	-	-	120
Al-300-54	61	10	7	7	15	77	22	1	<1	-	-	62
Mg-380-32	46	5	4	16	29	47	38	-	<1	13	-	416
Mg-340-42	67	7	4	9	14	71	20	-	1	-	7	265
Mg-300-54	57	11	7	10	16	67	23	<1	1	-	8	158
Au-380-34	68	9	6	7	10	82	17	1	<1	-	-	188
Au-340-42	67	8	4	9	12	79	20	1	<1	-	-	223
Au-300-50	59	12	6	10	13	74	22	2	<1	<1	-	159
Cu-380-30	64	9	6	6	15	76	20	1	1	2	-	200
Cu-340-34	60	7	7	8	17	71	24	1	1	3	-	267
Cu-300-48	65	6	4	10	16	70	24	3	-	-	-	245

* Peak Assignments: C₁ = \underline{C} - R (R = C, H) O₁ = \underline{O} = C
C₂ = \underline{C} - O O₂ = \underline{O} - C
C₃ = \underline{O} = \underline{C} - OR

**JFTOT Preheater Tube Composition - Test Temperature in °C - Station in Millimeters

Table 3. Tube Locations of Maximum Deposit For Three Control Temperatures

Tube control temp. =	Deposit Peak Locations, mm		
	300°C	340°C	380°C
<u>Metal Surface</u>			
1018 Mild Steel	52	40	32
Mg/304 SS	52	40	34
Cu/304 SS	46	36	30
	(301°C)*	(325°C)*	(340°C)*
Au/304 SS	52	40	32
Al/304 SS	52	44	34
304 SS	50	40	34
	(298°C)*	(335°C)*	(345°C)*

* Approximate Tube Temperature, °C, at location, estimated from Figure 8.

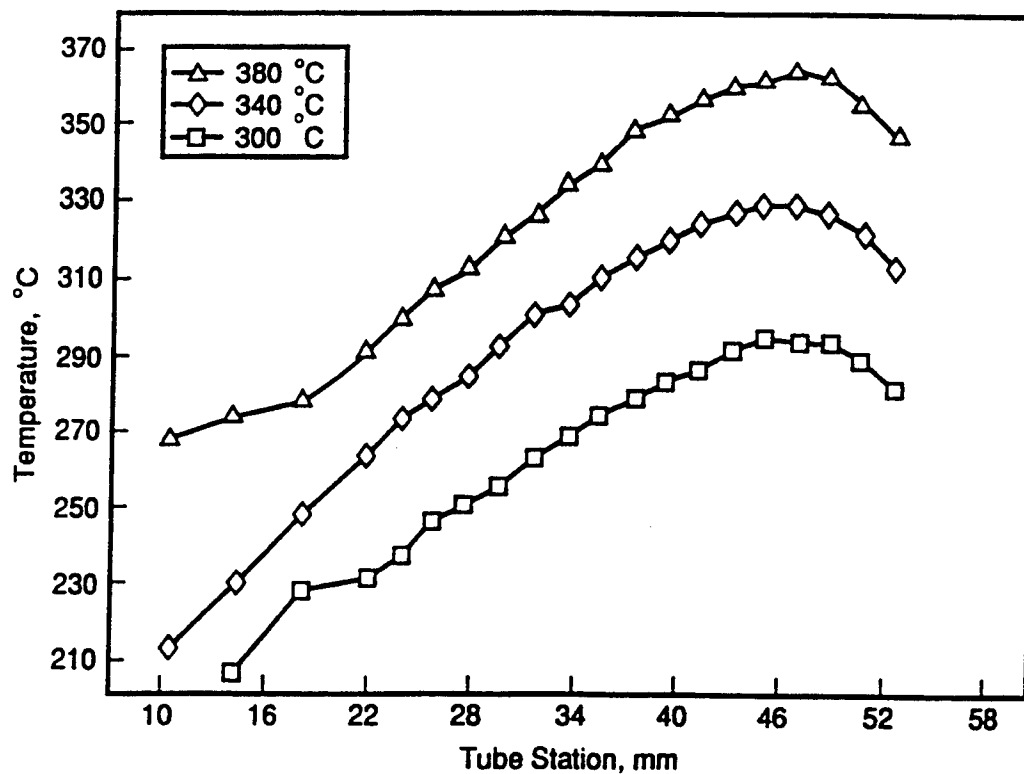


Figure 1. HLPS temperature profile of three temperatures using 304 stainless steel heater tubes

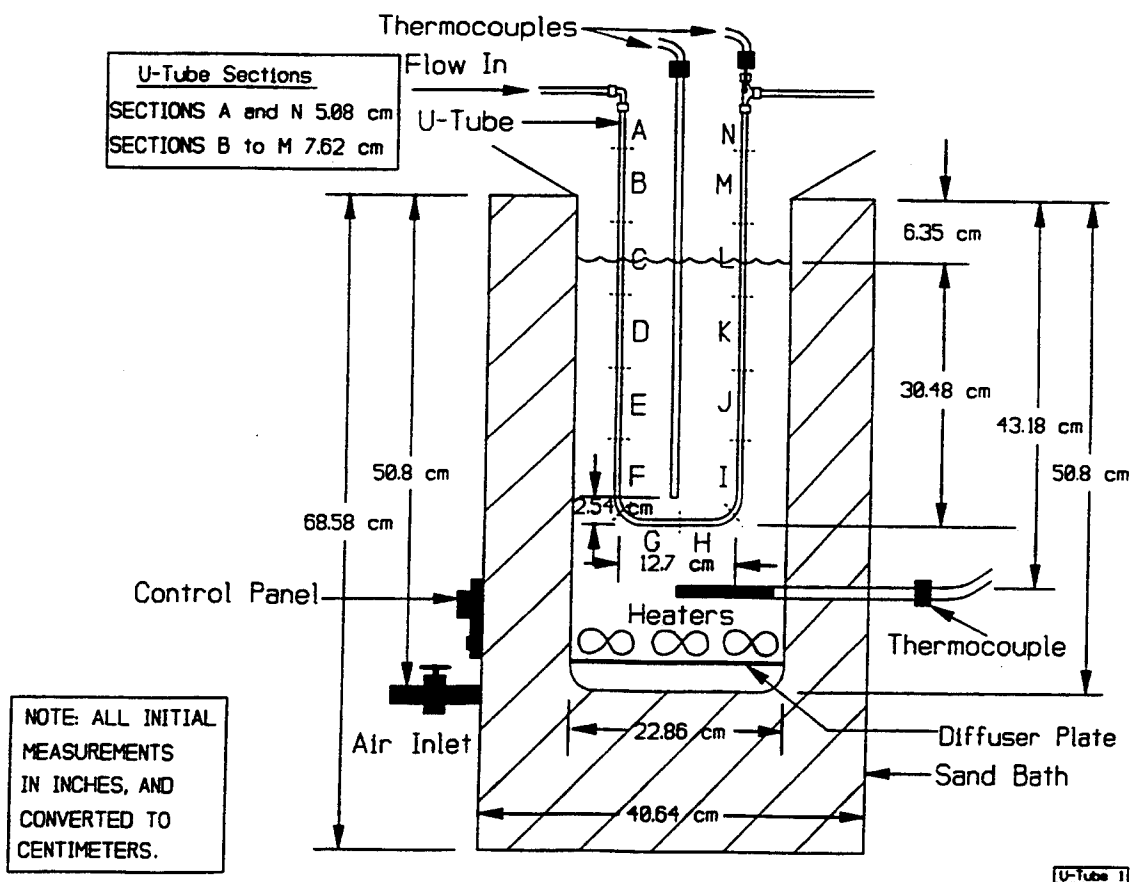
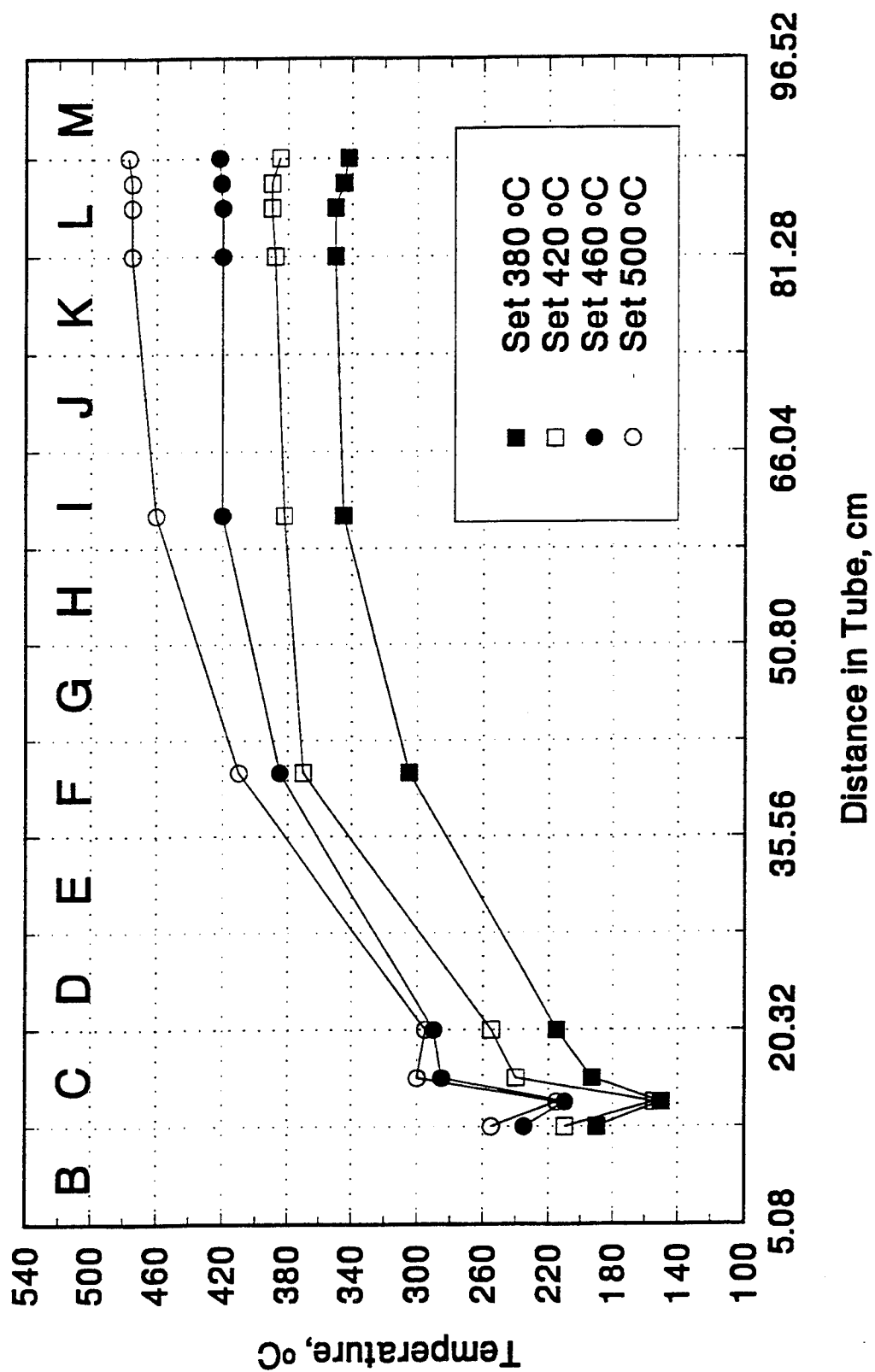


Figure 2. Diagrammatic Sketches of Single Tube Heat Exchanger

Figure 3. Fuel temperature profiles in STHE

Flow Rate = 10 mL/minute



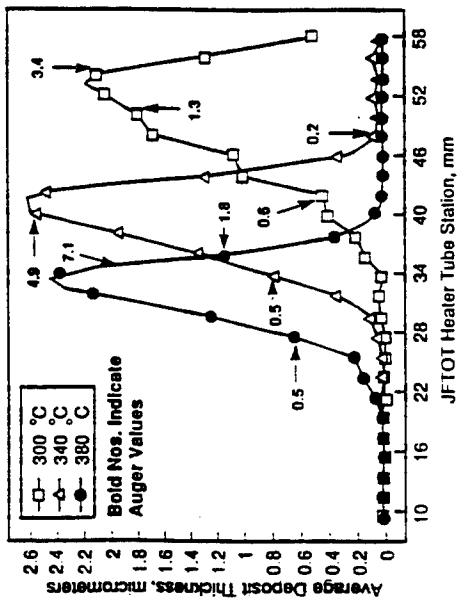


Figure 4. Deposit thickness on mild steel heater tube run at 300°C, 340°C, and 380°C

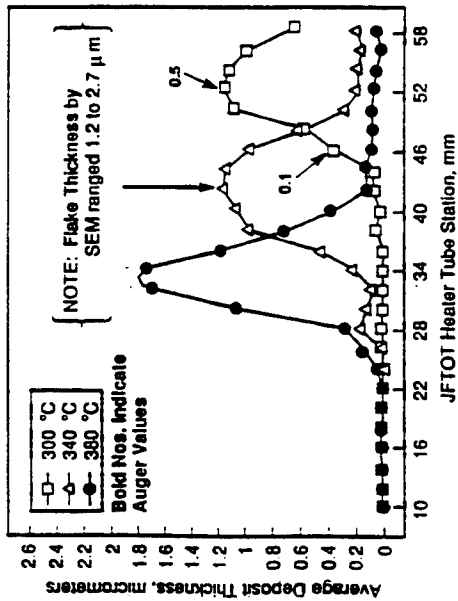


Figure 6. Deposit thickness on aluminum-plated heater tube run at 300°C, 340°C, and 380°C

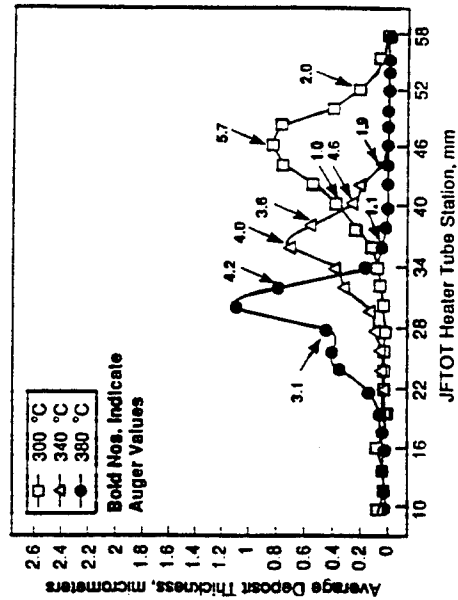


Figure 8. Deposit thickness on copper-plated heater tube run at 300°C, 340°C, and 380°C

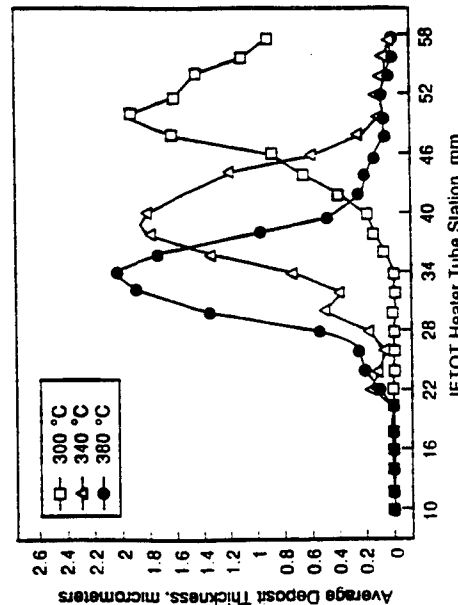


Figure 5. Deposit thickness on 304 stainless steel heater tube run at 300°C, 340°C, and 380°C

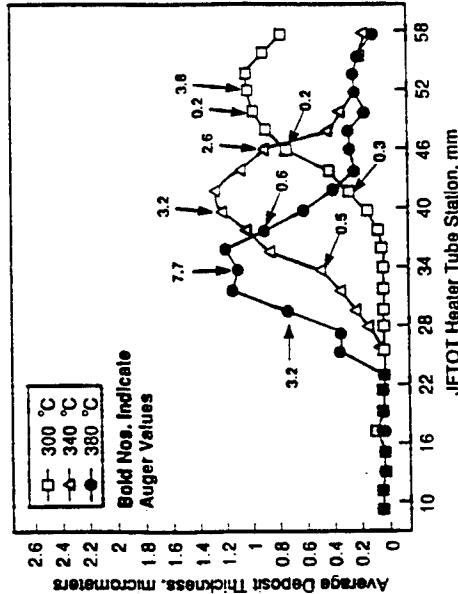


Figure 7. Deposit thickness on magnesium-plated heater tube run at 300°C, 340°C, and 380°C

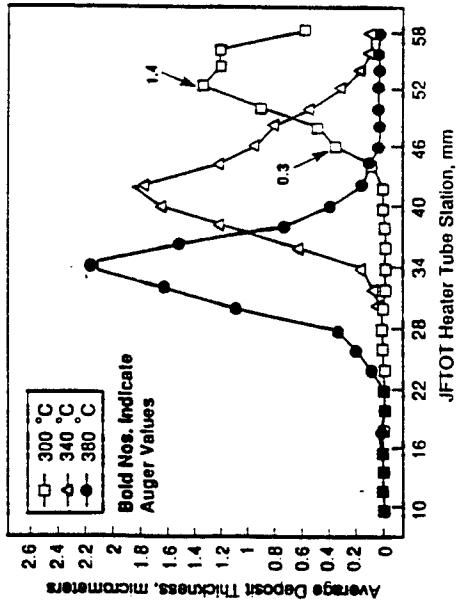


Figure 9. Deposit thickness on gold-plated heater tube run at 300°C, 340°C, and 380°C

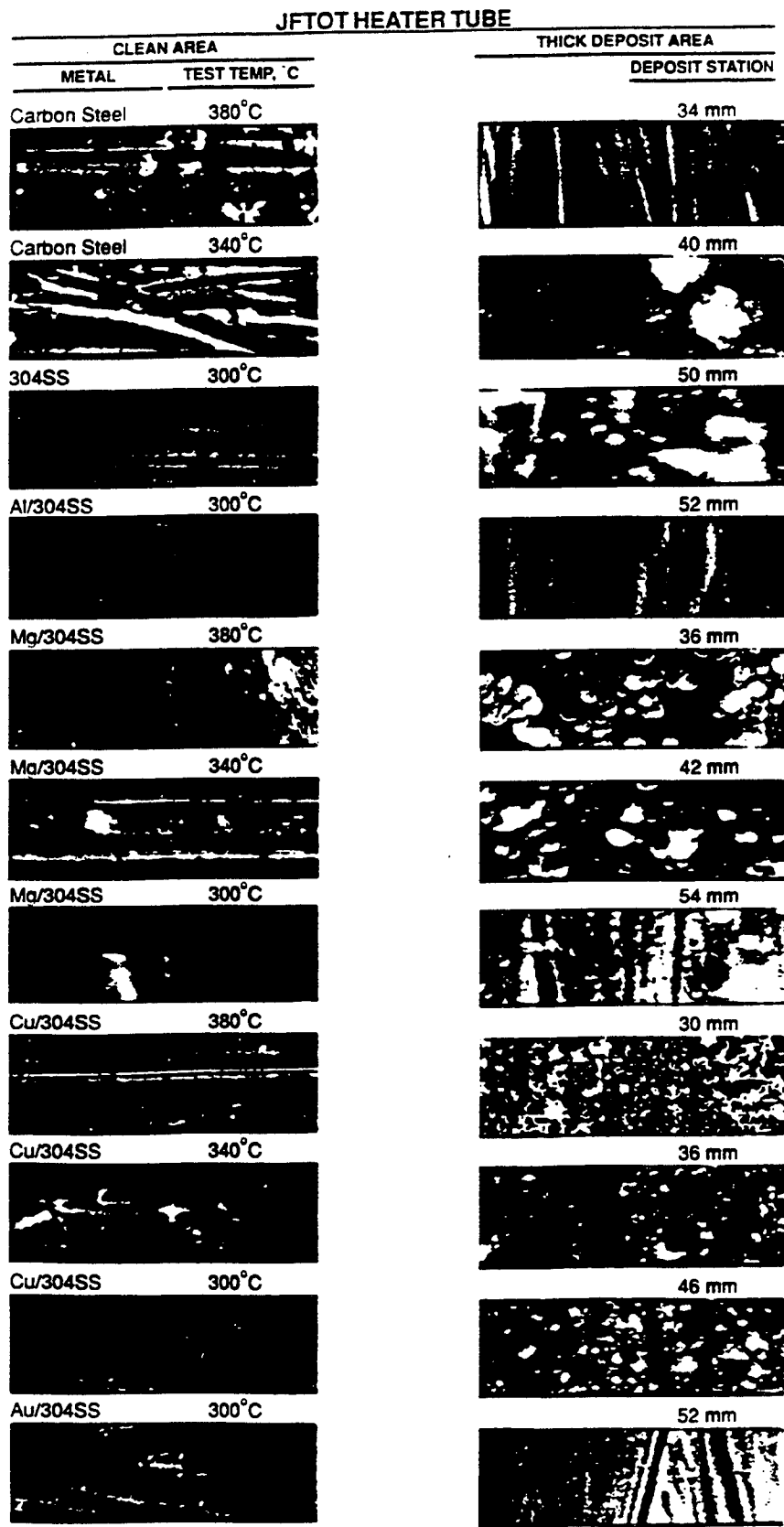
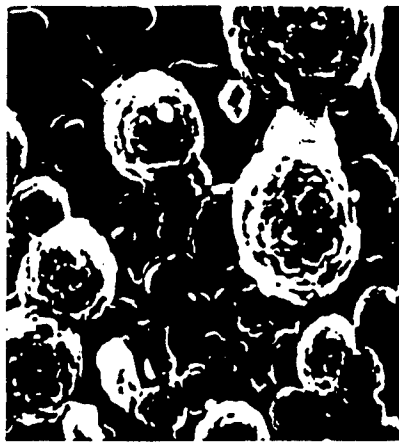
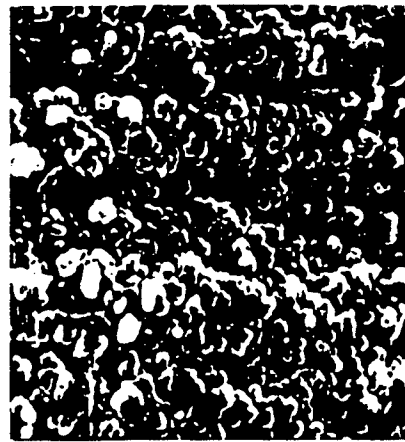


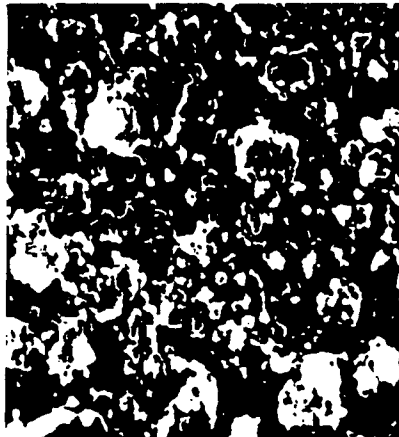
Figure 10. SEM Photographs of clean and thick deposit areas of JFTOT test tubes (height of photographs = 10 μ m)



Magnesium on 304SS



Aluminum on 304SS



Copper on 304SS



Gold on 304SS

Figure 11. SEM Photographs of 380°C JFTOT tube deposits at 7000x magnification (width of photographs = 10 μ m)

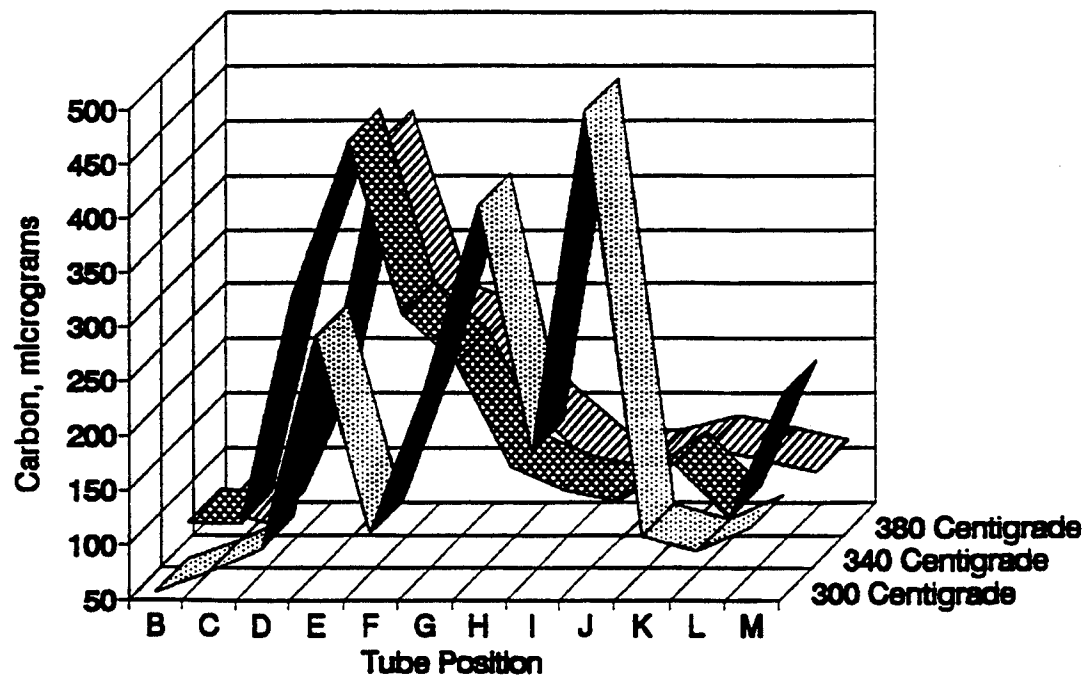


Figure 12. Carbon Burnoff data for STHE tube sections from Jet A at 300°, 340°, and 380°C

DISTRIBUTION LIST

Department of Defense

DEFENSE TECH INFO CTR	12	CDR	
CAMERON STATION		DEFENSE FUEL SUPPLY CTR	
ALEXANDRIA VA 22314		ATTN: DFSC Q BLDG 8	1
		DFSC S BLDG 8	1
		CAMERON STA	
		ALEXANDRIA VA 22304-6160	

Department of the Army

DEPARTMENT OF THE ARMY		PROG EXEC OFFICER	
MOBILITY TECH CTR BELVOIR		COMBAT SUPPORT	
ATTN: AMSTA RBF (M E LEPERA)	10	ATTN: SFAE CS TVL	1
AMSTA RBXA (R B TOBEY)	1	SFAE CS TVM	1
10115 GRIDLEY RD STE 128		SFAE CS TVH	1
FT BELVOIR VA 22060-5843		CDR TACOM	
		WARREN MI 48397-5000	
SARDA		PROG EXEC OFFICER	
ATTN: SARD TL	1	ARMAMENTS	
PENTAGON		ATTN: SFAE AR HIP	1
WASHINGTON DC 20310-0103		SFAE AR TMA	1
CDR AMC		PICATINNY ARSENAL NJ 07806-5000	
ATTN: AMCRD S (V FALCHETTA)	1		
5001 EISENHOWER AVE		DIR	
ALEXANDRIA VA 22333-0001		ARMY RSCH LAB	
		ATTN: AMSRL CP PW	1
TARDEC		2800 POWDER MILL RD	
ATTN: AMSTA CMA	1	ADELPHIA MD 20783-1145	
AMSTA CMB	1		
AMSTA R	1	VEHICLE PROPULSION DIR	
AMSTA RG	1	ATTN: AMSRL VP (MS 77 12)	1
AMCPM ATP	1	NASA LEWIS RSCH CTR	
CDR TACOM		21000 BROOKPARK RD	
WARREN MI 48397-5000		CLEVELAND OH 44135	
PROG EXEC OFFICER		CDR ARO	
ARMORED SYS MODERNIZATION		ATTN: AMXRO EN (D MANN)	1
ATTN: SFAE ASM S	1	RSCH TRIANGLE PK	
SFAE ASM AB		NC 27709-2211	
SFAE ASM BV	1		
SFAE ASM CV	1	CDR ARMY NRDEC	
SFAE ASM AG	1	ATTN: SATNC US (J SIEGEL)	1
CDR TACOM		SATNC UE	1
WARREN MI 48397-5000		NATICK MA 01760-5018	
PROG EXEC OFFICER		CDR ARMY CRDEC	
ARMORED SYS MODERNIZATION		ATTN: SMCCR RS	
ATTN: SFAE ASM FR	1	APG MD 21010-5423	
SFAE ASM AF	1		
PICATINNY ARSENAL NJ 07806-5000		CDR APC	
		ATTN: SATPC Q	1
		SATPC QE (BLDG 85 3)	1
		NEW CUMBERLAND PA 17070-5005	

PROG MGR PETROL WATER LOG
ATTN: AMCPM PWL
4300 GOODFELLOW BLVD
ST LOUIS MO 63120-1798

1

CDR TRADOC
ATTN: ATCD SL 5
INGALLS RD BLDG 163
FT MONROE VA 23651-5194

1

PROG MGM MOBILE ELEC PWR
ATTN: AMCPM MEP
7798 CISSNA RD STE 200
SPRINGFIELD VA 22150-3199

1

CDR ARMY QM SCHOOL
ATTN: ATSM CD
ATSM PWD
FT LEE VA 23001-5000

1

1

CDR
ARMY BIOMED RSCH DEV LAB
ATTN: SGRD UBZ A
FT DETRICK MD 21702-5010

1

Department of the Navy

OFC OF NAVAL RSCH
ATTN: ONR 464
800 N QUINCY ST
ARLINGTON VA 22217-5660

1

CDR
NAVAL RSCH LABORATORY
ATTN: CODE 6181
WASHINGTON DC 20375-5342

1

CDR
NAVAL SEA SYSTEMS CMD
ATTN: SEA 03M3
2531 JEFFERSON DAVIS HWY
ARLINGTON VA 22242-5160

1

CDR
NAVAL PETROLEUM OFFICE
CAMERON STA T 40
5010 DUKE STREET
ALEXANDRIA VA 22304-6180

1

CDR
NAVAL SURFACE WARFARE CTR
ATTN: CODE 63
CODE 632
CODE 859
3A LEGGETT CIRCLE
ANNAPOLIS MD 21401-5067

1

1

Department of the Navy/U.S. Marine Corps

HQ USMC
ATTN: LPP
WASHINGTON DC 20380-0001

1

PROG MGR GROUND WEAPONS
MARINE CORPS SYS CMD
2033 BARNETT AVE
QUANTICO VA 22134-5080

1

PROG MGR COMBAT SER SPT
MARINE CORPS SYS CMD
2033 BARNETT AVE STE 315
QUANTICO VA 22134-5080

1

Department of the Air Force

HQ USAF/LGSSF
ATTN: FUELS POLICY
1030 AIR FORCE PENTAGON
WASHINGTON DC 20330-1030

1

SA ALC/SFT
1014 ANDREWS RD STE 1
KELLY AFB TX 78241-5603

1

AIR FORCE WRIGHT LAB
ATTN: WL/POSF
1790 LOOP RD N
WRIGHT PATTERSON AFB
OH 45433-7103

1